universität
wien

DIPLOMARBEIT

Titel der Diplomarbeit

„The influence of free fatty acids on the development of liver inflammation"

Verfasser

Mario Kuttke, B.Sc.

angestrebter akademischer Grad

Magister der Naturwissenschaften (Mag.rer.nat.)

Wien, 2012

Studienkennzahl lt. Studienblatt:	A 490
Studienrichtung lt. Studienblatt:	Diplomstudium Molekulare Biologie
Betreuerin / Betreuer:	A.o.Univ.-Prof.Dipl.-Ing.Dr. Marcela Hermann

Danksagung

Zuerst möchte ich mich bei a.o.Univ.-Prof. Dipl.-Ing. Dr. Marcela Hermann für die Betreuung meiner Diplomarbeit bedanken.

Besonderer Dank gilt a.o.Univ-Prof. Dr. Bettina Grasl-Kraupp für die fachliche Unterstützung und Betreuung während der praktischen Durchführung der Arbeit.

Weiters bedanke ich mich bei Sandra Sagmeister, Therese Böhm, Nora Bintner, Waltraud Schrottmaier, Melanie Pichlbauer, Marzieh Nejabat, Teresa Riegler, Bettina Wingelhofer und Christiane Maier für die ausgezeichnete Zusammenarbeit im Labor und die Unterstützung in allen Lebenslagen.

Birgit Mir-Karner, Helga Koudelka und Krystyna Bukowska danke ich für ihre Hilfsbereitschaft und für die kollegiale Zusammenarbeit.

Mein größter Dank gilt meinen Eltern, Ursula und Heinz, und meiner Großmutter, Theresia, die mir mein Studium ermöglicht und mich immer unterstützt haben, sowie meinem Bruder, Alex, der in allen Lebenslagen für mich da ist.

TABLE OF CONTENTS

Table of Contents

2

Introduction

Hepatocellular carcinoma (HCC)

Hepatocellular carcinoma (HCC) is one of the most common cancers worldwide and the third most common cause of cancer death. It accounts for 85-90% of liver cancers and develops in the background of chronic liver inflammation caused by viral infections by hepatitis B (HBV) and hepatitis C virus (HCV) infections, intoxications (e.g. aflatoxin B1), alcohol abuse and non-alcoholic steatohepatitis (NASH) (Yang & Roberts, 2010; Blonski, Kotlyar & Forde, 2010; Oyagbemi, Azeez & Saba, 2010). Other factors increasing the risk of developing HCC are iron overload syndrome, tobacco use (Blonski, Kotlyar & Forde, 2010) and genetic conditions like hemochromatosis and α1-antitrypsin deficiency (Berasain, Castillo, Perugorria, Latasa, Prieto, & Avila, 2009). All these conditions may result in liver fibrosis and cirrhosis, which are detectable in 70-90% of all HCC cases (El-Serag & Rudolph, 2007).

The incidence in HCC has been increasing over the last decades. When in 2002 626,000 incident cases emerged and 598,000 patients died of HCC worldwide, these numbers increased to 748,000 new cancer patients and 696,000 deaths in 2008. As most cases of liver cancer are detected at very late stages, the numbers of new cases and deaths, unfortunately, are of similar height (Yang & Roberts, 2010). Nowadays, HCC has become the fastest growing cause of cancer death among male US adults (El-Serag & Rudolph, 2007) with a 5-year survival rate below 9% (Berasain, Castillo, Perugorria, Latasa, Prieto, & Avila, 2009)

80% of HCC cases occur in developing countries in sub-Saharan Africa and Eastern Asia mostly because of intoxications and viral infections. But since 1978, HCC incidence has been decreasing in these areas, but has been increasing in developed countries. There is also a shift to younger ages (around 45-60 years) in age distributions of todays HCC patients noticed, when compard to the late 1990s (around 65 years) (El-Serag & Rudolph, 2007). Among the factors causing the increase and age shift in developed countries - and which are thought to become even more prominent in the near future - are the metabolic syndrome, diabetes mellitus and NASH (Yang & Roberts, 2010).

Hepatocarcinogenesis

Hanahan and Weinberg proposed six changes in normal cells in their 2000 review 'The Hallmarks of Cancer' (Hanahan & Weinberg, 2000), which are necessary for the development of malignant cancer (see Figure 1) and added two more so-called 'Emerging Hallmarks' and two 'Enabling Characteristics' (see Figure 2) to their 2011 published review 'The Hallmarks of Cancer: The next Generation' (Hanahan & Weinberg, 2011). According to this widely accepted hypothesis, a cell must 1) gain self-sufficiency in growth signals, 2) gain insensitivity to anti-growth signals, 3) gain a limitless replicative potential, 4) evade apoptosis, 5) sustain angiogenesis and 6) gain the ability to invade the surrounding tissue. Two abilities that have been proposed and have now been added to the former 6 hallmarks are 7) the ability to deregulate and reprogram the cellular metabolism to enable further cell growth and proliferation, and 8) the capability to evade the immune system. Especially the latter is a quite interesting characteristic as many tumors attract immune cells in order to make them

release chemicals (e.g. reactive oxygen species), which are mutagenic and could lead to genetic changes in tumor cells, or growth factors to sustain proliferation, survival factors that help circumvent apoptosis, proangiogenic factors or matrix-modifying enzymes for the invasion of surrounding tissue and metastasis (Hanahan & Weinberg, 2011).
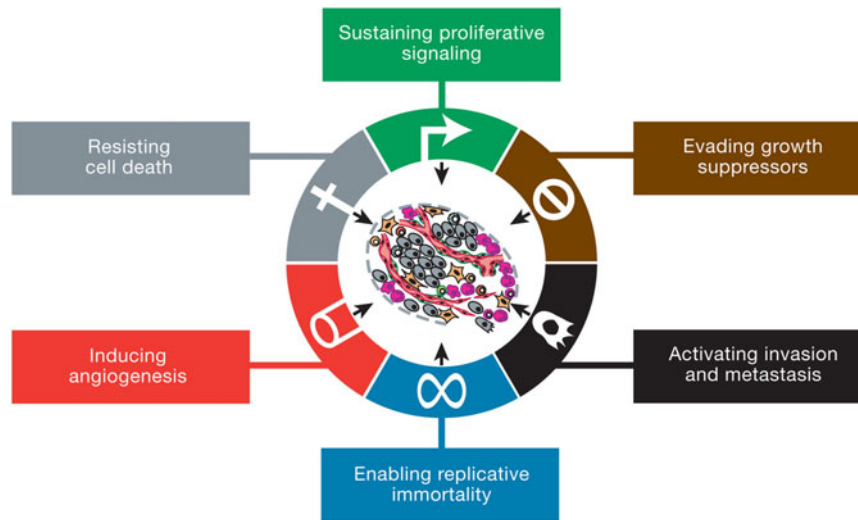
Figure 1: The Hallmarks of cancer. Taken from: Hanahan & Weinberg, Hallmarks of Cancer: The next Generation, 2011.

The two 'enabling characteristics' that help cells acquire functions for the transformation into tumor cells are 'genome instability and mutation' and 'tumor-promoting inflammation'. 'Genome instability and mutation' is generated through defects in mechanisms responsible for either detecting DNA damage or repairing DNA damage or preventing mutagenic substances from causing damage in the cell. All these changed mechanisms result in a certain instability of the genome enabling an evolving tumor cell to accumulate favorable mutations and at the same point maintaining a minimum stability for further proliferation (Hanahan & Weinberg, 2011).

'Tumor-promoting Inflammation' is a second important characteristic enabling the generation and promotion of preneoplastic lesions by resulting in release of the already mentioned growth factors, survival factors, proangiogenic factors and matrix-modifying enzymes as well as reactive oxygen species. Almost every neoplastic lesion is believed to contain immune cells, mostly of the innate immune system, and this accumulation of immune cells seems to be important for the very first stages of preneoplastic progression into neoplastic lesions leading to the development of cancer (Hanahan & Weinberg, 2011).

Introduction
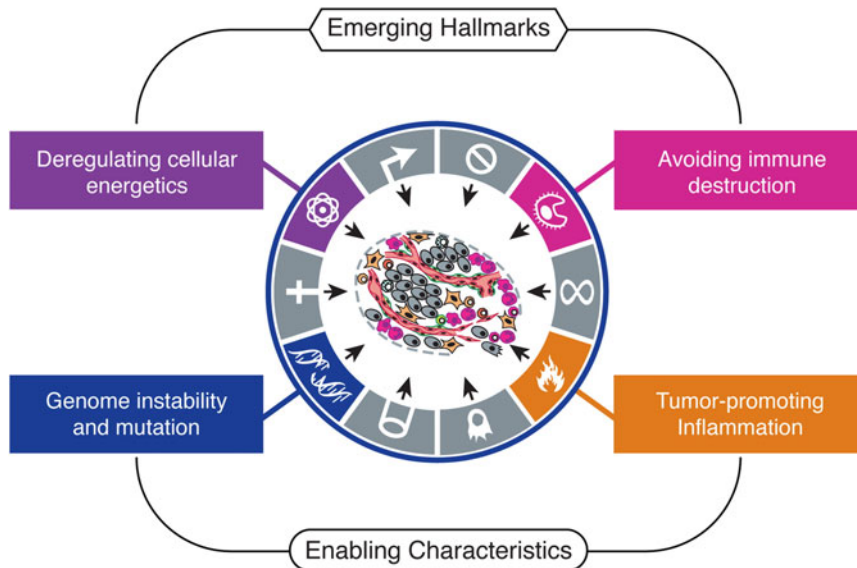
Figure 2: Emerging hallmarks and enabling characteristics. Taken from: Hanahan & Weinberg, Hallmarks of Cancer: The next Generation, 2011.

HCC development is almost undetectable in patients suffering from liver diseases without liver cirrhosis, but increases dramatically when a cirrhotic liver develops. Therefore cirrhosis seems to be a prerequisite for liver tumor formation (El-Serag & Rudolph, 2007; see also Figure 3).

NASH is found to develop into a cirrhotic stage in 10-29% of patients within 10 years and is distinguished from a simple fatty liver (hepatosteatosis) by inflammation caused by infiltration of immune cells, damage and death of hepatocytes and sometimes even fibrosis (Cohen, Horton & Hobbs, 2011).
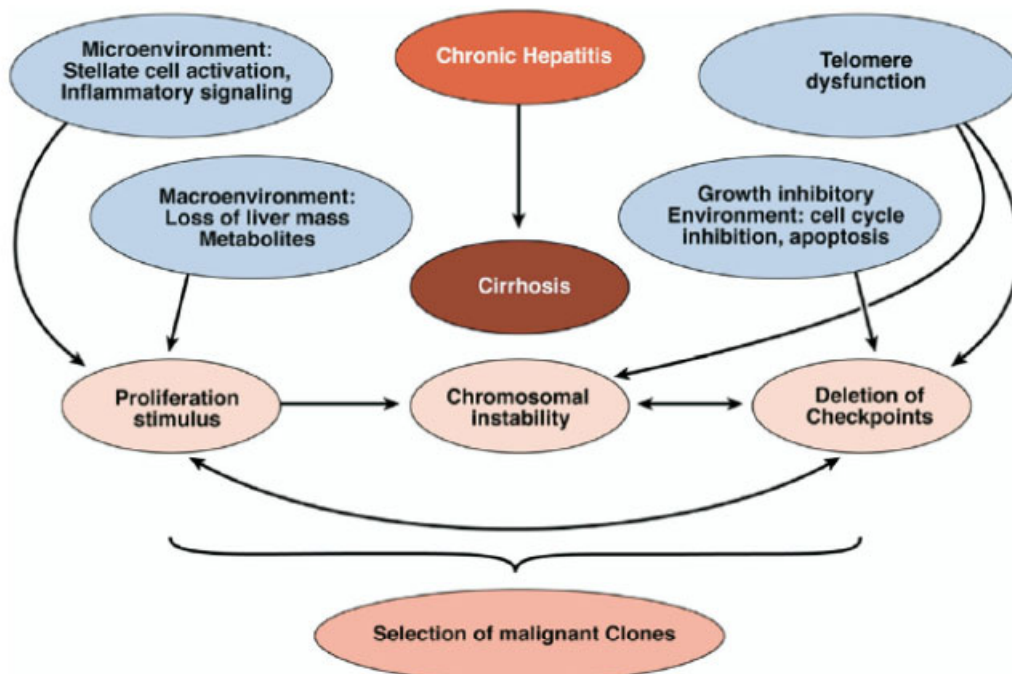
Figure 3: Mechanisms inducting liver cancer at the cirrhotic stage. Taken from El-Serag & Rudolph, 2007.

Hence, inflammation in the liver seems to play a mature part in the development and progression of cirrhosis and furthermore, liver cancer. This could be demonstrated by Park and colleagues (Park et al., 2010) who showed a tumor promoting effect of low-grade inflammation caused by genetic and

dietary obesity in a mouse model of liver cancer. These mice did not develop liver cancer when they were kept on a normal diet and were administered a carcinogenic chemical, but did so when they were genetically obese or kept on a high fat diet. They also showed that the pro-inflammatory cytokines IL-6 and TNFα where elevated in this low-grad inflammatory stage and that these cytokines are needed for propagation of steatohepatitis and tumor-promotion. Therefore obesity seems to be a bona fide tumor promotor as soon as carcinogenesis is initiated, most probably due to its ability to induce inflammation.

Obesity

Overweight is defined by the World Health Organization (WHO) by a body-mass-index (BMI) of more than $25kg/m^2$ and less than $30kg/m^2$, which is also referred to as 'grade-1-overweight'. Obesity is defined by a BMI of more than $30kg/m^2$.

Excess body weight is associated with an increase in total cancer risk, with the highest increase being found in HCC. This was shown in several studies, for example in a 2007 published meta-analysis of 11 studies clarifying the risk of developing HCC. Both, overweight and obese patients were examined and a 17% increase in risk of developing HCC in overweight patients, and an 89% increase in developing HCC in obese patients was found (Blonski, Kotlyar, & Forde, 2010). Although there are several other studies proposing (similar or) even higher risk factors for the development of HCC in overweight, obese or diabetic patients, all studies did find a positive correlation of cancer incidence with increasing excess body weight.

Furthermore, excess body weight was shown to result in a 1.52-fold and 1.62-fold increase in total cancer-related death in men and women, respectively. The relative risk of men with a BMI higher than $35kg/m^2$ for death from liver cancer was even 4.52-fold increased when compared to men with normal weight (Calle, Rodriguez, Walker-Thurmond & Thun, 2003).

Obesity is often accompanied by high blood pressure, peripheral insulin resistance and type-2-diabetes (T2D). Especially peripheral insulin resistance in muscle, liver and adipose tissue leads to decreased glucose uptake in these tissues (resulting in hyperglycemia), uninhibited glycogenolysis in the liver (but interestingly with retained lipogenesis) (Cohen, Horton, & Hobbs, 2011) and uninhibited lipolysis in adipose tissue. Usually, binding of insulin to the insulin receptor results in PI3K activation, which further results (via PKB/Akt and PKC-λ/ζ) in GLUT4 translocation to the plasma membrane and increases glucose transport into the cell. In adipocytes, insulin usually also inhibits lipolysis and therefore release of free fatty acids (FFA) (via hormone-sensitive lipase and adipose triglyceride lipase) into the plasma and inhibits glycogenolysis in the liver (Schenk, Saberi & Olefsky, 2008). But the exact interplay is not fully resolved yet, as there are findings in mice with reduced synthesis, mobilization, or β-oxidation of fatty acids, which show hepatic steatosis without insulin resistance. Findings in human individuals suffering from genetic defects in APOB or ATGL show similar effects, namely increased hepatic TG contents or even steatosis without insulin insensitivity (Cohen, Horton, & Hobbs, 2011).

Adipose tissue in obese individuals contains very often a high fraction of bone marrow-derived macrophages and the amount increases with the degree of obesity. These macrophages express

TNFα and IL-6 and IκB and contribute to insulin resistance, glucose intolerance and hyperinsulinemia (Schenk, Saberi, & Olefsky, 2008).

As two-thirds of US adults are already overweight and one-third are obese, and obesity is a major risk factor for NAFLD and NASH, other liver diseases and liver cancer, these metabolic disorders might become major health problems in the future (Yang & Roberts, 2010; Schenk, Saberi & Olefsky, 2008).

Non-alcoholic fatty liver disease (NAFLD)

Non-alcoholic fatty liver disease (NAFLD) comprises a set of liver disorders ranging from simple hepatic steatosis to non-alcoholic steatohepatitis (NASH, which includes hepatocyte death, fibrosis and cirrhosis) (Masterton, Plevris & Hayes, 2010). It is the most common liver disease in the US, affecting about 24% of the US population, and about 10-35% of adults worldwide (Park et al., 2010; Masterton, Plevris & Hayes, 2010). The prevalence of NAFLD increases with increasing degree of obesity, ranging from 9% in individuals with a BMI below $25kg/m^2$ to 51% in individuals with a BMI higher than $35kg/m^2$ (Cohen, Horton, & Hobbs, 2011).

NAFLD is considered to develop because of two 'hits', the first one being steatosis, which is storage of fat in the liver, followed by oxidative stress leading to inflammation (Masterton, Plevris & Hayes, 2010). Steatosis develops when more food is consumed than needed for energy production and the storage capacity of adipocytes is reaching its maximum, resulting in the alternative deposition of fat in the liver. This progression is a severe problem as the uptake of free fatty acids (FFAs) into the liver is not thought to be regulated (Savage & Semple, 2010). This assumption is supported by the finding, that in genetic diseases, like glycogen storage disease type 1a and citrin deficiency, which result in an increase in the production of fatty acids, the increased flux of FFAs to the liver is sufficient to cause steatosis (even in the absence of insulin resistance) (Cohen, Horton, & Hobbs, 2011).

In the human body excess nutrients are stored mainly as triglycerides (TG) for future breakdown and energy production (catabolism), as they provide a higher caloric density (9kcal/g) compared to carbohydrates (4.5kcal/g) and proteins (4kcal/g). As increased liver TG levels are the hallmark of NAFLD (Greenfield, Cheung, & Sanyal, 2008), steatosis therefore is defined either by hepatic TG levels being higher than 55mg/g of liver or TG droplets within hepatocytes exceeding 5% of the cytoplasm (Cohen, Horton, & Hobbs, 2011).

Unfortunately, the exact pathogenesis in cellular and molecular terms of steatosis and the possible progression to NASH and cirrhosis have not been entirely elucidated yet (Masterton, Plevris & Hayes, 2010), as has the contribution of insulin resistance in the development of NAFLD. Insulin resistance might be a cause or a consiquence of NAFLD (Cohen, Horton & Hobbs, 2011).

NAFLD together with hypertension, insulin resistance, obesity and dyslipidaemia are summarized as the 'metabolic syndrome' or 'syndrome X'. Several studies found a positive correlation in the number of features defining the metabolic syndrome with the chance of developing NASH (Greenfield, Cheung, & Sanyal, 2008).

Non-alcoholic steatohepatitis (NASH)

In some cases NAFLD proceeds to non-alcoholic steatohepatitis (NASH), which is characterized by infiltration of the liver by immune cells, death of hepatocytes, production of collagen by stellate cells (fibrosis) and sometimes also cirrhosis. Exact numbers are missing, but about one-third of NAFLD patients who undergo liver biopsy show indications of NASH (Cohen, Horton, & Hobbs, 2011). Patients suffering from hepatocellular carcinoma (HCC) are in 70-90% of all cases also diagnosed with cirrhosis (El-Serag & Rudolph, 2007) and sometimes also with just some features of NASH and are therefore categorized as 'cryptogenic cirrhosis'. This leads to the assumption that HCC might develop at different stages of NASH (Greenfield, Cheung, & Sanyal, 2008), but there definitely is a lot of data confirming the association between chronic inflammation and cancer development (Berasain, Castillo, Perugorria, Latasa, Prieto, & Avila, 2009).

NASH, like NAFLD, might be subclinical for years and might just show elevated liver transaminases, like aspartate aminotransferase (AST), and alanine aminotransferase (ALT). Fatty liver might be detected on ultrasound and tomography, whereas liver biopsy remains the only diagnostic method to estimate the progression of NAFLD/NASH as it is still impossible to distinguish NAFLD from NASH by imaging technologies (Greenfield, Cheung, & Sanyal, 2008).

Adipose tissue might also play a role in the pathogenesis of NASH due to its ability to secrete a variety of factors (e.g.: CCL2, IL-1b, MIF, adiponectin, leptin; Schenk, Saberi, & Olefsky, 2008; Toffanin, Friedman, & Llovet, 2010), among them tumor-necrosis-factor-α (TNFα) and interleukin-6 (IL-6) (Schenk, Saberi, & Olefsky, 2008). Both factors are elevated in livers and blood of NASH patients. The major source of at least TNFα was found to be adipose tissue associated macrophages, whose number positively correlates with BMI, but the exact mechanisms of activation and infiltration of macrophages are not fully clarified yet. All the cytokines produced by adipocytes and macrophages, such as TNFα, IL-6 or leptin, result in an increase in activity of hormone sensitive lipase which leads to an elevation of free fatty acid (FFA) levels in the circulation. This elevation of FFAs and their unregulated uptake into the liver (Savage & Semple, 2010) is believed to be the cause for lipotoxicity resulting in hepatocyte injury (Greenfield, Cheung & Sanyal, 2008).

Leptin seems to act as a mediator between adipose tissue and the innate immune system, as leptin levels are elevated in obesity and the metabolic syndrome. Leptin promotes proliferation of mononuclear cells and increases the activity of diacylglycerol acyl transferase (DGAT), which facilitates the binding of a single FFA to a molecule of diacylglycerol to form a molecule of triacylglycerol (or triglyceride, TG) and therefore removes the otherwise toxic FFAs from the circulation. Furthermore leptin promotes the production of collagen in activated stellate cells, which is a prerequisite for fibrosis. The production of collagen is also stimulated by insulin (Greenfield, Cheung & Sanyal, 2008).

Besides inflammation, ER stress resulting in activation of the unfolded protein response (UPR) seems to play a role in NASH development. Both, inflammation and UPR activation result in NF-κB and JNK activation (Cohen, Horton, & Hobbs, 2011).

In the following, free fatty acids and inflammation are discussed in more detail.

Introduction

Free fatty acids (FFAs)

Triglycerides (TG) are composed of a molecule of glycerol and three molecules of fatty acids, each of which is coupled to the glycerol via an ester bond. Glycerol is an intermediate of glycolysis and gluconeogenesis, whereas there are three different sources of fatty acids for triglyceride production in the liver: 1) diet, 2) lipolysis by adipocytes and 3) de-novo-lipogenesis (DNL). Fatty acids from diet result from lipolysis via lipases (e.g. lipoprotein lipase) and fatty acids from DNL mainly are a result of carbohydrate derived acetyl-coenzyme A (acetyl-CoA) (Cohen, Horton, & Hobbs, 2011, see Figure 4). About 60% of FFAs in liver TGs derive from adipose tissue, 15% of FFAs in liver TGs derive from diet and 25% derive from de-novo lipogenesis (DNL) (Savage & Semple, 2010), the latter (DNL) is increased in patients with NAFLD. This is most probably because of SREBP1c-mediated induction of DNL by insulin (Greenfield, Cheung, & Sanyal, 2008). Activation of SREBP1 further stimulates glycolysis. n3-PUFA reduce the amount of SREBP1 resulting in downregulation of stimulatory effects caused by insulin and reduction of DNL (Masterton, Plevris, & Hayes, 2010). Another cause of increased levels of fatty acids resulting in hepatic steatosis is decreased TG removal via VLDL particles (He, Lee, Febbraio, & Xie, 2011). During fasting, exercise, stress or inflammation lipolysis in adipose tissue is activated resulting in an increase of FFA levels. These levels are reported to range from 90-1200µM, with basal levels around 300-500µM (Lee, Zhao, & Hwang, 2009).
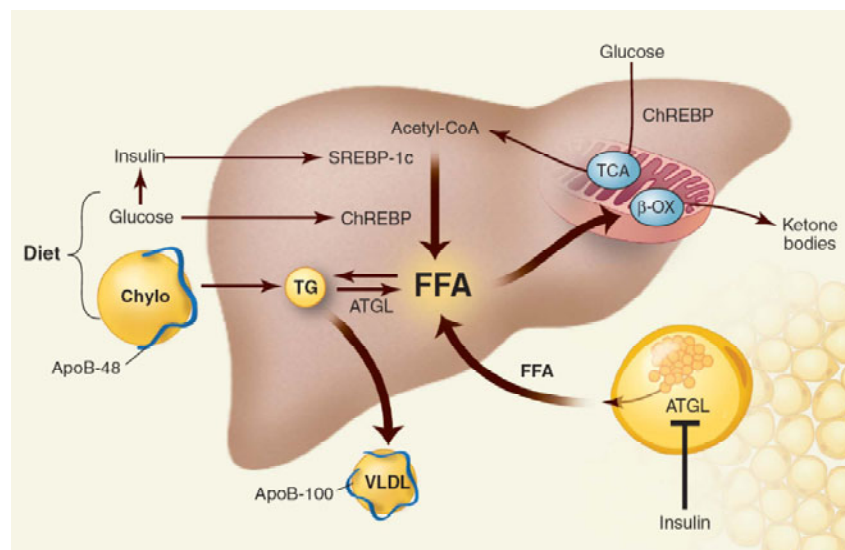
Figure 4: Metabolism of triglycerides in the liver. Taken from: Cohen, Horton & Hobbs, 2011.

Free fatty acids (FFAs) are either released from the cell membrane by phospholipases or taken up by the cell from the unbound pool of fatty acids (in contrast to the albumin-bound fatty acids) in the blood. The unbound fatty acids are in equilibrium with the albumin-bound forms. The concentration of these unbound fatty acids is believed to be at least 3 orders of magnitude lower than the total concentration of the fatty acids, placing it in physiological concentrations of ≤50nM. Furthermore, the physiological, molar ratio of fatty acids to BSA (v) was calculated to be ~0.1:1 – 3:1. Uptake of FFAs was reported to be a linear function of total FFA concentration or a saturable function of the unbound FFA concentration in primary hepatocytes. More than 90% of FFA uptake in hepatocytes is now believed to occur via a saturable pathway at FFA:BSA ratios of ~3:1. This leads to the conclusion that FFA uptake (at least in hepatocytes) is facilitated and occurs via transporters, in contrast to unfacilitated uptake via passive diffusion through the lipid bilayer. Experiments further showed that fatty acid uptake is temperature sensitive (Berk & Stump, 1999).

Richieri and colleges (Richieri, Anel, & Kleinfeld, 1993) reported that the concentration of unbound FFA at a given chain length and FFA:BSA ration depend on degree of 'unsaturation' due to increased water-solubility with increasing number of double bonds. Furthermore, the presence of albumin prevents the formation of stable micelles in aqueous solutions, thereby strengthening the assumption of FFA uptake from the unbound pool of FFAs.

Effects of impaired metabolism of FFAs

Fatty acids are either stored as TGs in adipose tissue, muscle and liver or they are used for energy production by oxidizing them to CO_2 via a process termed 'β-oxidation' in the mitochondria. The rate limiting step in this process is the binding of fatty acids to L-carnitine, with is used as a transporter. The ligation of carnitine and fatty acids is catalyzed by the enzyme carnitine palmitoyltransferase-I (CPT-I) (Schenk, Saberi, & Olefsky, 2008).

When storage or oxidation of FFAs are already maximized, fatty acid intermediates like ceramide or diacylglycerol accumulate and these intermediates are hypothesized to inhibit insulin signaling (either via activation of the mTOR/p70S6K, JNK, IKK and PKC pathways or via inhibition of AKT/PKB signaling by ceramide). Fatty acids have been shown to induce insulin resistance in part through inhibitory IRS-1 phosphorylation resulting in inhibition of the association of IRS-1 with the insulin receptor (Schenk, Saberi, & Olefsky, 2008). In muscle, insulin signaling can also be inhibited by FFAs resulting in decreased glucose uptake and increased insulin secretion by the pancreas (Greenfield, Cheung, & Sanyal, 2008). Furthermore, FFAs are precursors of regulators of immune reactions.

Types and effects of free fatty acids

Omega-3 (n3 or Ω3), n6 and n9 (oleic acid derived) polyunsaturated fatty acids (PUFAs) have immunomodulatory effects (Greenfield, Cheung, & Sanyal, 2008).

Omega-3 (n3 or Ω3) fatty acids derive from α-linolenic acid (ALA) and have to be taken up by diet as they cannot be synthesized in the human body. α-Linolenic acid is metabolized in the liver to eicosapentaenoic acid (EPA) and docosahexaenoic acid (DHA). These two fatty acids are precursors for eicosanoids, lipid mediators of inflammatory responses (Wall, Ross, Fitzgerald, & Stanton, 2010; see Figure 5).

EPA has been reported to reduce inflammation by inhibiting the production of TNF and IL-1 and treatment of various cancer cell lines with EPA showed less proliferation and invasiveness. Omega-3 fatty acids have further been shown to reduce primary tumor growth and metastasis in mice and humans (Boutros, Somasundar, Razzak, Helton, & Espat, 2010), as well as lymphocyte proliferation and neutrophil chemotaxis (Greenfield, Cheung, & Sanyal, 2008).

Although the exact molecular mechanisms of the anti-tumorigenic properties of n3-PUFA are not entirely elucidated yet, these kinds of fatty acids are thought to replace arachidonic acid in phospholipids in the cell membrane thereby reducing or even inhibiting COX-2 mediated production of pro-inflammatory eicosanoids and reducing production of VEGFs. This is especially true in the membrane of erythrocytes, neutrophils, monocytes and liver cells (Wall, Ross, Fitzgerald, & Stanton,

2010). Other hypotheses suggest n3-PUFA-mediated alterations in AP1 and NF-κB signaling leading to reduced production of pro-inflammatory cytokines like TNFα (Boutros, Somasundar, Razzak, Helton, & Espat, 2010).

Especially the conversion of the n3-PUFA EPA by COX and LOX enzymes results in less inflammatory or anti-inflammatory acting eicosanoids like the 3-series prostaglandins or the 5-series leukotrienes (see Figure 5). EPA has further been shown to decrease the degradation of IκB, the inhibitor of the transcription factor NF-κB in human monocytes. NF-κB regulates the transcription of cytokines (IL-1, IL-2, IL-6, IL-12 and TNFα), chemokines (IL-8, MCP-1) and inflammation-associated enzymes like iNOS or COX-2. DHA can be converted into resolvins by LOX (most probably by 5-LOX and 15-LOX; Gleissman, Johnsen, & Kogner, 2010), which are local-acting mediators resulting in reduction of neutrophil infiltration and lowering of overall inflammatory responses (Wall, Ross, Fitzgerald, & Stanton, 2010). Protectins and resolvins are also needed for the resolution of an inflammatory response (Gleissman, Johnsen, & Kogner, 2010).

A study examining the relationship between plasma free fatty acid levels and levels of inflammatory markers in 1,123 persons found a positive correlation between the total n3-PUFA concentration with lower IL-6, TNFα and CRP levels and higher levels of anti-inflammatory markers (Wall, Ross, Fitzgerald, & Stanton, 2010).

Omega-6 (n6 or Ω6) fatty acids derive from linoleic acid (LH), which is further converted into arachidonic acid in the liver. This fatty acid is a precursor for pro-inflammatory eicosanoids like prostaglandin E_2 (PGE_2) and leukotriene B_4 (LTB_4). PGE_2 can induce the production of IL-6 in macrophages, whereas LTB_4 induces the production of TNFα, IL-1β and IL-6 by macrophages and acts as a chemoattractant for leukocytes and might also activate neutrophils (Wall, Ross, Fitzgerald, & Stanton, 2010).

As modern western diets contain high contents of n6-PUFA and low contents of n3-PUFA, enzymes which are needed for the conversion of both types of fatty acids primarily convert n6-PUFA rather than n3-PUFA due to their higher availability. At a ratio of n3-PUFAs to n6-PUFAs of 1:4 these enyzmes would convert n3 rather than n6 fatty acids, but due to the increased consumption of vegetable oils the ratio is 1:16 (n3:n6) providing higher amounts of n6 fatty acids (Wall, Ross, Fitzgerald, & Stanton, 2010).

As unsaturated fatty acids contain double bonds they may react with oxygen and form peroxidized fatty acids as it is the case when fat containing food is heated for a long time at temperatures above 100°C. Furthermore, these oxidized PUFAs can cause lipid peroxidation in the membrane of cells (Sagmeister, 2009) and this might result in a change of eicosanoid production (Greenfield, Cheung, & Sanyal, 2008).
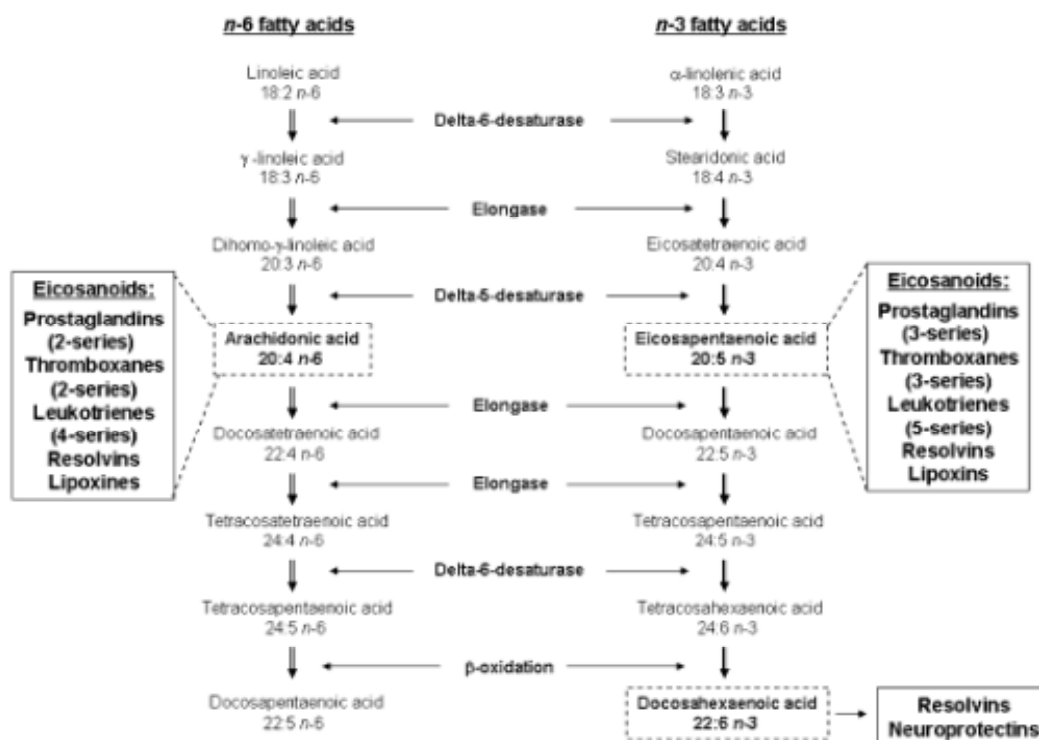
Figure 5: conversion of n6 and n3-PUFA into physiologically active molecules. Taken from: Wall, Ross, Fitzgerald, & Stanton, 2010.

For conversion or β-oxidation, fatty acids have to be taken up into the cell which occurs either by uptake via CD36 (or fatty acid translocase; FAT), liver fatty acids-binding protein (L-FABP) or fatty acid transport proteins (FATPs) (He, Lee, Febbraio, & Xie, 2011). Furthermore, FFAs may induce signaling via binding to specific fatty acid receptors.

Free fatty acid receptors

CD36

CD36 (or fatty acid translocase; FAT; see Figure 6) is a ~88KDa glycoprotein which is expressed in a variety of cell types including endothelial cells, macrophages, dendritic cells, hepatocytes, adipocytes, cardiac and skeletal myocytes and epithelial cells. Besides its function in angiogenesis and as a pattern recognition receptor (PRR), CD36 is a translocase for long-chain fatty acids in adipocytes, myocytes, enterocytes, hepatocytes, Kupffer cells and hepatic stellate cells (He, Lee, Febbraio, & Xie, 2011; see also) and might interact with other membrane receptors such as TLR, integrins and tetraspanins. Its expression is controlled by PPARγ, pregnane X receptor (PXR; liver-specific) and liver X receptor (LXR; liver-specific) and is upregulated upon binding of a ligand (Silverstein, Li, Park, & Rahaman, 2010). Its expression is also increased significantly in hepatocytes by a high-fat diet, therefore contributing in the development of obesity and correlating positively with liver fat content in NAFLD patients. This is further supported by the 2.6-fold increase in CD36 protein levels and the 1.7-fold induction of hepatic TG storage in HFD-fed mice (He, Lee, Febbraio, & Xie, 2011).

Inhibition of CD36-facilitated uptake of lipids prevented lipotoxicity (Silverstein & Febbraio, 2009), further supporting its role in hepatic lipid uptake. In macrophages, CD36 is the major receptor responsible for the uptake of oxidized low-density lipoprotein (LDL) suggesting a role in the

progression of macrophages into lipid-laden foam cells in the development of atherosclerosis (He, Lee, Febbraio, & Xie, 2011). The binding of oxidized LDL by macrophages via CD36 leads to activation of the transcription factor NF-κB, partly through interaction with a TLR4/6 heterodimer (Stewart, et al., 2010). Activation of CD36 on endothelial cells results in activation of fyn-kinase and p38-MAPK (Silverstein, Li, Park, & Rahaman, 2010).
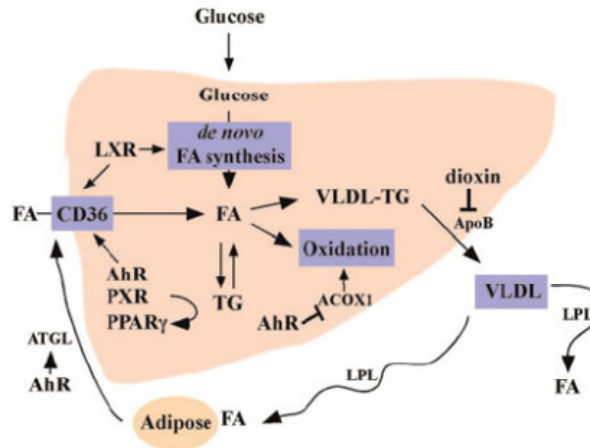
Figure 6: Function and regulation of CD36 in hepatic lipid metabolism. Taken from: He, Lee, Febbraio, & Xie, 2011.

Toll-like receptors

Toll-like receptors (TLRs) are germ-line encoded pattern recognition receptors (PRRs) involved in the detection of conserved pathogen associated molecular patterns (PAMPs) and are mainly expressed in macrophages and adipocytes. They are type I transmembrane receptors with an extracellular leucine-rich repeat and a cytoplasmic Toll/interleukin-1 receptor homology domain. So far 13 different TLRs have been identified in humans (Lee, Zhao, & Hwang, 2009). Their signaling is propagated through myeloid differentiation primary response gene 88 (MyD88), TRIF and TRAM which leads to activation of NF-κB. Ligand-mediated activation of CD36 by oxidized LDL (oxLDL) results in interaction of Lyn-kinase with CD36 and further in heterodimer formation of TLR4/6, which subsequently associate with CD36. This was shown by co-precipitation experiments performed in THP1 monocytes which were activated by oxLDL. Ligand internalization resulted in signaling from the CD36/TLR4/TLR6 complex leading to transcription of IL-1β, production of ROS via MyD88 and activation of NF-κB (Stewart, et al., 2010).

TLRs were further shown to be able to bind saturated fatty acids including lauric and palmitic acid, and unsaturated fatty acids. The expression of TLR4 can be increased by high glucose and by oxLDL and the activation of TLR4 by saturated fatty acids (in macrophages and endothelial cells) leads to activation of NF-κB and the expression of IL-1, IL-6 and IL-8. Activation of TLRs occurs via formation of dimers, homodimers in the case of TLR3 and TLR4, and heterodimers in the case of TLR4/6, TLR1/2 and TLR2/6. The latter might also form a complex with CD36. MyD88 dependent signaling (downstream of TLR) includes activation of p38MAPK and JNK and furthermore NF-κB and AP1, resulting in the expression of pro-inflammatory cytokines. MyD88-independent signaling leads to delayed activation of NF-κB. Whereas TLR2 and TLR4 can be activated by saturated fatty acids, like palmitic acid, the binding of n3-PUFAs, inhibits this SFA-induced activation. The n3-PUFA EPA was shown to inhibit SFA-induced expression of COX-2 in murine macrophages and TNFα in human THP1 cells. Most probably the inhibitory effect of n3-PUFA on SFA-induced activation of TLRs, especially

TLR4, is by inhibiting TLR-dimerization and translocation into lipid rafts along with attenuation of adaptor (MyD88 and TRIF) recruitment (Lee, Zhao, & Hwang, 2009).

TLRs are also expressed in liver cells; for example, TLR4 has been detected on all types of liver cells and is involved not only in the production of pro- and anti-inflammatory cytokines but also in the generation of ROS. TLR2 expression has been reported in hepatocytes, Kupffer cells, stellate cells and endothelial cells, and its activation leads to the production of pro-inflammatory cytokines (Gao, Jeong, & Tian, 2008).

G-protein coupled receptors

G-protein-coupled receptors (GPR) are seven-transmembrane-receptors which activate G-proteins. Activation results in downstream signaling via cAMP, phospholipase-C and mitogen-activated protein kinases (MAPKs). GPRs capable of binding FFA are distinguished by the length of FFA they bind; short-chain FFAs can activate GPR41 and GPR43; medium-chain FFAs activate GPR84 and long-chain FFAs activate GPR40 and GPR120. The activation of the latter was shown by the increase in [Ca^{2+}] and ERK activation upon stimulation of GPR120 by FFAs. This receptor is expressed in adipocytes, pro-inflammatory macrophages and negligibly in muscle and hepatocytes.

Stimulation of GPR120 with DHA or a synthetic agonist (GW9508) resulted in anti-inflammatory effects in macrophages shown by the inhibition of TAK1 phosphorylation and activation resulting in attenuation of both TLR (TLR2/3/4) and TNFα inflammatory signaling pathways. This most probably occurs via association of β-arrestin2 with the cytoplasmic domain of GPRs followed by receptor internalization. Upon internalization of the complex, β-arrestin2 associates with TAB1 thereby blocking TAB1-TAK1 association and inhibiting TAK1-mediated downstream signaling via IKKβ/NF-κB and JNK/AP1 (see Figure 7).
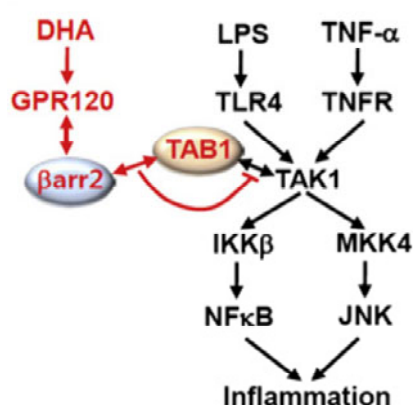
Figure 7: possible mechanism of n3-PUFA-mediated attenuation of TLR and TNFR signaling via GPR120. Taken from: Oh, et al., 2010.

GPR120 was further shown to play a role in n3-PUFA mediated insulin sensing as demonstrated by comparing obese WT with GPR120-KO mice. Both groups of mice became equally obese and insulin resistant, but n3-PUFA supplement improved insulin sensitivity in WT but not in GPR120-KO mice. Furthermore, HFD led to an increase in liver TGs, DAGs, SFAs, monounsaturated FAs and n6-PUFA in both groups of mice. n3-PUFA supplement reduced the increase of these lipids in WT but not in GPR120-KO mice. This points to an important role of GPR120 in n3-PUFA-mediated reversal of steatosis as this was also observed in several studies of obese patients.

Introduction

In 3T3-L1 adipocytes, DHA stimulation of GPR120 led to an increased GLUT4 translocation to the cell surface and an increased glucose uptake. In the HFD or obese mouse model, GPR120 expression was induced in adipose-tissue-associated-macrophages as well as in Kupffer cells (Oh, et al., 2010).

Peroxisome proliferator activated receptors

Peroxisome proliferator activated receptors (PPARs) are nuclear receptors, which are capable of binding fatty acids, especially n3-PUFA, and eicosanoids and act as transcription factors in the cell. PPAR-mediated signaling is important in many cellular processes including differentiation, inflammation, cancer progression, insulin sensing and several metabolic disorders (Wall, Ross, Fitzgerald, & Stanton, 2010).

Especially PPARα was shown to be activated by n3-PUFA in the liver which resulted in upregulation of genes involved in fatty acid and lipid metabolism ('β-oxidation') and suppression of TNFα and IL-6 production. A further study demonstrated the prevention of steatohepatitis in mice infused with an PPARα agonist (Masterton, Plevris, & Hayes, 2010).

Nucleotide-binding oligomerization domain proteins

Nucleotide-binding oligomerization domain proteins (NODS) are cytoplasmic pattern recognition receptors that can be activated by saturated fatty acids (like lauric acid) resulting in the activation of the transcription factor NF-κB. Activation of NODs is thought to occur via homodimer formation and further recruitment of RICK/RIP2 which leads to the activation of NF-κB and subsequent inflammatory gene expression and activation of p38MAPK and JNK. As it is the case with TLRs, the SFA-induced activation of NF-κB and expression of IL-8 could be inhibited by n3-PUFA via binding to NODs (Lee, Zhao, & Hwang, 2009).

TR4/NR2C2

TR4/NR2C2 is a nuclear receptor which is expressed in testis, brain, kidney, liver and adipose tissue. FFAs and eicosanoids might bind TR4, thereby enhancing its activity as a transcription factor. TR4 plays a role in the regulation of lipid metabolism and gluconeogenesis. Male TR4-KO mice were shown to be resistant against HFD-induced obesity, hepatic steatosis, white adipose tissue inflammation, insulin resistance and glucose intolerance. Their livers showed reduced lipid accumulation compared to controls. The expression of several genes in the livers of TR4-KO mice was reduced including CD36, Cidea and Cidec (cell death–inducing DFFA-like effector a and c, respectively), which are involved in triglyceride accumulation in lipid droplets and regulation of lipolysis, Mogat1 (monoacylglycerol O-acyltransferase 1), which is important in TG synthesis and PPARγ. In addition, TR4 also seems to regulate CD36 expression in macrophages (Kang, et al., 2011).

Inflammation and inflammation associated factors

As already mentioned, inflammation seems to play an important role in the development and promotion of preneoplastic into neoplastic lesions and was therefore considered an 'enabling characteristic' for the development of cancer by Hanahan and Weinberg (Hanahan & Weinberg, 2011). During inflammation, several factors are secreted for sustaining proliferation (growth factors), for circumventing apoptosis (survival factors), for angiogenesis and for the invasion of surrounding tissue and metastasis (matrix-modifying enzymes).

Elevated levels of the pro-inflammatory cytokines TNFα, IL-6 and C-reactive protein (CRP) have been found in diabetic and insulin resistant patients. Furthermore, JNK and IKK were found to be upregulated and activated resulting in the phosphorylation of AP1 (cFos/c-Jun) and NF-κB, both of which activate inflammatory pathways. This activation of pro-inflammatory cytokines, kinases and transcription factors found already at an insulin resistant stage, which is often associated with or leads to NAFLD, might provide an explanation for the inflammation that results in the progression to NASH (Schenk, Saberi, & Olefsky, 2008).

A second possibility for the activation of inflammatory pathways (NF-κB and JNK) is the production of ROS caused by the increased demands on the ER by the accumulation of intracellular lipids which is observed in obesity and NAFLD. Oxidative stress can further induce DNA damage and result in the generation of favorable genetic changes predisposing for the development of cancer (Toffanin, Friedman, & Llovet, 2010).

Park and colleagues (Park, et al., 2010) showed that lipid accumulation furthermore results in a low-grade inflammation leading to an increase in IL-6 and TNFα levels via production by adipocytes and Kupffer cells. Both cytokines are critical for the development of steatohepatitis and the induction of cell proliferation through JAK/STAT and ERK activation leading to HCC development (Toffanin, Friedman, & Llovet, 2010). In addition, the transcription factor STAT3 is not only involved in proliferation, but also in survival, angiogenesis, invasion and tumor promoting inflammation. In epithelial cells active STAT3 leads to the upregulation of chemokines for the attraction of immune and inflammatory cells. These cells further propagate STAT3 activation in epithelial cells through release of IL-6 (via JAKs; Janus kinases) and other cytokines (Li, Grivennikov, & Karin, 2011) as well as growth factors (via EGFR or VEGFR; Berasain, Castillo, Perugorria, Latasa, Prieto, & Avila, 2009).

Especially tumor–associated macrophages (TAMs) might play a major role in this process as they are the most abundant type of immune cells in the tumor microenvironment and they may contribute to tumor growth not only by releasing factors like IL-6 or TNFα but also epidermal growth factor receptor (EGFR) ligands and CXCL12 (Berasain, Castillo, Perugorria, Latasa, Prieto, & Avila, 2009).

Tumor growth is further supposed to be supported by IL-6 via the upregulation of anti-apoptotic factors like Bcl-xL or promitogenic factors like mcl-1, c-Fos, c-Myc and c-Jun. Under normal conditions STAT3 activity is regulated by suppressors of cytokine signaling (SOCS, especially SOCS3), which are activated by STATs, thereby forming a negative feedback loop. Hepatocyte specific deletion of SOCS3 resulted in an increase in the number and size of tumors in DEN-induced HCC in mice. STAT3 activity in tumor cells promotes IL-6, IL-10 and VEGF production. Loss of SOCS3 expression in liver parenchymal cells showed enhanced liver regeneration and neoplastic transformation (Berasain, Castillo, Perugorria, Latasa, Prieto, & Avila, 2009).

Introduction

Furthermore, the NF-κB and STAT3 pathways are cross-linked. NF-κB activation results in expression of IL-6 and COX2, which in turn lead to the activation of STAT3. Genes associated with tumor progression (Bcl-xL, survivin, mcl1, VEGF and MMP9) are regulated by both factors (Berasain, Castillo, Perugorria, Latasa, Prieto, & Avila, 2009).

NF-κB gets activated in inflammatory cells either by activation of TLR and downstream signaling via MyD88 or by the pro-inflammatory cytokines TNFα and IL-1β. The importance of this transcription factor in tumor development was shown by several deletion or inhibition experiments. When IKKβ, the beta-subunit of the IκB kinase, was deleted in myeloid cells, a reduction in the number of tumors was found in a model of colitis-associated cancer. The deletion of IKKβ in Kupffer cells in a model of chemically induced HCC did also result in a reduction in tumor load, and further less production of TNFα, IL-6, HGF and inhibition of hepatocyte proliferation. In a mouse model of inflammation driven HCC, were multi drug resistance protein 2 (Mdr2) was knocked out resulting in the development of HCC at 8-10 months of age, the inhibition of the degradation of IκB (inhibitor of κB signaling) in the liver blocked tumor development (Berasain, Castillo, Perugorria, Latasa, Prieto, & Avila, 2009) most likely due to the TNF dependent activation of NF-κB for HCC development in this model and the possible requirement of NF-κB for the production of chemokines for the recruitment of inflammatory cells thereby maintaining a tumor promoting microenvironment (Grivennikov & Karin, 2011). The tumor promoting effect of NF-κB is most likely a result of its ability to prevent apoptosis and its regulation of genes involved in epithelial-mesenchymal transition (EMT) (Berasain, Castillo, Perugorria, Latasa, Prieto, & Avila, 2009).

In contrast, hepatocyte-specific ablation of NF-κB signaling via deletion of the IKKβ gene resulted in a higher liver tumor incidence in DEN treated animals, most probably through enhanced JNK1 activity (Berasain, Castillo, Perugorria, Latasa, Prieto, & Avila, 2009) and increased DEN induced hepatocyte death resulting in increased compensatory proliferation of premalignant hepatocytes. In contrast to the Mdr2-knock-out model, the DEN induced HCC model is not TNF/TNFR dependent (Grivennikov & Karin, 2011). In the following, inflammation-associated factors important for this work are discussed more precisely.

TNFα

Tumor necrosis factor α (TNFα) is a pro-inflammatory and pleiotropic cytokine produced by different types of cells including macrophages, T-cells and adipocytes (Schenk, Saberi, & Olefsky, 2008; Toffanin, Friedman, & Llovet, 2010; Grivennikov & Karin, 2011). TNFα plays an important role as a tumor promoting agent in a variety of cancers including obesity-induced HCC and is needed for obesity-induced hepatosteatosis and steatohepatitis. Its cancer promoting characteristic is most likely caused by its ability to activate the transcription factors NF-κB and AP1 (cFos/c-Jun), both of which stimulate cell proliferation and survival. TNFα-mediated NF-κB activation further stimulates the production of ROS (Toffanin, Friedman, & Llovet, 2010) and the production of IL-6 (Park, et al., 2010). This was also shown by the inhibition of TNFα which reduced the production of IL-6 (Grivennikov & Karin, 2011).

In hepatocytes, TNFα (together with IL-6, IL-1 and IFN-γ) stimulates the production of high levels of secreted PRRs (Gao, Jeong, & Tian, 2008). Its expression and protein levels were also found to be

elevated in normal liver and HCC of obese mice (Toffanin, Friedman, & Llovet, 2010; Park, et al., 2010) and were increased in obese humans (Grivennikov & Karin, 2011).

Lipid accumulation seems to be dependent on TNFα-mediated signaling, as TNFR1-KO mice showed reduced lipid accumulation and infiltration of macrophages and neutrophils induced by HFD (Toffanin, Friedman, & Llovet, 2010). Knock-out of TNFR1 furthermore resulted in the attenuation of HCC development and neutralization of TNFα using specific antibodies led to apoptosis of transformed hepatocytes, thereby supporting the assumption of its role in initiation and promotion of liver cancer (Berasain, Castillo, Perugorria, Latasa, Prieto, & Avila, 2009).

TNFα is produced as a ~24kDA precursor, which, upon cleavage and shedding from the cell membrane (~17kDa), becomes active. This shedding event is catalyzed mainly by ADAM17/TACE (Becker, Gilles, Sommerhoff, & Zahler, 2002).

COX-2

Cyclooxygenase 2 or prostaglandin synthase 2 (PTGS2) catalyzes the conversion of unsaturated fatty acids into eicosanoids. Arachidonic acid (n6-PUFA) is the preferred substrate resulting in the production of pro-inflammatory eicosanoids (e.g.: 2-series prostaglandins, 4-series leukotrienes), whereas n3-PUFAs might act as competitive inhibitors (Lee, Zhao, & Hwang, 2009) and might also be converted to non- or even anti-inflammatory eicosanoids (3-series prostaglandins, 5-series leukotrienes) (Wall, Ross, Fitzgerald, & Stanton, 2010). Expression of COX2 can be enhanced in a TLR4-dependent manner, resulting in elevated PGE_2 production.

Prostaglandin E_2 (PGE_2) activates the expression of amphiregulin in colon cancer cells through elevation of cAMP levels and protein kinase A (PKA) activation and elevated levels were also found in liver cancer, probably contributing to carcinogenesis. Enhanced COX-2 expression was further observed in chronic liver inflammation, cirrhosis, human and experimental HCC. (Berasain, Castillo, Perugorria, Latasa, Prieto, & Avila, 2009).

iNOS

Inducible nitric oxide synthase (iNOS) is an enzyme expressed in macrophages that catalyzes the reaction of arginine with NADPH and oxygen to yield nitric oxide (NO) which is used in antimicrobial and antitumor activities. Upon excess production of NO tissue damage and inflammation develop. NO production via iNOS in macrophages is induced by LPS, TNFα or IFNγ via the transcription factor NF-κB. Saturated and unsaturated fatty acids were shown to induce NO production in murine macrophages at low concentrations mostly via activation of NF-κB in a time dependent manner (de Lima, de Sa Lima, Scavone, & Curi, 2006).

IL-6

Interleukin 6 (IL-6) is a cytokine that acts either directly via the binding to the IL-6 receptor and its co-receptor gp130 or indirectly via the binding to the soluble form of the IL-6 receptor and further to

Introduction

gp130 on the surface of a target cell via 'trans-signaling' (Li, Grivennikov, & Karin, 2011). Production of IL-6 can be induced by IL-1 and TNF signaling (Park, et al., 2010). This leads to downstream activation of STAT3 (Grivennikov & Karin, 2011). Il-6 can propagate inflammation and stimulates triglyceride secretion (Park, et al., 2010).

Increased levels of IL-6 were found in obese mice (Toffanin, Friedman, & Llovet, 2010) (Park, et al., 2010) and are associated with most HCC risk factors including hepatosteatosis, obesity and liver cirrhosis. IL-6 is a critical tumor promotor in HCC, as IL-6 deficient mice were resistant to HCC development when treated with diethylnitrosamine (DEN). The source of IL-6 in this model seemed to be Kupffer cells. These cells were further capable of binding IL-1α, which might have been released by damaged hepatocytes, leading to IL-6 production by Kupffer cells and resulting in proliferation of surviving hepatocytes which might harbor oncogenic mutations (Grivennikov & Karin, 2011).

Furthermore, IL-6 KO mice showed reduced lipid accumulation and reduced infiltration of macrophages and neutrophils induced by HFD (Toffanin, Friedman, & Llovet, 2010).

Male mice showed enhanced liver tumor development compared to females when treated with DEN and did also show higher levels of DEN-induced IL-6 production. This higher level could be decreased to the level observed in female mice upon treatment with an estrogen receptor agonist, indicating a suppressive function of estrogen signaling in IL-6 mediated inflammation in females (Berasain, Castillo, Perugorria, Latasa, Prieto, & Avila, 2009; Yang & Roberts, 2010).

ADAM17/TACE

Tumor necrosis factor alpha converting enzyme (TACE) or a disintegrin and metalloproteinase (ADAM) 17 is a zinc-containing sheddase (or α-secretase) that cleaves membrane-bound proteins from the cell surface thereby converting them into their mature, soluble form in a process termed 'ectodomain-shedding'. ADAMs are type-I transmembrane proteins which contain an inhibitory pro-domain, a catalytic metalloproteinase domain, a disintegrin domain, an EGF-like domain, a transmembrane domain and a cytoplasmic domain (see Figure 8; Scheller, Chalaris, Garbers, & Rose-John, 2011). ADAM17 has been found to be upregulated in chronic liver injury and human HCC tissue (Berasain, Castillo, Perugorria, Latasa, Prieto, & Avila, 2009) and also seems to play a role in development as knock-out mice show perinatal lethality due to defective cardiac valvulogenesis (Gutiérrez-López, et al., 2011).

The first protein recognized to be shed by TACE was TNFα, but TGFα, HB-EGF, amphiregulin, p55-TNFαR, p75-TNFαRII, IL-6R, HER-4, Notch, L-selectin, ICAM-1, VCAM-1, RANKL, CSF-1 and VEGFR2 (Scheller, Chalaris, Garbers, & Rose-John, 2011) are also shed by TACE. These proteins are mostly shed at basal levels by other sheddases than TACE (e.g.: ADAM10, MMP7; Alvarez-Iglesias, Wayne, O'Dea, Amour, & Takata, 2005), but stimulation-induced increase in shedding is most likely due to TACE. Doedens et al. showed that TACE activity on murine monocytes (DRM cells) could be increased when cells were stimulated with a phorbol ester (PMA), which did not affect the abundance of TACE on the cell surface. Basal shedding which was not caused by TACE could also be detected (Doedens, Mahimkar, & Black, 2003). Alvarez-Iglesias et al. (Alvarez-Iglesias, Wayne, O'Dea, Amour, & Takata, 2005) showed LPS-induced increase in TACE activity in a human monocytic cell line (THP1). LPS-treatment did also not change TACE abundancy on the cell surface. The same group showed an

increase in TACE activity on MonoMac-6 cells upon treatment with PMA. Scott et al. (Scott, et al., 2011) found LPS-induced and ROS-dependent TACE activation without altering TACE abundancy on the cell membrane in primary human monocytes.

ADAM17/TACE is produced as a zymogen which has to be activated by the removal of an inhibitory cysteine switch, which inhibits TACE activity at the catalytically active, zinc-ion containing site (Scott, et al., 2011). Control of proteolytic cleavage might also occur via spatial segregation of the enzyme and its substrates. The covalent modification of the inhibitory pro-domain by oxidation via ROS (and maybe - although unlikely - RNS) has also been postulated, as has the presence of TACE inhibitors complexed with TACE in unstimulated cells (Doedens, Mahimkar, & Black, 2003). In primary human cells the pro-domain is most likely removed intracellularly, therefore pro-domain removal at the site of action, at the cell membrane, seems unlikely (Scott, et al., 2011). Gutiérrez-López et al. showed that in human leukocytes and endothelial cells the tetraspanin CD9 interacts with TACE and this interaction results in reduced TACE-mediated shedding of TNFα and ICAM-1. This could be abrogated by treatment with PMA, which resulted in dissociation of CD9 with TACE (Gutiérrez-López, et al., 2011).

Signaling involved in direct TACE activation seems to be dependent on p38MAPK, which gets activated by ROS, at least in primary human monocytes. Furthermore, there seems to be a threshold of p38MAPK activation below which TACE activity does not increase (Scott, et al., 2011)

It is now suggested, that full activation of TACE requires all steps including expression, translocation to the cell membrane, disulfide bridge rearrangement, spatial distribution and abrogation of inhibition. As all this is concluded from in-vitro studies, the exact in-vivo regulation of TACE has still to be fully elucidated. This might still take some time as appropriate in-vivo models, like mouse models, might show different substrate specificities, as for example murine IL-6R is shed by ADAM10, whereas it is shed by ADAM17/TACE in humans (Scheller, Chalaris, Garbers, & Rose-John, 2011).
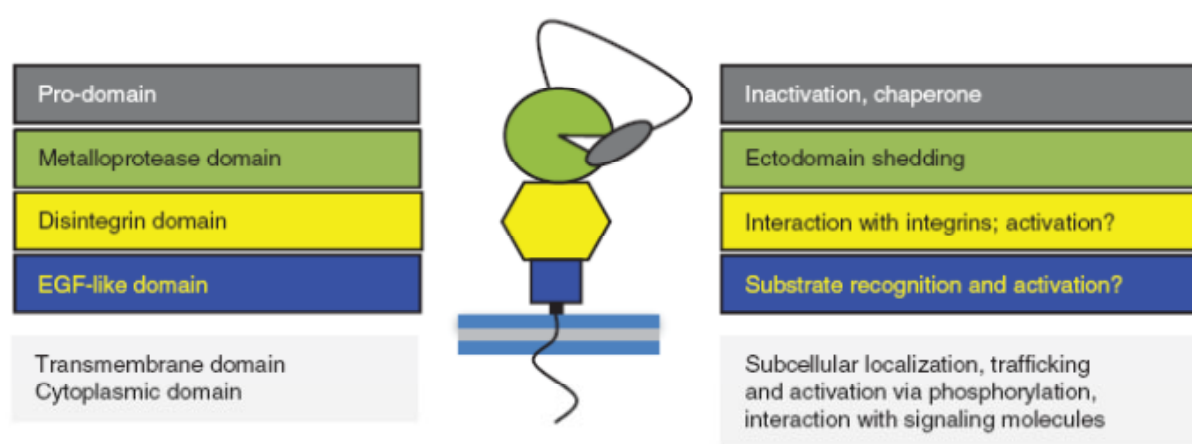
Figure 8: Schematic structure and domains of ADAM17/TACE. Taken from: Scheller, Chalaris, Garbers, & Rose-John, 2011.

Aims of the thesis

Hepatocellular carcinoma is one of the most common causes of cancer related death worldwide and develops in the background of chronic liver inflammation which might be caused by a fatty liver. As free fatty acids (FFA) levels are increase in individuals suffering from obesity and non-alcoholic fatty liver disease (NAFLD) we were interested in the role FFAs play in the onset of liver inflammation. Therefore we studied the effects of FFAs on transcription, kinase phosphorylation, protein secretion and activity and the in-vivo effects of oil-treatment on rats.

The aims of this thesis were:

(i)   To analyze the viability of primary rat liver cells in response to increasing concentrations of α-linolenic acid (ALA), as this FFA is reported to have anti-inflammatory properties.

(ii)   To study the secretion of tumor-necrosis-factor-α from primary rat liver cells treated with FFAs. TNFα levels are increased in diet-caused obesity which causes hepatosteatosis and steatohepatitis and the cytokine further acts as a tumor promoting agent.

(iii)   To examine the possible involvement of p38MAPK and Erk, both of which are kinases involved in stress induced pathways, in FFA-mediated inflammatory signaling.

(iv)   Investigation of changes in the expression of the inflammation-associated genes iNOS, COX-2, TNFα and IL-6 in cells treated with free fatty acids.

(v)   Inhibition of CD36, a translocase and receptor of free fatty acids and examination of the resulting changes in gene expression and signaling in primary rat endothelial cells and Kupffer cells.

(vi)   Establishment of a real-time enzyme assay measuring the activity of ADAM17/TACE on live primary rat Kupffer cells using a fluorogenic substrate, as this specific enzyme is responsible for the conversion of a variety of proteins involved in inflammatory responses and is reported to be overexpressed in HCC.

(vii)   Comparison of in vivo changes in oil-treated rats and water-treated controls with a special focus on the levels of free fatty acids and alterations in total gene expression in the liver.

Materials and methods

Materials

Reagent	Supplier
Acrylamide	Biorad (Hercules, CA)
Agarose	Biozym (Hessisch Oldendorf, Germany)
α-linolenic acid	Sigma (St.Louis, MO)
Ammonium-persulfat (APS)	Sigma (St. Louis, MO)
Ascorbat	Merck (Darmstadt, Germany)
50 bp DNA marker	Fermentas (Burlington, Ontario)
5x Biorad protein assay	Biorad (Hercules, CA)
Bovine serum albumin (BSA)	Sigma (St. Louis, MO)
Bovine serum albumin (BSA), fatty acid free	Sigma (St. Lois, MO)
Bromophenol blue	Sigma (St. Louis, MO)
Calciumchloride	Merck (Darmstadt, Germany)
Chloroform	Merck (Darmstadt, Germany)
Collagenase, Typ2 CLS2	Worthington (Lakewood, NJ)
Dabcyl-TNFα-Edans	Bachem (Bubendorf, Switzerland)
10mM dNTP mix	Fermentas (Burlington, Ontario)
Dexamethasone	Serva (Heidelberg, Germany)
Dimethylsulfoxide (DMSO)	Sigma (St. Louis, MO)
ECL-Plus Western Blotting Detection Kit	GE Healthcare (Uppsala, Schweden)
Ethylenediaminetetraacetic acid (EDTA)	Sigma (St. Louis, MO)
Ethanol	Merck (Darmstadt, Germany)
Ethidiumbromide	Sigma (St. Louis, MO)
Fetal calf serum (FCS)	PAA (Pasching, Austria)

Materials and methods

Gentamycin	Serva (Heidelberg, Germany)
Glucagon	Sigma (St. Louis, MO)
Glucose	Merck (Darmstadt, Germany)
Glutamax	Invitrogen (Carlsbad, California)
Glycerin	Sigma (St. Louis, MO)
Glycin	Sigma (St. Louis, MO)
Heparin sodium salt	Serva (Heidelberg, Germany)
HEPES	Sigma (St. Louis, MO)
Hexamer Primer	Fermentas (Burlington, Ontario)
Insulin	Sigma (St. Louis, MO)
Isopropanol	Merck (Darmstadt, Germany)
KH_2PO_4	Merck (Darmstadt, Germany)
Linoleic acid	Sigma (St.Louis, MO)
Lipofectamin	Invitrogen (Carlsbad, California)
Lipopolysaccharid (LPS):	Sigma (St. Louis, MO)
6x loading dye	Fermentas (Burlington, Ontario)
Methanol	Merck (Darmstadt, Germany)
β-Mercaptoethanol	Sigma (St. Louis, MO)
5x MMLV Buffer	Fermentas (Burlington, Ontario)
MMLV reverse transcriptase	Fermentas (Burlington, Ontario)
NaCl	Merck (Darmstadt, Germany)
Na-Deoxycholat	Sigma (St. Louis, MO)
Na_2HPO_4	Merck (Darmstadt, Germany)
$NaH_2HPO_4*2H_2O$	Merck (Darmstadt, Germany)
NaOH	Merck (Darmstadt, Germany)
Na_3VO_4	Merck (Darmstadt, Germany)
NP-40	Sigma (St. Louis, MO)

Nuclease free water	Promega (Madison, WI)
Palmitic acid	Sigma (St. Louis, MO)
Penicillin G sodium salt	Sigma (St. Louis, MO)
Penicillin-streptomycin	PAA (Pasching, Austria)
Percoll	GE Health care (Uppsala, Schweden)
PMSF (protease inhibitor)	Roche (Basel, Switzerland)
Potassium chloride, KCl	Merck (Darmstadt, Germany)
Pyruvat	Sigma (St. Louis, MO)
Ponceau S	Sigma (St. Louis, MO)
Skim milk	Sigma (St. Louis, MO)
Sodium dodecyl sulfate (SDS)	Sigma (St. Louis, MO)
Sulfosuccinimidyl oleate sodium (SSO)	Santa Cruz Biotechnology (Santa Cruz, CA)
Streptomycin sulfate salt	Sigma (St. Louis, MO)
TAPI-2	Enzo Life Sciences (Farmingdale, NY)
Taqman Gene Expression Assays	Applied Biosystems (Carlsbad, California)
TaqMan® universal master mix	Applied Biosystems (Carlsbad, California)
TEMED (N,N,N',N'-Tetramethylendiamine)	Sigma (St. Louis, MO)
TMB Substrate Kit	Thermoscientific, Rockford
TriFast	Peqlab (Erlangen, Germany)
Triiodthyronin	Serva (Heidelberg, Germany)
Tween 20	Biorad (Hercules, CA)
Trizma base	Sigma (St. Louis, MO)
Trypan blue	Invitrogen (Carlsbad, California)

Table 1: Reagents and supplier.

Materials and methods

Buffers and solutions

20mM Tris.HCl pH 7.4

50mM Tris.HCl pH 7.4

250mM Tris.HCl pH 7.4

ADAM17/TACE Activity Substrate solution
Dabcyl-TNFα-Edans (DABCYL-Leu-Ala-Gln-Ala-Val-Arg-Ser-Ser-Ser-Arg-EDANS Trifluoroacetate salt; Bachem): 1mg of Dabcyl-TNFα-Edans was dissolved in 635,4µl 20mM Tris.HCl pH 7.4 to yield a 1mM stock solution which was stored at -20°C until used.

ADAM17/TACE Activity Inhibitor solution
TAPI-2: (IC3; N-(R)-(2-(Hydroxyaminocarbonyl)methyl)-4-methylpentanoyl-L-t-butyl-glycine-L-alanine 2-aminoethyl amide; Enzo Life Sciences): 1mg of TAPI-2 was dissolved in 481,6µl 20mM Tris.HCl pH7.4 to yield a 5mM stock solution which was stored at -20°C until used.

1x Assay Buffer for ELISA
5 g BSA, 0.5 ml Tween 20 in 1 liter 1xPBS pH 7.4

BSA buffer pH 7.4
contains per liter: 8.3 g NaCl, 0.5 g KCl, 2.4 g HEPES, 6 ml 1M NaOH, 1 g Bovine Serum Albumin (BSA) 96%, 10 mg Gentamycin

Collagenase buffer pH 7.5
contains per liter: 6.8g NaCl, 0.4g KCl, 1g glucose, 1g HEPES, 60mg penicillin G sodium salt, 100mg streptomycin sulphate salt, 110mg pyruvat, 294mg $CaCl_2$, 0.0013% BSA, 0.7nM Glucagon, 10nM Triiodthyronin, 6.7nM Insulin, 100nM Dexamethasone, 400mg collagenase

Hank's buffered salt solution (HBSS) for ADAM17/TACE activity assay
0.137M NaCl, 5.4mM KCl, 0.25mM Na_2HPO_4, 0.44mM KH_2PO_4, 1.3mM $CaCl_2$, 1.0mM $MgSO_4$, 4.2mM $NaHCO_3$

10x HBSS buffer for HC-Percoll solution
80g NaCl, 4g KCl, 2g $MgSO_4.7H_2O$, 0.6g KH_2PO_4, 10g Glucose, 0.6g $Na_2HPO_4.2H_2O$, in 1 liter ddH_2O

Laemmle electrophoresis buffer
3 g Trizma Base, 14.4 g Glycin, 1 g SDS in 1 liter ddH_2O

5x reducing Laemmle sample loading buffer
300mM Tris.HCl pH 6.8, 60% Glycerol, 10% SDS, 0.025 % Bromophenol blue, 7% β-Mercaptoethanol

1x PBST
1x PBS (pH 7.4) supplemented with 0,05% Tween 20

Percoll solutions for NPC purification
Stock Percoll Solution (SPS) contains 90% Percoll and 10% 10x PBS
50% Percoll-solution: 50% SPS + 50% PBS
25% Percoll-solution: 25% SPS + 75% PBS

Percoll solution for HC purification
Stock Isoosmotic Percoll (SIP) contains 90% Percoll and 10% 10x HBSS

Perfusion buffer pH 7.4
contains per liter: 6.8 g NaCl, 0.4 g KCl, 1g glucose, 1g HEPES, 200µl 4N NaOH, 60mg penicillin G sodium salt, 100mg streptomycin sulphate salt, 12.4 mg heparin sodium salt, 110mg pyruvat, 0.0013% BSA, 0.7nM Glucagon, 10nM Triiodthyronin, 6.7nM Insulin, 100nM Dexamethasone.

1x Phosphate Buffer Saline (PBS) pH 7.4
5.68g NaCl, 1.44g Na_2HPO_4, 2.96g $NaH_2PO_4.2H_2O$ in 1 liter

10x Ponceau-S-Solution
2% Ponceau, 10% acetic acid in 1x PBS

RIPA Buffer
500mM NaCl, 50mM Trisma base pH 7.4, 0.1% SDS, 1% NP-40, 0.5% Na-Deoxycholat, 1mM Na_3VO_4, 1mM PMSF

1x TBST
1x TBS (pH 7.4) supplemented with 0.05% Tween 20

Transfer buffer
3 g Trizma base, 14.4 g Glycin, 5% Methanol in 1 liter of ddH_2O

Tris based buffer
50mM Tris.HCl pH 8.0; 100mM NaCl; 10mM $CaCl_2.2H_2O$; 0.01% Triton-X-100

1x Tris-borat-EDTA buffer (TBE)
10.8 g Trizma base, 5.5 g boric acid, 4 ml 0.5 M EDTA (pH 8) in 1 liter of ddH_2O

1x Tris buffered saline (TBS) pH 7.4
0.05 M Trizma base, 0.3 M NaCl

1x Wash Buffer for ELISA
1x PBS (pH7.4) supplemented with 0.05% Tween 20

Western blot stripping solution pH 2.2
15g Glycine, 10ml 10% SDS (or 1g SDS), 10ml Tween 20 in 1 liter of ddH_2O

Media

HC culture medium
Williams-Medium E (Invitrogen, San Diego, CA), 10µl/ml Glutamax, 20mM HEPES, 10µg/ml Gentamycin, 0.0013% BSA, 0.7nM Glucagon, 10nM Triiodthyronin, 6.7nM Insulin, 100nM Dexamethasone, 0.151mM Ascorbat.

HC plating medium
HC culture medium supplemented with 10%FCS

Materials and methods

NPC medium
RPMI1640 (Sigma), 10%FCS, 0.01g Gentamycin per liter medium

Kupffer cell medium
RPMI1640 (Sigma), 10%FCS, 0.01g Gentamycin per liter medium

Endothelial cell medium
EBM-2 + EGM-2MV (Lonza, Basel, Switzerland)

Washing medium
Minimum essential medium (Sigma St. Louis, MO) supplemented with: 20mM HEPES, 10µg/ml Gentamycin, 10µl/ml Glutamax

ECII medium
RPMI1640 (Sigma), 20% FCS, 170µM Penicillin, 70µM Streptomycin and 1µM Dexamethasone

HAM's tissue culture medium and Leibovitz L-15 medium
Were kind gifts from the laboratory of Dr. Brigitte Marian.

Cell culture

Animals and in vivo treatment
Wistar rats were kept at the 'Division for Decentralized Biomedical Facilities of the Medical University of Vienna' under standard SPF conditions. Female wistar rats (8-10 weeks of age) were treated once or daily on 6 consecutive days with a dose of 1ml Mazola® oil per 100g body weight by gavage. Control groups were given the same volume of water by gavage. Rats were sacrificed 20 hours after the last administration.

Collagenase perfusion of the rat liver
The livers of untreated or oil-treated rats were perfused with collagenase according to the technique of Seglen (Seglen, 1976) with modifications described (Parzefall, Monschau, & Schulte-Hermann, 1989; Pertoft & Smedsrod, 1987). Perfusions were kindly performed by Dr. Sandra Sagmeister, Mag. Therese Böhm and Marzieh Nejabat, MD. Wistar rats were anesthetized with a chlorinated hydrocarbon of similar vapour pressure as isoflurane. Therefore the animals were gased with a mixture of dinitrogen oxide (N_2O) at 1200 ml/min and oxygen at 800 ml/min which is passed through a vaporizer filled with a chlorinated hydrocarbon and set to a concentration of 4 %. The abdomen was cut open, a cannula was inserted into the portal vein and ligated. The lower vena cava was immediately cut and perfusion was started. First perfusion buffer was pumped through the liver with a flow rate of 15 ml/min. After approximately ten minutes the liver was freed of blood. The perfusion continued with pumping collagenase buffer with a flow rate of 10 ml/min through the liver. The temperature of both buffers was 37°C. On average the liver tissue was sufficiently decomposed after 10 minutes. The softened liver was excised and put into ice-cold washing medium (adapted from Sagmeister, 2009). The liver capsule was cut open with sterile scissors and cells were collected in washing medium by gentle shaking of the capsule. The gained cell suspension was filtered through a 105µm mesh (Polyester precision mesh) to get rid of non-separated cells. This was repeated approximately 4 times using a total volume of 100ml washing buffer until no more cells could be collected by shaking the capsule.

Purification of primary rat non-parenchymal cells (NPCs)

The filtered cell suspension was centrifuged for 5 min at 55xg and 4°C. The pellet was used for purification of hepatocytes, the supernatant was centrifuged for 10min at 1200xg and 4°C to collect NPCs. The resulting pellet was resuspended in 10ml of BSA buffer and carefully pipetted onto a two-step discontinuous NPC percoll gradient (20ml of a 50% Percoll underneath 19ml of a 25% Percoll) which was centrifuged at 1200xg for 30min and 4°C without any acceleration or deceleration, to avoid any mixing of the two Percoll solutions. The fraction containing NPCs located at the interface of the 25% and 50% Percoll solutions was collected, diluted with BSA buffer and centrifuged for 10min at 1200xg and 4°C. The resulting pellet was resuspended in NPC medium and cells were counted and viability was determined in a Neubauer counting chamber.

Purification of primary rat hepatocytes

The pellet obtained after the first centrifugation step was resuspended in 20ml washing medium and centrifuged for 5min at 300rpm (=17xg) to get rid of residual collagenase buffer. The resulting pellet was resuspended in 25ml washing medium and mixed with 24ml SIP. This Percoll-cell suspension was centrifuged for 10min at 550rpm and 4°C. The supernatant was discarded and the pellet was resuspended in 40ml washing medium followed by centrifugation for 2min at 550rpm and 4°C to get rid of residual Percoll. The pellet was resuspended in 25ml washing medium and centrifuged for 5min at 300rpm and 4°C. The pellet was resuspended in 20ml washing medium and centrifuged for 5min at 300rpm and 4°C. Following this, the pellet was resuspended in HC plating medium and counted and viability was determined in a Neubauer counting chamber.

Determination of cell viability

Viability of primary rat liver cells was determined by the trypan blue dye exclusion test after purification in a Neubauer counting chamber. Trypan blue stained cells were considered dead because of damaged cell membranes allowing the dye to enter the cell. 50µl of cell suspension were mixed with 50µl of trypan blue dye and vital and dead cells were counted. Only the vital cell count was used for calculation of cells to be plated.

Culture of primary rat non-parenchymal cells

NPCs were plated onto collagen coated dishes after counting and allowed to adhere for 2h in NPC medium. Cells were checked for adherence visually and washed once with 1x PBS to get rid of nonattached cells and cell debris. This was followed by treatment of the cells.

If desired, NPCs were separated into Kupffer cells and endothelial cells by selective adherence. The NPC fraction was therefore plated onto non-coated dishes and Kupffer cells were allowed to adhere for 30-40 min. After this period of time the supernatant containing endothelial cells was collected, centrifuged for 5 min at 1000rpm and resuspended in endothelial cell medium. Following counting of endothelial cells they were plated onto collagen-coated dishes.

Culture of primary rat hepatocytes

Percoll-purified primary rat hepatocytes were plated onto collagen coated dishes and allowed to adhere for 2h in hepatocyte plating medium. Cells were checked for adherence visually followed by treatment of the cells.

Culture of cell lines

THP1 cells were kept in RPMI 1640 medium supplemented with 10% fetal calf serum at 37°C and 5% CO_2 in a humidified atmosphere. Medium was changed every 2-3 days and cells were passaged every 4-6 days.

Materials and methods

ECII cells were kept in RPMI 1640 medium supplemented with 20% FCS, 170µM Penicillin, 70µM Streptomycin and 1µM Dexamethasone at 37°C and 5% CO_2 in a humidified atmosphere on collagen-coated dishes.

Treatment of cells with free fatty acids

Free fatty acids were dissolved in ethanol upon arrival and stored as 50mM stocks solutions in liquid nitrogen to prevent oxidation. Appropriate volumes of stock solution were dissolved in the respective treatment media (*HC culture medium supplemented with 0.1% BSA* for HCs, *NPC medium* for NPCs, *RPMI 1640 supplemented with 10% FCS* for THP1 monocytes, *ECII medium* for ECII cells) and solutions were dispersed by sonication.

FFA concentration	EtOH
500µM	1%
250µM	0.5%
100µM	0.2%
75µM	0.15%
50µM	0.1%
25µM	0.05%
10µM	0.02%
1µM	0.002%

Table 2: FFA concentrations used for cell treatment and their corresponding concentrations of ethanol in the medium.

Treatment of cells with Sulfosuccinimidyl oleate sodium (SSO)

Cultured primary rat non-parenchymal cells were treated with 500µM SSO for 30min followed by addition of palmitic acid (10µM final concentration), ethanol (0.02% final concentration) or LPS (final concentration 10ng/ml). The time point of PA, EtOH or LPS treatment, respectively, was considered as time point = 0. DMSO served as solvent control as SSO was dissolved in DMSO and stored as stock solution of 250mM.

Cytotoxicity assay

Cell viability was measured by uptake of neutral red into lysosomes of viable cells in 24-well plates (BD Falcon; $2x10^5$ of primary HCs, THP1, ECII per well, respectively) or 12-well plates (BD Falcon; $1.5x10^6$ of NPCs per well). After plating cells were allowed to attach for 2h. This was followed by incubation for 24h with medium containing 0.1% BSA (HCs) or 10% FCS (NPCs, THP1) or 20% FCS (ECII) and varying concentrations of free fatty acids (ranging from 0 - 500µM) or the corresponding ethanol concentrations (see Table 2). Cells were incubated with their respective treatment medium (without FFAs, but) supplemented with 50mg/L neutral red. Each neutral red solution was incubated at 37°C for 30min and filtered before application to get rid of non-dissolved neutral red crystals. After a 2h incubation period cells were washed twice with 1xPBS and lysed with a 1% acetic acid solution in 70% ethanol for 10min. Absorbance of 100µl of each well's supernatant was measured at 562nm. Cell viability of each treatment was assayed in triplicate and calculated as fold corresponding ethanol control.

Detection of mRNA

RNA isolation using the TriFast reagent

RNA isolation using the TriFast reagent is based upon the method of Chomczynski & Sacchi (Chomczynski & Sacchi 1987). Medium was sucked off and cells were washed once with 1xPBS. TriFast reagent was added to each well (usually 300µl for a 6-well) and cells were scraped off. The TriFast lysed cell suspension was transferred into 2ml Eppendorf tubes and stored at -20°C or immediately used for RNA isolation. Chloroform (1/5 of the used TriFast volume) was added and tubes were gently inverted for 15sec and allowed to rest for 10min at room temperature. Tubes were then centrifuged for 15min at 12000xg and 4°C. The upper, aqueous phase was transferred into a new tube, isopropanol (1/2 of the used TriFast volume) was added and RNA was precipitated over night at -20°C. On the following day the tube was centrifuged for 8min at 12000xg and 4°C to collect the RNA. The supernatant was discarded and the pellet was washed gently with 70% ethanol. The pellet was again centrifuged for 8min at 12000xg and 4°C and the residual ethanol was discarded. The pellet was allowed to dry and dissolved in DEPC-treated water. The RNA concentration was measured with a Nanodrop ND-1000 spectrophotometer. Samples were stored at -80°C until used.

RNA isolation using miRNeasy Mini kit (Qiagen)

RNA of hepatocytes and non-parenchymal cells of oil-treated and control rats was isolated using the miRNeasy Mini kit (Qiagen). First, cells ($15x10^6$ NPCs or $2x10^6$ HCs, respectively) were resuspended in 700µl QIAzol Lysis Reagent (Quiagen) and homogenized by centrifugation for 2 min at 13000xg in QIAshredder homogenizer spin columns (Qiagen). The lysed and homogenized flow-through was stored at -80°C until used for RNA isolation.

For RNA isolation, samples were thawed at room temperature. 140µl of chloroform were added to each sample and tubes were shaken vigorously for 15 sec. Tubes were placed at room temperature for 3 min followed by centrifugation for 15 min at 12000xg and 4°C. The upper, aqueous phase was transferred into a new tube, 1.5 volumes of ethanol were added and mixed by pipetting. The samples were loaded into RNeasy Mini columns (Qiagen) and centrifuged for 15 sec at 13000xg and room temperature and flow-through was discarded. Columns were washed once with 700µl of RWT buffer (Qiagen) and twice with 500µl RPE buffer (Qiagen). This was followed by elution of the RNA by addition of 30µl of RNAse-free water (Qiagen) to each column and centrifugation for 1 min at 13000xg. Isolated RNA samples were stored at -80°C until used.

Reverse transcription PCR

For reverse transcription of RNA into cDNA 1µg of RNA was filled up with DEPC-treated water to a total volume of 15µl. 0.625µl of random hexamer primer were added and samples were heated for 2min at 72°C. To each sample 9.375µl of mastermix (see Table 3) were added and samples were incubated for 1 hour at 42°C for reverse transcription, followed by incubation for 5min at 94°C to inactivate the MMLV reverse transcriptase. Samples were then filled up to a total volume of 100µl with DEPC-treated H_2O and stored at -20°C.

Reagent	Volume [µl]
5x MMLV buffer	5
10mM dNTPs	1.5625
RNAse Inhibitor	0.625
DEPC-treated H_2O	1.1875
MMLV reverse transcriptase	1
Total	*9.375*

Table 3: Mastermix for reverse transcription of one RNA sample.

Polymerase chain reaction (PCR)

1µl of cDNA was mixed with 24µl of mastermix (see Table 4). PCR was performed in a thermocycler (C1000, Thermal Cycler, Biorad) using primers, temperatures and durations listed in Table 5 and Table 6.

Reagent	Volume [µl]
Forward primer	1
Reverse primer	1
DEPC H_2O	9.5
2x mastermix	12.5
Total	*24*

Table 4: Mastermix for standard PCR.

Stage	Temperature	Duration
Cycle 1	95°C	5 min
Cycle 2		
- Denaturation	94°C	30 sec
- Annealing	60°C	30 sec
- elongation	72°C	30 sec
Cycle 3	72°C	7 min

Table 5: Cycles for standard PCR, for the amplification of cDNA in hepatocytes cycle 2 was repeated 35-times, in endothelial and Kupffer cells 40-times, if not stated otherwise.

Primer	Sequence	Product size
CD36-for	5' GTA TGG TGT GCT GGA CAT TG 3'	162bp
CD36-rev	5' CCA GTT ATG GGT TCC ACA TC 3´	
β-actin-for	5'- ATG TTG CCC TAG ACT TCG AG – 3'	175bp
β-actin-rev	5'- TCA TGG ATG CCA CAG GAT TC - 3'	

Table 6: Primers used for standard PCR (Eurogentec).

Quantitative real-time PCR (qRT-PCR)

For qRT-PCR analysis 1µl cDNA was mixed with 11.5µl of qRT-PCR mastermix (see Table 8). 12µl of this mixture were transferred into a Fast Optical 96-Well Reaction Plate (Applied Biosystems). All samples were measured in duplicates in an ABI-PRISM 7500 Sequence detection system (Applied Biosystems).

Stage	Temperature	Duration	Cycles
1	50°C	2 min	1
2	95°C	10 min	1
3	95°C	15 sec	40
	60°C	1 min	40

Table 7: Cycles for qRT-PCR

The Ct-values of each measured probe were normalized to β-2-microglobulin. The resulting gene expression levels were calculated according to the ΔΔ-Ct method (Applied Biosystems).

Reagent	Volume [µl]
Primer	0.625
DEPC-treated H_2O	4.625
2x GE mastermix	6.25
total	*11.5*

Table 8: Mastermix for qRT-PCR.

Taqman Gene Expression Assay	Assay ID
COX-2	Rn01483828_m1
iNOS	Rn00561646_m1
TNFα	Rn99999017_m1
IL6	Rn99999011_m1
β2-Microglobulin	Rn00560865_m1

Table 9: Taqman Gene Expression Assays used for qRT-PCR.

Agarose-gel electrophoresis

RNA samples from in-vivo treated rats or PCR products were run on a 1.5% agarose gel to estimate the integrity of the RNA visually or for densitometry of PCR-products, respectively. The desired amount of agarose was dissolved in 1xTBE and heated in a microwave. The agarose gel was poured into a gel apparatus (BioRad) together with ethidium bromide (3.5μl - 7μl depending on the volume of the agarose gel). After the gel solidified, 1μl of each sample (diluted with 4μl of DEPC-treated water and 1μl of a 6x loading dye) was loaded onto the gels. Samples were run for approximately 25 min at 80V. The separated bands were visualized by UV light in a Geldoc2000.

Bioanalyzer

Isolated RNA samples from in-vivo treated rats were analyzed on RNA 6000 nanochips (Agilent Technologies) in an Agilent 2100 Bioanalyzer (Agilent Technologies) for RNA integrity before having them analyzed on a RNA-mircoarray. Only RNAs with integrity units (RIN) above 8 were used for the mircoarray.

Analysis of RNA samples was done according to manufacturer's instructions as described in Agilent's RNA 6000 Nano Kit Quick Start Guide. Briefly, the RNA 6000 Nano gel was filtered through a spin filter and aliquoted. The RNA 6000 Nano dye was equilibrated to room temperature for 30min, vortexed, spun down and 0.5μl of dye were added to 32.5μl of filtered gel. The solution was vortexed and centrifuged for 10min at 13000xg and room temperature. 9μl of gel-dye mix was added to a RNA 6000 Nano chip. Then, 5μl of RNA 6000 Nano marker were added to each sample well and to the ladder well, respectively. 1μl of ladder was added to the ladder well and 1μl of sample was added to each sample well, respectively. The chip was vortexed for 1min in the IKA vortexer at 2400rpm. The chip was transferred to the Agilent 2100 Bioanalyzer and analysis was started.

RNA-microarray Array Transcriptome Analysis

RNA-microarray Array Transcriptome Analysis using the GeneChip Rat Genome 230 (Affymetrix) was kindly carried out by Markus Jeitler, BSc. at the Core Facility Genomics of the Medical University of Vienna led by Dr. Martin Bilban.

Detection of protein

Protein isolation

The medium was removed and the cells were washed once with ice-cold 1xPBS. Then the cells were scraped off in RIPA buffer (75 μl per 6-well) on ice to be able to detect phosphorylation of proteins. The samples were homogenized by sonication for 1sec (Bandelin electronic sonopuls) and centrifuged for 5 min at 15000xg and 4 °C. Protein samples were stored at -20 °C.

Determination of protein concentrations

Protein concentration was determined according to Bradford using a 1:5 dilution of 5x Protein assay reagent (Biorad). To estimate the concentrations of the protein samples a standard curve was done using BSA as standard protein. Concentrations ranged from 0 – 6µg/µl were used for the standard curve. 1µl of each sample was added to 9µl of water in a 96-well. 100µl of 1x Protein assay reagent was added to each standard and sample well and the absorbance at 595nm was measured in a plate reader (Tecan infinite 200Pro using Tecan i-control 1.7.1.12 software). The concentration of each sample was calculated from duplicates.

SDS-PAGe

Equal amounts of each protein sample were filled up with RIPA buffer to 10µl. 2µl of 6x Laemmle sample loading buffer were added and samples were heated for 5min at 95°C. Then samples and the protein ladder (PageRuler™ Plus Prestained Protein Ladder, Fermentas) were loaded onto 12% SDS-polyacrylamide gels and separated according to their molecular weight. Gel electrophoresis was performed at 60V for focusing proteins in the stacking gel and changed to 120V upon beginning of separation in the resolving gel. Stacking and resolving gels were mixed as described in the tables below.

Stacking gel	volume for 2 gels [ml]
Acryamide/Bisacrylamide (40%)	0.5
1 M Tris pH 6.8	0.625
10% SDS	0.05
H_2O	3.8
10% APS	0.025
TEMED	0.005

Table 10: Reagents and used volumes for 2 stacking gels.

Resolving gel (12%)	Volumes for 2 gels [ml]
40% Acrylamide/Bisacrylamide	3.6
1.5 M Tris pH 8.8	3
10% SDS	0.12
H_2O	5.2
10% APS	0.06
TEMED	0.006

Table 11: Reagents and used volumes for one resolving gel.

Transfer

The separated proteins were transferred from the gel to the membrane via wet blot in a blotting apparatus (Biorad). Therefore the gel was layered onto matching piece of PVDF membrane (GE-healthcare) which was previously wetted with methanol followed by ddH_2O and transfer buffer. The gel and membrane were covered with Whatman filter papers and sponges on both sides. The blotting apparatus was filled up with transfer buffer and transfer was performed over night at 25V and 4°C. Following the transfer, the membranes were stained with a Ponceau-S solution to make sure that the transfer from the gel to the membrane worked properly, that samples were loaded equally and no air bubbles disturbed the transfer.

Immunodetection

The stained membrane was washed with ddH_2O to get rid of any residual Ponceau-S solution and incubated for approx. 5 min in the respective buffer that the primary antibody was diluted in. This was followed by blocking of the membrane with BSA (2-5%) or skim milk powder (2-3%) in the same

buffer at room temperature for 2 hours. After blocking, the membrane was incubated over night at 4°C with the primary antibody.

Antibody	Dilution	Fc-Domain	Incubation	MW [kDa]	Supplier
ppp38	1:1000 (PBST; 3% skim milk)	Mouse	Over night	38	Sigma
p38	1:1000 (PBST; 3% skim milk)	Rabbit	Over night	38	
ppERK1/2	1:10000 (TBST; 3% BSA)	Mouse	Over night	42/44	Cell signaling
ERK1/2	1:1000 (TBST; 2% BSA)	Rabbit	Over night	42/44	Cell signaling
ppTAK1	1:1000 (TBST; 5% BSA)	Rabbit	Over night	82	Cell signaling
TAK1	1:1000 (TBST; 5% BSA)	Rabbit	Over night	82	Cell signaling
β-Actin	1:10000 (PBST; 1% skim milk)	Mouse	1 hour	42	Sigma

Table 12. Primary antibodies, dilutions, incubation periods and molecular weight.

On the following day the membrane was washed 3 times for about 10 minutes in PBST/TBST, depending on the buffer of the primary antibody. Then the membrane was incubated with a HRP-conjugated secondary antibody (see Table 13).

Antibody	Dilution	Incubation	Supplier
Goat anti mouse Ig	1:10000	2 hours	
Goat anti rabbit Ig	1:10000	2 hours	

Table 13. Secondary antibodies, dilutions and incubation periods.

After incubation with the secondary antibody, the membrane was again washed 3 times for about 10 minutes in PBST/TBST. Then the membrane was rinsed with the developing reagent *ECL-Plus Western Blotting Detection* Kit (GE Healthcare) for about 5 minutes. Finally the chemiluminiscence was detected via CL-XPosure (ThermoScientific) in a developing machine.

Blotted membranes were subsequently used for hybridization with further varying primary and secondary antibodies. Upon detection of any previously used antibody, membranes had to be incubated with stripping buffer to remove these residual previously used antibodies. This was done by incubating the membrane twice for 10 min with stripping buffer, followed by incubation for 2x 10 min with 1x PBS and 2x 5 min with TBSt. After that, membranes had to be blocked again.

Enzyme-linked immunosorbent assay (ELISA)

Rat TNFα Matched Antibody Pairs for ELISA kit (BenderMedSystems) was used for ELISA analysis of primary rat cell supernatant according to manufacturer's instructions. 96-well plates for ELISA (BD Falcon) were used for coating with TNFα coating antibody. A 1:1 mixture of TMB and H_2O_2 (TMB Substrate Kit, Thermoscientific) was used as substrate solution for the conjugated HRP. The reaction was stopped by addition of 4N H_2SO_4.

Human TNFα Matched Antibody Pairs for ELISA kit (BenderMedSystems) was used for ELISA analysis of human cell line supernatant according to manufacturer's instructions. 96-well plates for ELISA (company) were used for coating with TNFα coating antibody. A 1:1 mixture of TMB and H_2O_2 (TMB Substrate Kit, Thermoscientific) was used as substrate solution for the conjugated HRP. The reaction was stopped by addition of 4N H_2SO_4.

Extraction of serum from rat blood

Rats were sacrificed by decapitation and blood was immediately collected in a 50ml tube. The blood was then transferred into a 15ml tube and allowed to clot at room temperature for at least 15 min to avoid water condensation and rupture of erythrocytes. This was followed by incubation of the blood

samples on ice for at least 1h. For separation of serum from cells the clotted blood was centrifuged for 15 min at 4°C and 2000xg. Supernatant was carefully collected and stored at -80°C until used for detection of free fatty acids.

Detection of free fatty acids

Concentrations of free fatty acids in sera of rats or supernatants of cells were determined using the *Free Fatty Acid Quantification Kit* (BioVision) according to manufactuer's instruction by Helga Koudelka.

ADAM17/TACE activity assay

THP1

For the final ADAM17/TACE activity assay $3x10^6$ THP1 cells were incubated for varying time periods in 5ml medium. LPS (10ng/ml) activated cells served as positive control, cells incubated in medium without LPS served as negative control. Following incubation, $2x10^5$ cells per 96-well were centrifuged at 1000rpm (=218xg) for 2min, resuspended in TACE assay buffer and transferred into a 96-well (Greiner 96 Flat Bottom Black plates). TACE inhibitor was added to wells if desired. Substrate was added to each well just before starting the measurement in a Tecan infinite 200Pro plate-reader (Tecan, Salzburg, Austria). The TACE activity of cells was assayed in duplicate.

Rat primary Kupffer cells

$2x10^5$ primary rat Kupffer cells were used per 96-well on Greiner 96 Flat Bottom Black plates (see also culture of Kupffer cells) in a total volume of 100µl of Kupffer cell medium. LPS (10gn/ml) activated cells served as a positive control, cells incubated in medium without LPS served as negative control. Following incubation, the medium was removed and TACE assay buffer was added. TACE inhibitor was added to wells if desired. Substrate was added to each well just before starting the measurement. The TACE activity of cells was assayed in duplicate.

Tecan infinite 200Pro plate-reader protocol

The Tecan infinite 200Pro plate-reader was heated to 37°C before starting the fluorescence measurements. Plates to be measured were shaken for 10 sec. and allowed to rest for another 10 sec. Then fluorescence of each well was measured at λ_{EM}: 485nm when excited at λ_{EX}: 360nm. This was followed by a waiting period of 4 min to allow the enzyme reaction to go on. This cycle was repeated 20-26 times (see Table 14).

Repeat	Action	Time period
1	Wait for temp. 36.5°C - 37.5°C	
1x Cycle	Shaking (orbital)	10 sec
	Wait	10 sec
	Measure fluorescence at 485nm	
	Wait	4 min

Table 14: Protocol for TACE activity measurement using the Tecan infinite 200Pro plate-reader.

Results

Viability of primary rat hepatocytes depending on EtOH concentration
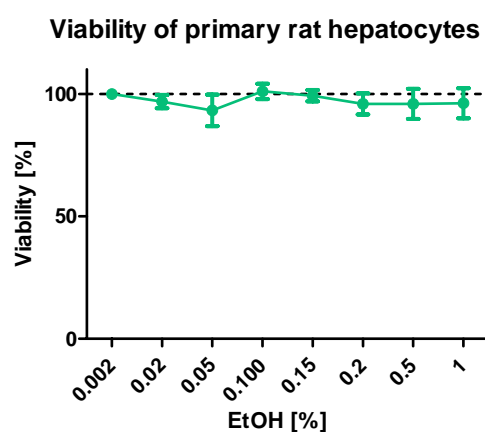

Figure 9: Viability of primary rat hepatocytes in response to increasing concentrations of ethanol as measured by neutral red assay. Values are expressed as fold of the lowest EtOH concentration (0.002%) and are represented as mean ±SEM, n=3.

Viability of primary rat hepatocytes in response to increasing concentrations of ethanol, which is used as solvent for the treatment of cells with fatty acids, was found to be not significantly altered at concentrations ranging from 0.002 to 1% (see Figure 9).

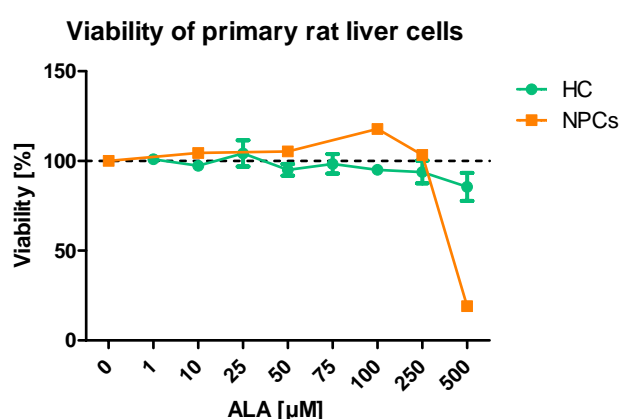## Viability of primary rat hepatocytes and non-parenchymal cells in response to α-linolenic acid

Figure 10: Viability of primary rat HCs and NPCs in response to increasing concentrations of α-linolenic acid as measured by neutral red assay. Values are expressed as fold respective ethanol control and are represented as mean ±SEM, HC: n=3, NPC: n=1.

Viability of primary rat liver cells when treated with increasing concentrations of α-linolenic acid was assayed by the uptake of neutral red in the medium by living cells. Therefore primary rat hepatocytes and mesenchymal cells were first purified from livers and incubated for 24 hours in the presence of α-linolenic acid or the corresponding concentration of solvent (see Table 2). Following this, neutral

red uptake of α-linolenic acid and solvent treated cells was assayed, respectively, and viability in response to α-linolenic acid was calculated as fold solvent control (see Figure 10).

Primary rat hepatocytes tolerate higher concentrations of α-linolenic acid than mesenchymal cells. At a concentration of 500µM the viability of hepatocytes decreased to 85.5% whereas at the same concentration the viability of mesenchymal cells was down to 19%.

Secretion of tumor-necrosis-factor-α from primary rat mesenchymal cells in response to free fatty acids

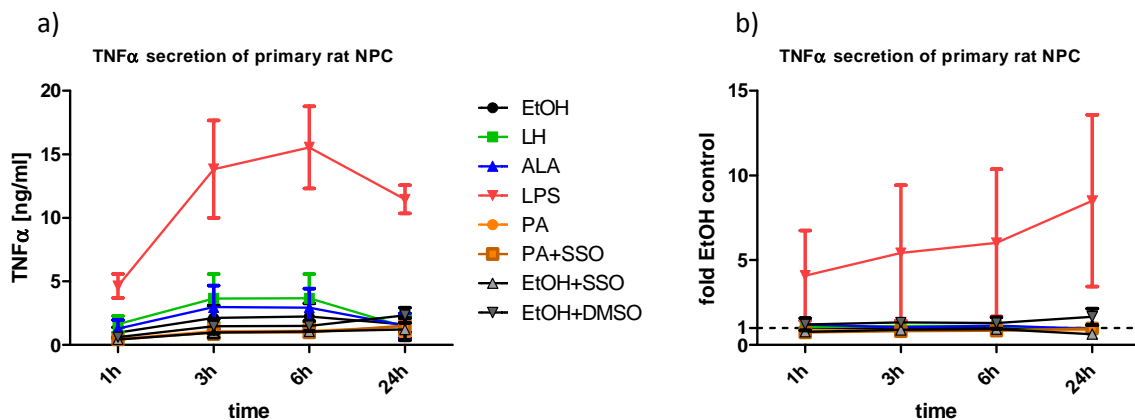**Figure 11: TNFα secretion into the supernatant of primary rat mesenchymal cells (NPCs) in response to free fatty acids (10µM), ethanol (0.02%), LPS (10ng/ml), SSO (250mM) or DMSO (0.1%), respectively, measured by ELISA. a) Absolute TNFα concentration in the supernatant of NPCs at different time points (see Table 15), b) TNFα secretion fold ethanol control. Values represent means ±SEM.**

TNFα	EtOH			LH			ALA			LPS		
[ng/ml]	Mean	SEM	N	Mean	SEM	n	Mean	SEM	N	Mean	SEM	N
1h	0,964	0,434	5	1,643	0,653	2	1,292	0,672	3	4,645	0,939	2
3h	2,129	0,989	6	3,665	1,902	3	2,968	1,715	4	13,822	3,833	2
6h	2,242	1,042	6	3,681	1,900	3	2,936	1,508	4	15,540	3,239	2
24h	1,626	0,621	5	1,422	0,9036	3	1,523	0,966	3	11,458	1,122	2
	PA			PA+SSO			EtOH+SSO			EtOH+DMSO		
	Mean	SEM	N	Mean	SEM	n	Mean	SEM	N	Mean	SEM	N
1h	0,490	0,231	2	0,418	0,202	2	0,434	0,199	2	0,624	0,217	2
3h	1,067	0,563	2	0,950	0,464	2	0,985	0,386	2	1,470	0,561	2
6h	1,114	0,484	2	0,990	0,325	2	1,064	0,302	2	1,485	0,410	2
24h	1,417	0,673	2	1,518	0,607	2	1,231	0,864	2	2,349	0,595	2

Table 15: Means of TNFα concentrations [ng/ml], SEM and n of experiments used in Figure 11a).

The secretion of tumor-necrosis-factor-α (TNFα) was assayed in primary rat mesenchymal cells after 1 hour, 3 hours, 6 hours and 24 hours of treatment with ethanol, free fatty acids (LH, PA, ALA), LPS, PA in combination with the CD36 inhibitor SSO and DMSO, respectively. Figure 11a shows the calculated absolute concentration in the supernatant of treated cells. LPS induced the highest secretion of TNFα in mesenchymal cells which was 4-times (1h), 5-times (3h), 6-times (6h) or even 8.5-times (24h) higher than from control cells. The used fatty acids, DMSO and the CD36 inhibitor SSO did not show any increase of TNFα secretion compared to the controls.

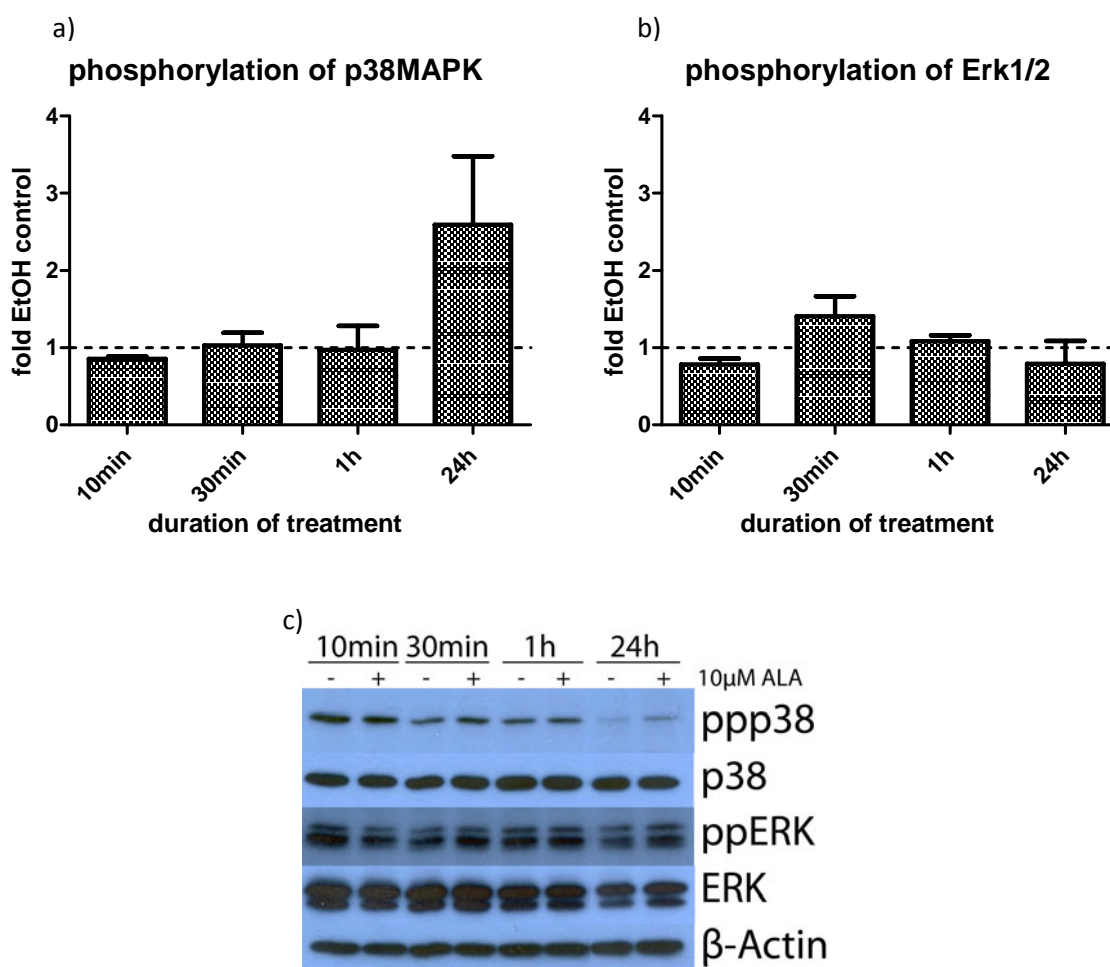## Effects of α-linolenic acid treatment on p38MAPK and Erk phosphorylation

Figure 12: p38MAPK phosphorylation and Erk phosphorylation in primary rat non-parchenchymal cells treated with 10μM α-linolenic acid for 10min, 30min, 1 hour and 24 hours. a) densitometric evaluation of the phosphorylation status of p38MAPK; b) densitometric evaluation of the phosphorylation status of ERK1/2; c) one of three similar blots.

	p38			ERK1/2		
	mean	SEM	n	mean	SEM	n
10min	0,856	0,026	3	0,784	0,076	2
30min	1,027	0,163	3	1,408	0,261	2
1h	0,970	0,314	3	1,085	0,077	3
24h	2,595	0,884	2	0,790	0,297	2

Table 16: mean volumes evaluated by densitometry of blots ± SEM and n of experiments used in Figure 12a) and b).

Phosphorylation of p38MAPK was not increased compared to solvent controls at time points 10min, 30min and 1 hour. After 24 hours a 2.5-fold increase could be detected. This might not only be a result of an actual change in phosphorylation, but also a result of the blot intensity itself, as the p38 phosphorylation in α-linolenic acid treated and control cells were generally low. Therefore every minor change in the volumes evaluated by densitometry leads to major changes in fold-control ratios. Phosphorylation of p38MAPK can be considered increased after 24 hours when treated with α-linolenic acid compared to solvent control, but probably not to that extent.

Results

Phosphorylation of ERK1/2 was slightly reduced after 10 min in α-linolenic acid treated cells. No significant change in α-linolenic acid treated cells compared to the solvent treated ones could be observed.

Effects of free fatty acids on mRNA expression levels of COX-2, iNOS and TNFα in primary rat liver cells
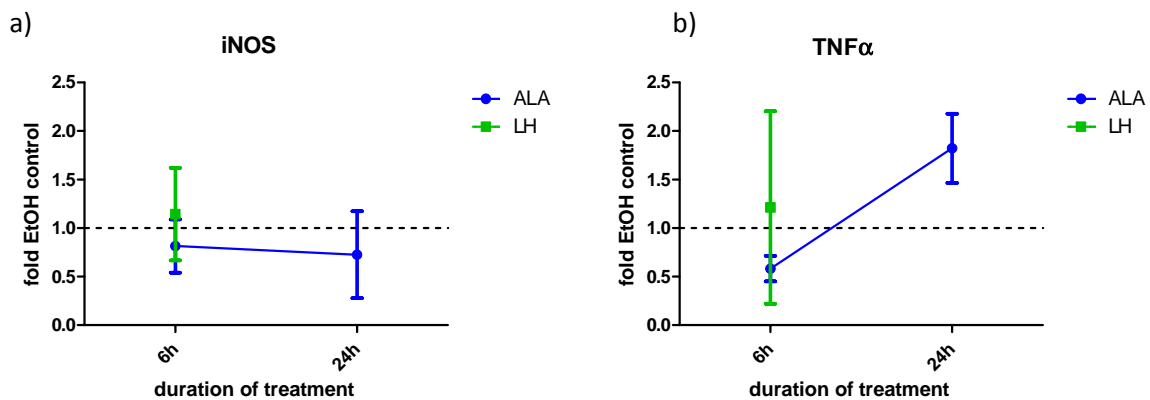
Gene expression levels in primary rat hepatocytes

Figure 13: Expression of iNOS (a) and TNFα (b) mRNA in response to 50µM of α-linolenic acid (ALA) or linoleic acid (LH) in primary rat hepatocytes after 6 and 24 hours of treatment, respectively. Values were calculated using the ΔΔCt method, normalized to β-2-microglobulin and expressed as fold ethanol control, values represent mean ±SEM.

	ALA			LH		
iNOS	**Mean**	**SEM**	**n**	**Mean**	**SEM**	**n**
6h	0,815	0,273	4	1,145	0,476	3
24h	0,727	0,447	3			
TNFα						
6h	0,583	0,132	2	1,212	0,991	2
24h	1,822	0,356	2			

Table 17: means of ΔΔCt values, SEM and n of experiments used in Figure 13a) and b).

COX-2 was undetectable in hepatocytes in response to free fatty acid treatment most of the time. iNOS and TNFα could be detected in most experiments, although neither iNOS nor TNFα were detectable after 24h when heptocytes were treated with 50µM linoleic acid (LH, see Figure 13).

Treatment of hepatocytes with linoleic acid did not significantly change expression of iNOS or TNFα. α-Linolenic acid reduced expression of TNFα 0.5-fold after 6 hours of treatment but increased the expression about 1.82-fold compared to solvent treated cells.

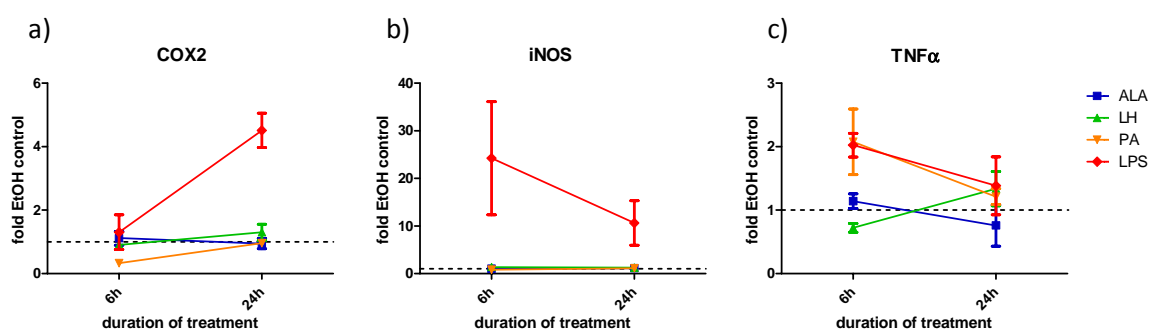## Gene expression levels in primary rat mesenchymal cells

Figure 14: Expression of COX2 (a), iNOS (b) and TNFα (c) mRNA in response to 10μM of α-linolenic acid (ALA), linoleic acid (LH), palmitic acid (PA) or 10ng/ml LPS in primary rat mesenchymal cells after 6 and 24 hours of treatment, respectively. Values were calculated using the ΔΔCt method, normalized to β-2-microglobulin and expressed as fold ethanol control, values represent mean ±SEM.

COX2	ALA			LH			PA			LPS		
	Mean	SEM	n	Mean	SEM	n	Mean	SEM	n	Mean	SEM	n
6h	1,116	0,216	4	0,909	0,012	2	0,332	0,080	2	1,304	0,545	2
24h	0,943	0,158	2	1,305	0,252	3	0,962	0,024	3	4,512	0,544	2
iNOS												
6h	1,012	0,322	3	1,386	0,358	3	0,827	0,023	2	24,249	11,856	3
24h	1,162	0,407	3	1,243	0,268	3	1,145	0,294	3	10,620	4,662	3
TNFα												
6h	1,141	0,114	4	0,720	0,069	3	2,075	0,516	3	2,023	0,187	2
24h	0,757	0,322	3	1,337	0,269	3	1,210	0,125	3	1,383	0,456	2

Table 18: Means of ΔΔCt values, SEM and n of experiments used in Figure 14a), b) and c).

COX-2 mRNA expression was elevated when mesenchymal cells were treated with LPS for 24h. α-Linolenic acid, linoleic acid and palmitic acid showed no elevation of COX-2 expression. Palmitic acid tended to reduce the expression of COX-2 mRNA after 6 hours of treatment.

mRNA levels of iNOS were only elevated when the cells were treated with LPS, leading to an 24-fold and 11-fold increase of expression after 6 and 24 hours of treatment, respectively.

The expression level of TNFα was slightly decreased when cells were treated with linoleic acid for 6 hours and around 2-fold increased after treatment with palmitic acid or LPS for the same period of time. α-Linolenic acid did not change the expression of TNFα compared to the ethanol controls. After 24 hours of treatment TNFα levels were as high as in the ethanol controls, regardless of the treatment.

Results

Effects of inhibition of CD36 by SSO on primary rat liver cells

As CD36 is one of the most studied receptors of free fatty acids and might also act as translocase for free fatty acids in several cell types (Silverstein & Febbraio, 2009; He, Lee, Febbraio, & Xie, 2011), we were interested whether inhibition of CD36 by sulfosuccinimidyl oleate (SSO) would result in any change in mRNA expression levels of inflammation-associated genes or phosphorylation of kinases in primary liver cells.

Therefore we first estimated the general expression of CD36 in hepatocytes, endothelial cells and Kupffer cells of the rat liver.

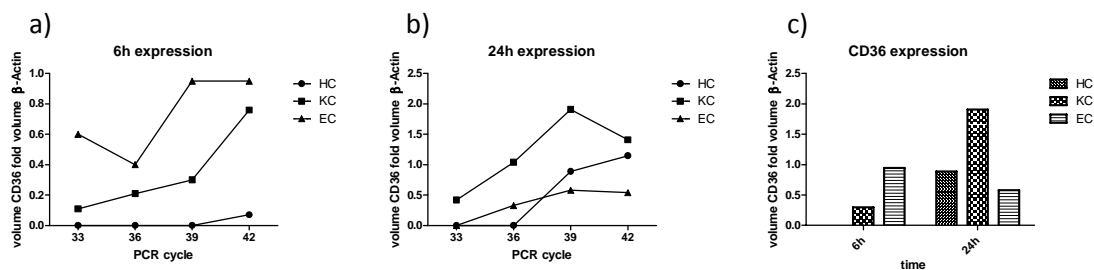### *Expression of CD36 in primary rat liver cells*

Figure 15: Expression of CD36 in primary rat hepatocytes (HC), Kupffer cells (KC) and endothelial cells (EC) expressed as densitometric volumes of CD36 fold volumes of β-actin. a) CD36 fold β-actin 6h after plating of cells at PCR cycles 33-42. b) CD36 fold β-actin 24h after plating of cells at PCR cycles 33-42. c) CD36 fold β-actin of HCs, KCs and ECs 6h and 24h after plating. Densitometric volumes were taken from PCR cycle 39.

RNA of cultured primary rat hepatocytes, Kupffer cells and endothelial cells from collagenase-perfused livers of untreated rats was harvested 6 hours and 24 hours after plating of the cells. Reverse-transcriptase-PCR was performed to convert RNA into cDNA. The obtained cDNA was used as template for PCR amplification using forward and reverse primers for CD36 and β-Actin. Amplified products from PCR cycles 33, 36, 39 and 42 were run on an agarose gel. Volumes of CD36 and β-actin PCR products of each cell type and PCR cycle were determined by densitometry and CD36-fold-β-actin ratios were calculated.

6 hours after plating of cells, CD36 expression was detectable in Kupffer cells and endothelial cells (see Figure 15a). Expression in hepatocytes could just be detected upon cycle 42. 24 hours after plating expression of CD36 was detectable in all three different cell types with Kupffer cells showing the highest expression, followed by hepatocytes and endothelial cells (see Figure 15b and c). Thus all three cell types express CD36 and might therefore be capable of detection of free fatty acids via CD36.

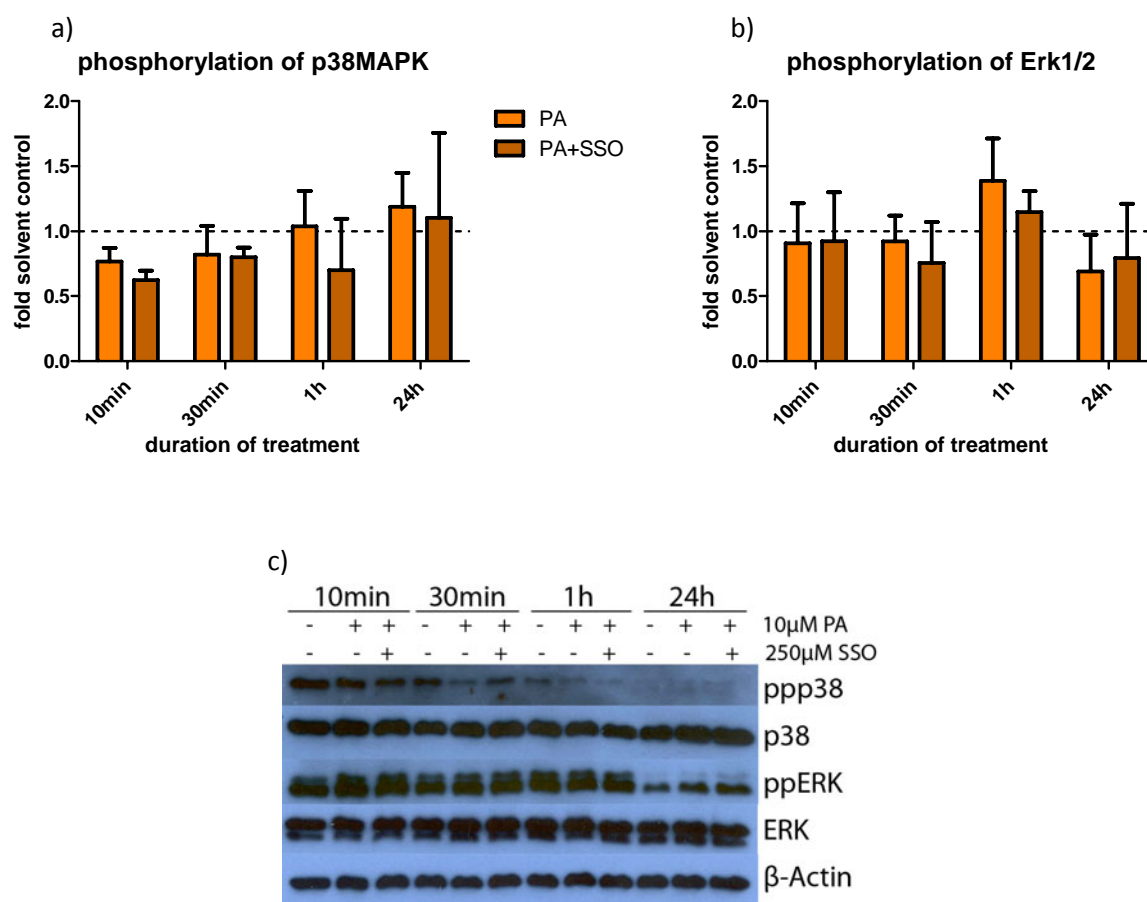### Effects of CD36 inhibition on the phosphorylation status of p38MAPK and ERK

Figure 16: Effects of PA treatment and inhibition of CD36 by SSO on primary rat non-parenchymal cells, respectively. Shown blot represents one of three independent experiments.

p38	PA			PA+SSO		
	mean	SEM	n	mean	SEM	n
10min	0,765	0,105	3	0,624	0,071	3
30min	0,819	0,221	3	0,798	0,075	3
1h	1,037	0,273	3	0,700	0,392	3
24h	1,188	0,261	3	1,103	0,654	3
ERK1/2	PA			PA+SSO		
	Mean	SEM	n	Mean	SEM	n
10min	0,907	0,308	3	0,924	0,376	3
30min	0,922	0,198	3	0,755	0,316	3
1h	1,386	0,326	3	1,147	0,160	3
24h	0,689	0,282	3	0,794	0,417	3

Table 19: mean volumes evaluated by densitometry of blots ± SEM and n of experiments used in Figure 16a) and b).

Phosphorylation of p38MAPK was reduced to about 77% of controls when primary rat mesenchymal cells were treated with palmitic acid for 10 min. Treatment with palmitic acid in combination with SSO resulted in a further decrease of p38MAPK phosphorylation to about 62% of controls (see Figure 16a) and Table 19). This suppressive effect of SSO was abrogated at time point 30min although SSO tended to reduce the phosphorylation of p38 more than palmitic acid alone. This trend could again be detected after 1 hour of treatment but was not significant. Phosphorylation was at the level of the controls after 24 hours.

Results

Treatment of primary rat mesenchymal cells with palmitic acid or palmitic acid in combination with SSO, respectively, had no significant effect on the phosphorylation status of Erk1/2, although palmitic acid tended to reduce it after 24 hours of treatment (see Figure 16b and Table 19).

Effects of CD36 inhibition on mRNA levels of COX-2, iNOS and TNFα in primary rat mesenchymal cells

For inhibition studies of CD36 by sulfosuccinimidyl-oleate (SSO) palmitic acid (PA) was used as a fatty acid as it showed the highest induction of inflammatory markers compared to α-Linolenic acid (ALA) and linoleic acid LH (see Figure 14).
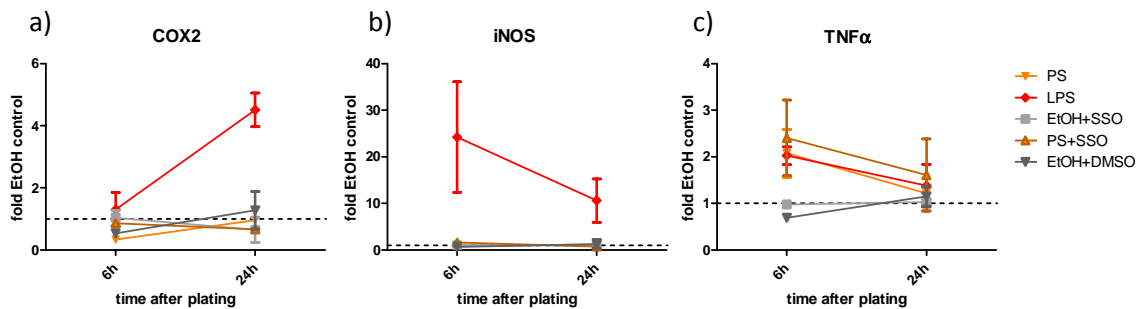

Figure 17: mRNA expression levels of COX2 (a), iNOS (b) and TNFα (c) in response to 10µM PA or 10ng/ml LPS or 250mM SSO in primary rat mesenchymal cells after 6h and 24h of treatment. Values were calculated using the ΔΔCt method, normalized to β-2-microglobulin and expressed as fold EtOH control, values represent mean ±SEM

COX2	PA			PA+SSO			LPS		
	Mean	SEM	n	Mean	SEM	n	Mean	SEM	n
6h	0,332	0,080	2	0,863	0,063	2	1,304	0,545	2
24h	0,962	0,024	3	0,669	0,031	2	4,512	0,544	2
	EtOH+SSO			EtOH+DMSO					
	Mean	SEM	n	Mean	SEM	n			
6h	1,035	0,240	2	0,536	0,014	2			
24h	0,649	0,402	2	1,277	0,600	2			
iNOS	PA			PA+SSO			LPS		
	Mean	SEM	n	Mean	SEM	n	Mean	SEM	n
6h	0,827	0,023	2	1,587	0,287	2	24,249	11,856	3
24h	1,145	0,294	3	0,722	0,437	2	10,620	4,662	3
	EtOH+SSO			EtOH+DMSO					
	Mean	SEM	n	Mean	SEM	n			
6h	1,048	0,197	2	0,691	0,044	2			
24h	1,010	0,460	2	1,262	0,950	2			
TNFα	PA			PA+SSO			LPS		
	Mean	SEM	n	Mean	SEM	n	Mean	SEM	n
6h	2,075	0,516	3	2,406	0,812	2	2,023	0,187	2
24h	1,210	0,125	3	1,608	0,774	2	1,383	0,456	2
	EtOH+SSO			EtOH+DMSO					
	Mean	SEM	n	Mean	SEM	n			
6h	0,974	0,072	2	0,690	0,039	2			
24h	1,031	0,189	2	1,152	0,213	2			

Table 20: means of ΔΔCt values, SEM and n of experiments used in Figure 17a), b) and c).

mRNA expression of COX-2 was decreased after 6 hours of treatment with palmitic acid compared to solvent control (approx. 0.33-fold). This effect was not seen after 24 hours. Mesenchymal cells treated with palmitic acid in combination with SSO did not showed any significant effect neither

compared to the treatment with palmitic acid alone nor to cells treated with ethanol and DMSO. LPS led to an increase in expression of COX-2 after 24 hours (approx. 4.5-fold)

iNOS expression was slightly reduced (0.86-fold) when cells were treated with palmitic acid for 6 hours and tended to be elevated (1.59-fold) when treated with palmitic acid and SSO for 6 hours. Neither of the controls showed any significant change in the mRNA expression levels of iNOS.

Palmitic acid, LPS and palmitic acid in combination with SSO resulted in an approx. 2-fold elevation of TNFα expression after 6 hours of treatment. After 24 hours the expression of TNFα was on the same level as the solvent control. Neither of the controls for the CD36 inhibitor SSO (EtOH+DMSO, EtOH+SSO) had any effect on TNFα expression.

Effects of CD36 inhibition on mRNA levels of COX-2, iNOS and TNFα in primary rat endothelial cells

As the expression analysis of primary rat mesenchymal cells was not always conclusive, we decided to separate this cell fraction into endothelial cells and Kupffer cells and analyzed the expression levels of inflammation associated genes in both cell types separately.
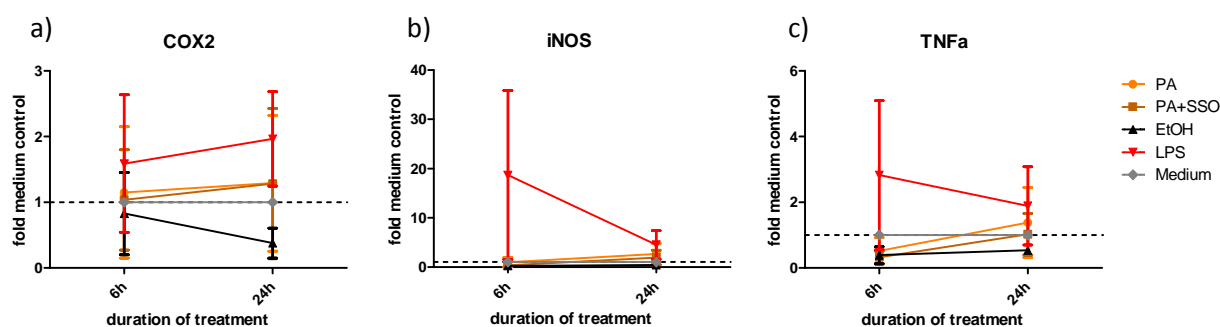

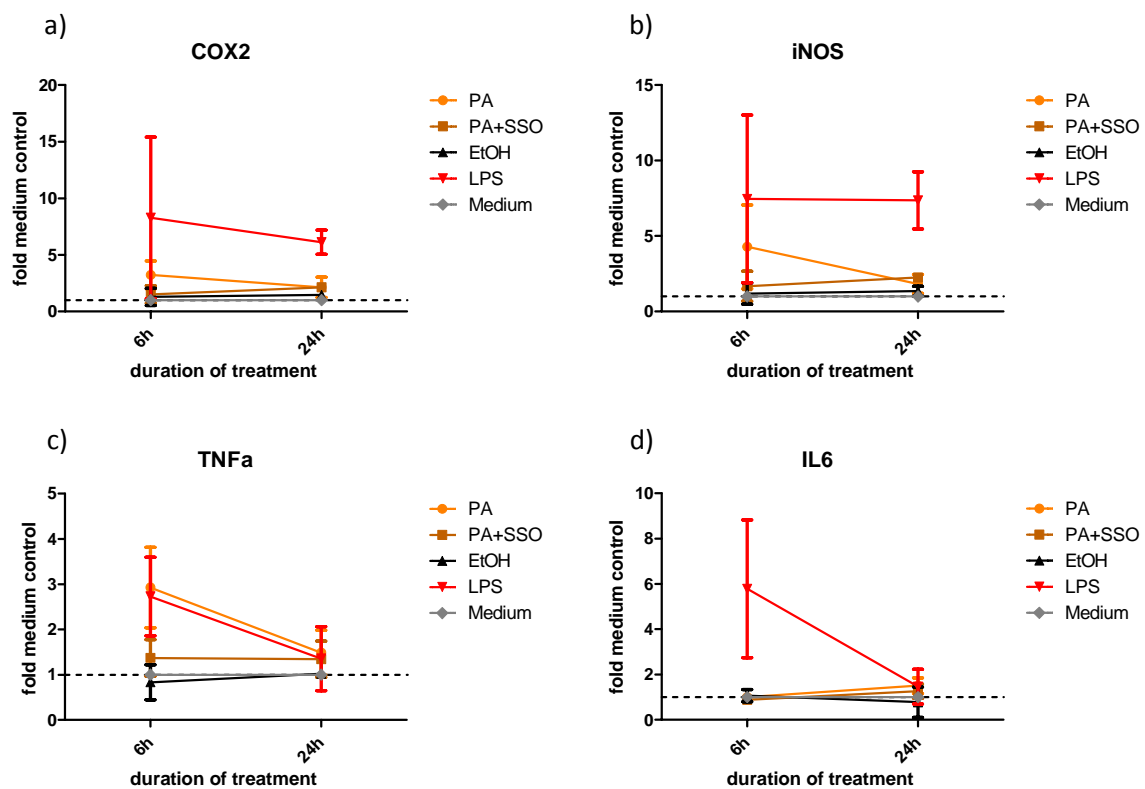**Figure 18: Expression of COX2 (a), iNOS (b) and TNFα (c) mRNA in response to 10µM PA or 0.02% EtOH or 10ng/ml LPS or 250mM SSO in primary rat endothelial cells after 6h and 24h of treatment, respectively. Values were calculated using the ΔΔCt method, normalized to β-2-microglobulin and expressed as fold medium control, values represent mean ±SEM.**

COX2	PA			PA+SSO			LPS			EtOH		
	Mean	SEM	n	Mean	SEM	n	Mean	SEM	N	Mean	SEM	n
6h	1,150	1,001	2	1,036	0,763	2	1,589	1,048	2	0,828	0,626	2
24h	1,290	1,035	2	1,285	1,146	2	1,965	0,721	2	0,378	0,226	2
iNOS	PA			PA+SSO			LPS			EtOH		
	Mean	SEM	n	Mean	SEM	n	Mean	SEM	n	Mean	SEM	n
6h	0,985	0,920	2	0,346	0,210	2	18,699	17,194	2	0,238	0,108	2
24h	2,668	2,162	2	1,928	1,469	2	4,500	2,922	2	0,404	0,157	2
TNFα	PA			PA+SSO			LPS			EtOH		
	Mean	SEM	n	Mean	SEM	n	Mean	SEM	n	Mean	SEM	n
6h	0,519	0,406	2	0,322	0,185	2	2,826	2,272	2	0,385	0,264	2
24h	1,385	1,070	2	1,026	0,638	2	1,889	1,198	2	0,531	0,057	2

Table 21: means of ΔΔCt values, SEM and n of experiments used in Figure 18a), b) and c).

The expression of COX-2 did not significantly change upon treatment with palmitic acid, nor was it changed by the treatment with the CD36 inhibitor SSO. LPS led to a 2-fold increase of expression after 24 hours. The solvent control decreased the expression after 24 hours of treatment.

Palmitic acid had no significant influence on iNOS expression after 6 and 24 hours. The combination of palmitic acid and SSO resulted in a decrease of iNOS expression after 6 hours and was increased,

Results

although not significantly, after 24 hours. LPS did increase the expression of iNOS in endothelial cells after 6 and 24 hours but with a high variation in intensity. The ethanol treatment resulted in a decrease of iNOS expression after 6 and 24 hours.

Expression of TNFα was slightly decreased upon treatment with palmitic acid after 6 hours, but was at the level of the medium control after 24 hours. Palmitic acid in combination with SSO had a similar effect, resulting in a decrease after 6 hours and coming back to the level of the medium control after 24 hours. LPS increased the expression of TNFα only after 6 hours and also slightly after 24 hours but with considerable variation in intensity at both time points. The treatment with ethanol reduced the expression at both investigated time points.

Effects of CD36 inhibition on mRNA levels of COX-2, iNOS, TNFα and IL6 in primary rat Kupffer cells

Figure 19: Expression of COX2 (a), iNOS (b), TNFα (c) and IL6 (d) mRNA in response to 10µM PA or 0.02% EtOH or 10ng/ml LPS or 250mM SSO in primary rat Kupffer cells after 6h and 24h of treatment, respectively. Values were calculated using the ΔΔCt method, normalized to β-2-microglobulin and expressed as fold medium control, values represent mean ±SEM.

COX2	PA			PA+SSO			LPS			EtOH		
	Mean	SEM	n	Mean	SEM	n	Mean	SEM	N	Mean	SEM	n
6h	3,242	1,232	2	1,289	0,765	2	8,286	7,120	2	1,289	0,765	2
24h	2,146	0,904	2	1,467	0,081	2	6,126	1,067	2	1,467	0,081	2
iNOS	PA			PA+SSO			LPS			EtOH		
	Mean	SEM	n	Mean	SEM	n	Mean	SEM	n	Mean	SEM	n
6h	4,289	2,778	2	1,681	0,981	2	7,466	5,548	2	1,191	0,701	2
24h	1,830	0,624	2	2,253	0,082	2	7,366	1,889	2	1,359	0,327	2
TNFα	PA			PA+SSO			LPS			EtOH		
	Mean	SEM	n	Mean	SEM	n	Mean	SEM	n	Mean	SEM	n
6h	2,926	0,886	2	1,371	0,404	2	2,7305	0,869	2	0,833	0,387	2
24h	1,489	0,495	2	1,345	0,399	2	1,359	0,706	2	1,026	0,079	2
IL6	PA			PA+SSO			LPS			EtOH		
	Mean	SEM	n	Mean	SEM	n	Mean	SEM	n	Mean	SEM	n
6h	1,003	0,132	2	0,877	0,054	2	5,789	3,042	2	1,064	0,272	2
24h	1,507	0,346	2	1,265	0,311	2	1,473	0,766	2	0,775	0,674	2

Table 22: means of ΔΔCt values, SEM and n of experiments used in Figure 19Table 11a), b), c) and d).

Palmitic acid increased the expression of COX-2 in primary rat Kupffer cells 3.2-fold after 6 hours of treatment and 2.1-fold after 24 hours. This could be reduced to 1.3-fold and 1.5-fold after 6 hours and 24 hours, respectively, by addition of the CD36 inhibitor SSO. The solvent control had no significant effect on expression of COX-2.

Expression of iNOS could also be induced by palmitic acid compared to the solvent control and led to a 4.3-fold and 1.8-fold increase after 6 hours and 24 hours, respectively. The elevation after 6 hours could be decreased by addition of SSO to 1.6-fold, but this had no effect after 24 hours. The solvent control had no significant effect on iNOS expression.

The Expression of TNFα was 2.9-fold increased when Kupffer cells were treated with palmitic acid for 6 hours. This could be decreased to 1.3-fold by SSO. The elevation caused by palmitic acid was reduced to 1.5-fold after 24 hours of treatment. The addition of SSO had a similar effect leading to an equal level of TNFα expression (1.3-fold). The elevation caused by palmitic acid alone was as high as the elevation caused by LPS (2.9-fold and 1.5-fold 6 and 24 hours, respectively, caused by palmitic acid and 2.7-fold and 1.4-fold 6 and 24 hours, respectively, caused by LPS). The solvent control had no significant effect on gene expression of TNFα.

Gene expression of interleukin6 (IL6) was also analysed in Kupffer cells as its action is in part regulated by TNFα. Palmitic acid did not significantly change the levels of IL6 expression (1-fold and 1.5-fold after 6 and 24 hours, respectively, compared to the solvent control), neither did the addition of SSO (0.8-fold and 1.3-fold after 6 and 24 hours, respectively). LPS induced IL6 expression after 6 hours to approx. 5.8-fold compared to the solvent control. This elevation was not seen after 24 hours.

Results

Real-time measurement of ADAM17/TACE activity on live cells using a fluorogenic substrate

Since TNFα secretion into the medium of primary rat mesenchymal cells could not always be measured to the same extent when cells were treated with free fatty acids and because the enzyme responsible for 80-90% of TNFα shedding (Arribas & Borroto, 2002) is also the sheddase for the soluble forms of TNFα receptors 1 and 2 (p75 TNFα-RII, p55 pro-TNFα-RI), which could have bound to secreted TNFα, we decided to directly measure the activity of this enzyme on primary rat Kupffer cells as these cells increased the expression of TNFα in response to the treatment with palmitic acid. As ADAM17/TACE is not only responsible for the shedding of TNFα, p75 TNFα-RII and p55 pro- TNFα-RI, but also for the shedding of IL6-Rα, HB-EGF, TGFα, proamphiregulin and HER-4, direct measurement of the activity of this enzyme becomes even more interesting (Arribas & Borroto, 2002).

As a substrate for ADAM17/TACE we decided to use the commercially available DABCYL-TNFα-Edans (Bachem, Switzerland) and performed the TACE assay using an excitation wavelength of 360nm and measuring the emission at 485nm.

Fluorescence of various buffers and media

First of all we had to choose a suitable buffer for the enzyme reaction. It should not show any fluorescence at the used excitation and emission wavelengths, not lead to hydrolysis of the substrate without any enzyme present, allow the hydrolytic reaction to occur and should not do any major damage to the cells for the time of incubation with the substrate.

Therefore we tested several buffers and media - that were either common or were reported to be used for the measurement of fluorescent reactions - for their fluorescence at the used wavelengths.
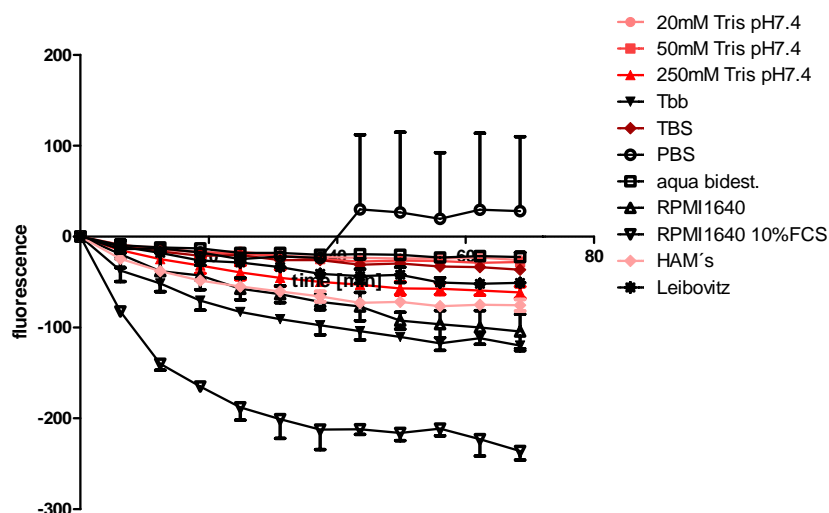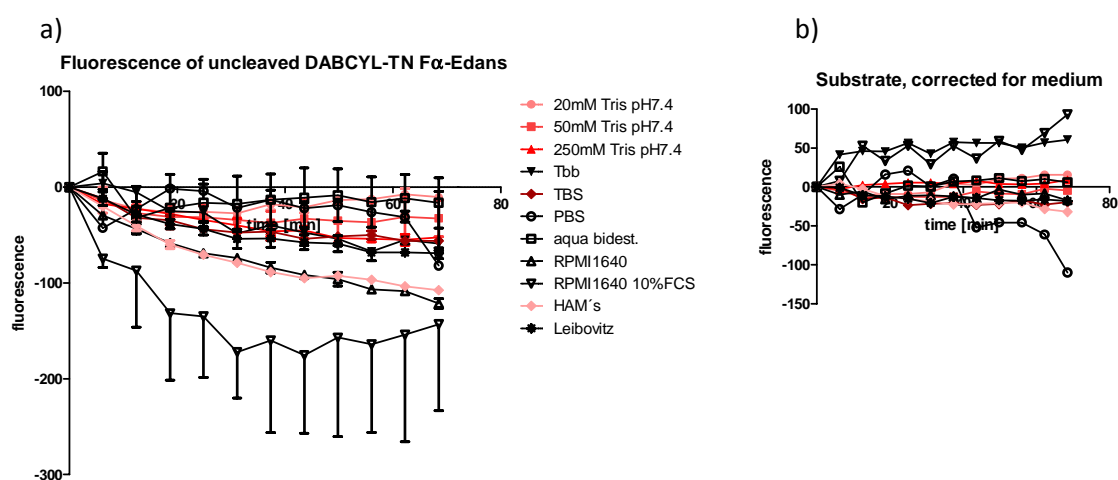

Figure 20: Fluorescence of various buffers and media. Fluorescence was measured once per cycle at λ_{em}: 485nm when samples were excited at λ_{ex}: 360nm in 12 cylces, 6.23min per cycle. Colored curves indicate buffers/media used for TACE activity measured on live cells due to their superior properties (see text and Figure 21 - Figure 25) compared to other buffers. Starting values were arbitrarily set to 0 and values represent arbitrary units ±SD of duplicates.

Fluorescence of 20mM Tris pH7.4, 50mM Tris pH7.4, 250mM Tris pH7.4, Tris-based-buffer (Tbb, see materials and methods), Tris-buffered-saline (TBS), phosphate-buffered-saline (PBS), distilled water

(aqua bidest.), RPMI-1640 medium, RPMI-1640 medium supplemented with 10%FCS (RPMI 1640 10%FCS), HAM's F-15 medium and Leibovitz L-15 medium was measured for 68 min at 37°C in duplicates at the used excitation and emission wavelengths (see Figure 20). Buffers and media with a minimal fluorescence were used for further experiments to estimate their applicability (20mM Tris pH7.4, 50mM Tris pH7.4, 250mM Tris pH7.4, TBS and HAM's).

The buffers with the lowest autofluorescence were found to be PBS, water, 20mM Tris pH7.4, 50mM Tris pH 7.4 and TBS (Figure 20).

Stability of DABCYL-TNFα-Edans in various buffers and media

Figure 21: a) Fluorescence of DABCYL-TNFα-Edans in various buffers and media. Fluorescence was measured once per cycle at λ_{em}: 485nm when samples were excited at λ_{ex}: 360nm in 12 cylces, 6.23min per cycle. Colored curves indicate buffers/media used for TACE activity measured on live cells due to their superior properties (see text and Figure 21 - Figure 25) compared to other buffers. Starting values were arbitrarily set to 0 and values represent arbitrary units ±SD of duplicates. B) values of Figure 20 were subtracted from values of Figure 21a) to compensate for buffer fluorescence.

The second important property, besides low autofluorescence, of a suitable buffer is guaranteeing the stability of the used substrate. Hydrolysis of the substrate without any proteinase present has to be excluded in order to develop a sensitive and quantifiable assay.

Fluorescence of 10µM DABCYL-TNFα-Edans in various buffers and media was measured every 6.23 minutes for about 68 minutes at 37°C (see Figure 21a). The fluorescence of the buffers and media was subtracted from the fluorescence of the substrate in the respective buffers and media (see Figure 21b), to exclude any buffer that shows a negative autofluorescence (e.g. Figure 20: RPMI1640 10%FCS) and hydrolysis of the substrate. A combination of these two effects would result in low fluorescence (the extent depending on the relative strength of the two effects) and therefore lead to the misleading conclusion that the buffer would be suitable.

Results

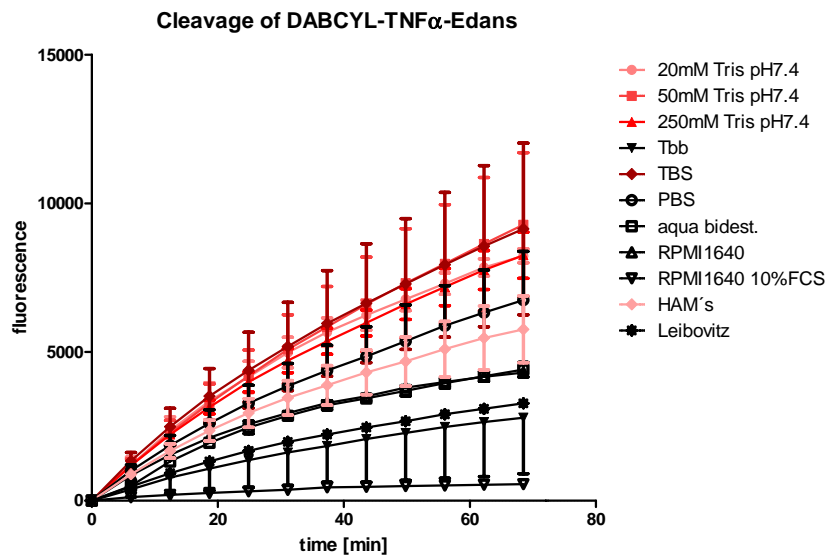## Cleavage of DABCYL-TNFα-Edans by trypsin measured in various buffers and media

Figure 22: Fluorescence of DABCYL-TNFα-Edans incubated with 1µg trypsin in various buffers and media. Fluorescence was measured once per cycle at λ_{em}: 485nm when samples were excited at λ_{ex}: 360nm in 12 cylces, 6.23min per cycle. Colored curves indicate buffers/media used for TACE activity measured on live cells due to their superior properties compared to other buffers. Starting values were arbitrarily set to 0 and values represent arbitrary units ±SD of duplicates.

The third property of the most appropriate buffer is its ability to allow the enzymatic reaction to happen. The cleaving reaction should also result in as much fluorescence as possible to ensure that the final assay has a maximum sensitivity. We therefore used trypsin as a proteinase for cleaving the substrate. This is possible because DABCYL-TNFα-Edans contains two arginin residues (DABCYL-Leu-Ala-Gln-Ala-Val-Arg-Ser-Ser-Ser-Arg-EDANS) which are potential cleavage sites for trypsin. The reaction was performed in the already mentioned buffers and media (Figure 22). The highest fluorescence of cleaved substrate by trypsin could be measured in 250mM Tris pH7.4, TBS, 20mM Tris pH7.4 and 50mM Tris pH7.4.

Signal-to-background ratio of DABCYL-TNFα-Edans in various buffers and media
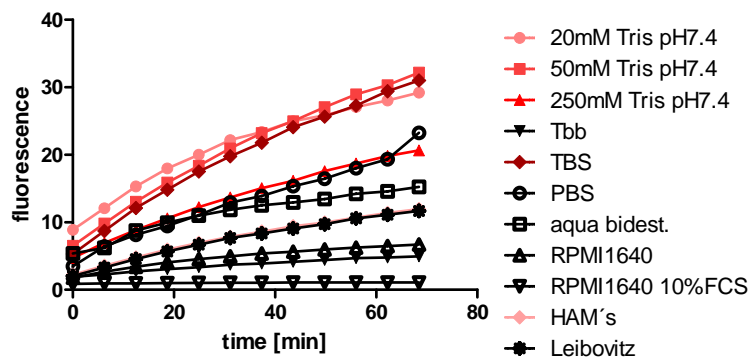
Figure 23: Arbitrary fluorescence units of DABCYL-TNFα-Edans incubated with 1µg trypsin (Figure 22) were divided by arbitrary fluorescence units of substrate alone (Figure 21a). Fluorescence was measured once per cycle at λ_{em}: 485nm when samples were excited at λ_{ex}: 360nm in 12 cylces, 6.23min per cycle. Colored curves indicate buffers/media used for TACE activity measured on live cells due to their superior properties compared to other buffers. Starting values were arbitrarily set to 0 and values represent arbitrary units ±SD of duplicates.

In addition to facilitate the stability of the substrate (see Figure 21b), the buffer of choice would have to allow the specific cleavage of the substrate to happen. The specificity of the reaction or the signal:background ratio was therefore calculated as the ratio of fluorescence of cleaved substrate to fluorescence of uncleaved substrate (see Figure 23). According to this calculation the Tris-buffers 20mM Tris pH7.4, 50mM Tris pH7.4, TBS and 250mM Tris pH7.4, together with PBS showed the highest signal-to-background ratios.

Difference in TACE activity of human monocytic THP1 cells depending on activation status
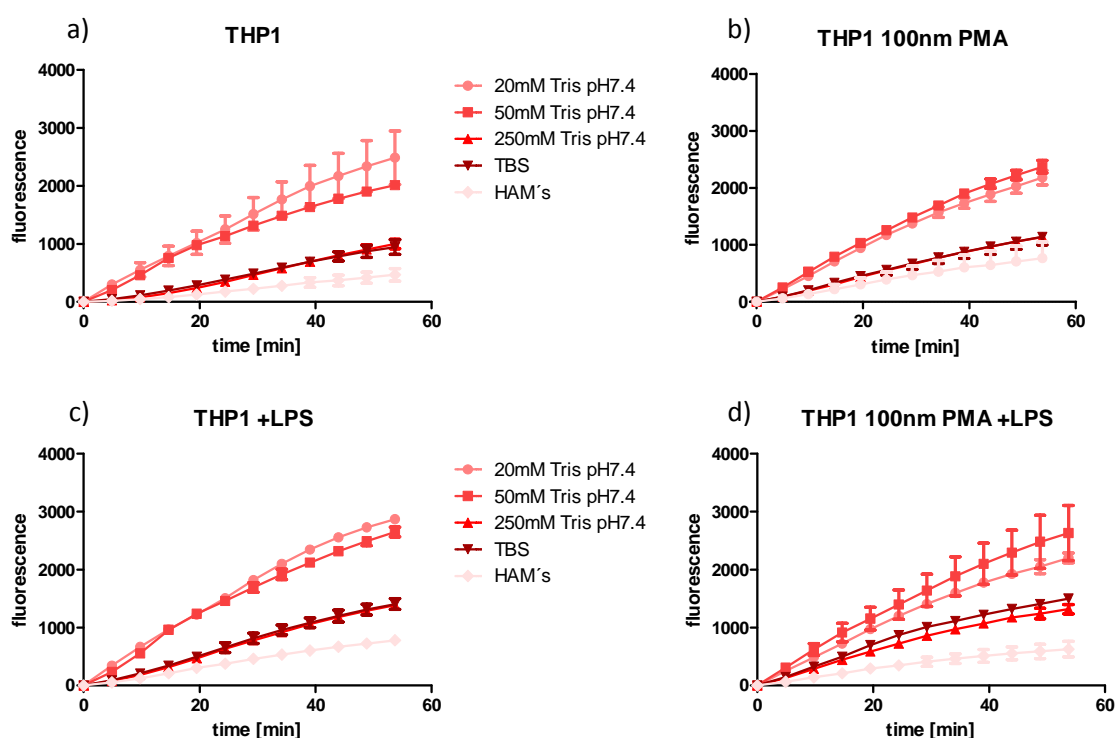
Figure 24: TACE activity measured by hydrolysis of DABCYL-TNFα-Edans by a) THP1 incubated for 27 hours in RPMI-1640; b) THP1 incubated for 27 hours in RPMI-1640 supplemented with 100nM PMA; c) THP1 incubated for 27h in RPMI-1640 including the last 3 hours with 10ng/ml LPS; d) THP1 incubated in RPMI-1640 supplemented with 100nM PMA for 27 hours including the last 3 hours with 10ng/ml LPS. Fluorescence was measured in 20mM Tris pH7.4, 50mM Tris pH7.4, 250mM Tris pH7.4, TBS and HAM's medium, respectively, at λem: 485nm when samples were excited at λex: 360nm in 12 cylces (4.88min per cycle). Starting values were arbitrarily set to 0 and values represent arbitrary units ±SD of duplicates.

The next step in testing assay conditions was to use live cells. Therefore we chose the human monocyte cell line THP1, as these cells express ADAM17/TACE on their cell surface (Alvarez-Iglesias, Wayne, O'Dea, Amour, & Takata, 2005; Gutiérrez-López, et al., 2011) and are quite easy to handle.

THP1 cells were incubated for 24 hours in RPMI 1640 without FCS in the absence or presence of 100nM PMA and were incubated for further 3 hours in the absence or presence of 10ng/ml LPS. TACE activity was measured in 20mM Tris pH7.4, 50mM Tris pH7.4, 250mM Tris pH7.4, TBS or HAM's medium, respectively (see Figure 24). These buffers and HAM's medium showed the best results in the preliminary experiments that were conducted to estimate the most appropriate buffer or medium for the reaction itself (see Figure 20, Figure 21, Figure 22 and Figure 23).

Results

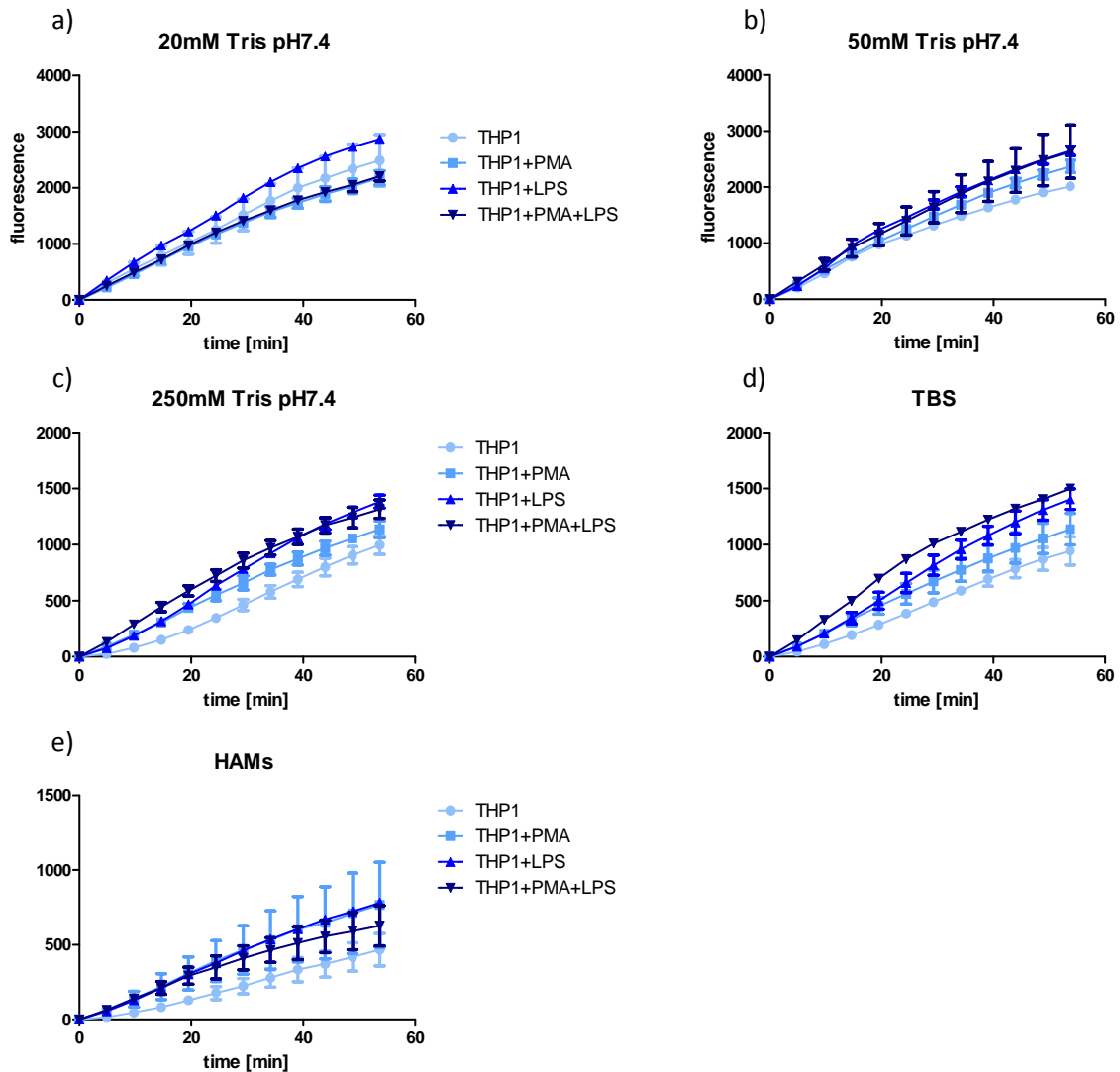The highest fluorescence independent of activation status could be detected in 20mM Tris pH7.4 and 50mM Tris pH7.4.

Figure 25: TACE activity measured by hydrolysis of DABCYL-TNFα-Edans by THP1 incubated for 27 hours in RPMI-1640 (THP1); THP1 incubated for 27 hours in RPMI-1640 supplemented with 100nM PMA (THP1+PMA); THP1 incubated for 27h in RPMI-1640 including the last 3 hours with 10ng/ml LPS (THP1+LPS); THP1 incubated in RPMI-1640 supplemented with 100nM PMA for 27 hours including the last 3 hours with 10ng/ml LPS (THP1+PMA+LPS). Fluorescence was measured once per cycle at λ_{em}: 485nm when samples were excited at λ_{ex}: 360nm in 12 cylces, 4.88min per cycle using a) 20mM Tris pH7.4, b) 50mM Tris pH7.4, c) 250mM Tris pH7.4, d) TBS, e) HAMs medium as buffer for measuring TACE activity. Starting values were arbitrarily set to 0 and values represent arbitrary units ±SD of duplicates.

The most prominent differences in TACE activity of THP1 cells due to their activation status could be detected in 250mM Tris pH7.4 and TBS followed by HAM's medium. Only a slight difference in TACE activity could be measured in 20mM Tris pH7.4 and 50mM Tris pH7.4 but nevertheless the increase in fluorescence after 54 minutes was highest using these two buffers, so we therefore tended to use one of these buffers for the final assay. As it later turned out, this might have been not the best decision, as it was the primary task to identify a buffer which showed the biggest difference in activity of TACE on live cells depending on the activation stage and not just the buffer showing the highest increase in fluorescence.

TACE activity in all buffers was highest in THP1 activated with PMA in combination with LPS followed by THP1 activated with LPS, and THP1 activated with PMA, with the exception of 20mM Tris pH7.4 and HAM's medium.
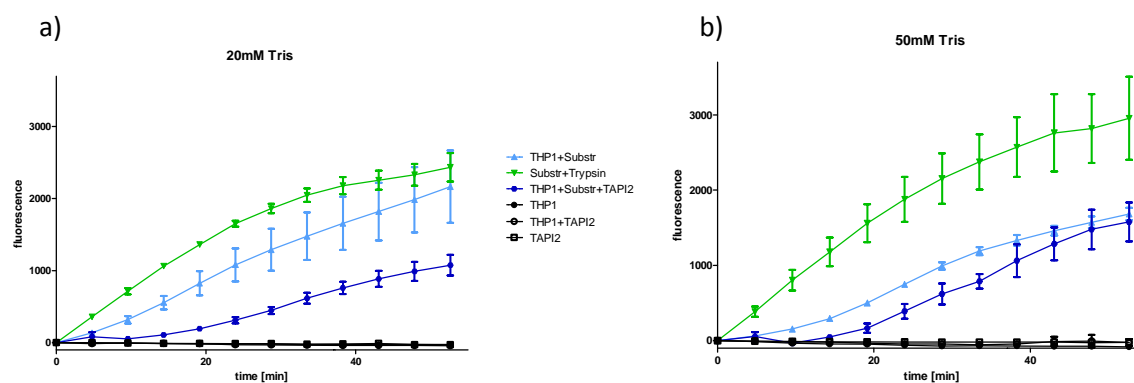
Inhibition of TACE activity in THP1 by TAPI-2

Figure 26: Fluorescence of cleaved substrate (Subst+Trypsin), THP1, THP1 with substrate (THP1+Substr), THP1 with substrate and TACE inhibitor (THP1+Substr+TAPI2), THP1 with TACE inhibitor (THP1+TAPI2) and TACE inhibitor (TAPI2), respectively, was measured in a) 20mM Tris pH7.4 and b) 50mM Tris pH7.4 at λ_{em}: 485nm when samples were excited at λ_{ex}: 360nm every 4.79min for 53min (12 cylces). Starting values were arbitrarily set to 0 and values represent arbitrary units ±SD of duplicates.

Time [min]	0	4.8	9.6	14.4	19.1	23.9	28.7	33.5	38.3	43.1	47.9	52.6
20mM Tris pH7.4	-	59.6%	17.0%	19.3%	23.3%	28.9%	34.6%	41.8%	45.9%	48.6%	49.8%	49.7%
50mM Tris pH7.4	-	87.0%	-21.4%	16.6%	33.1%	52.2%	62.6%	66.3%	79.7%	88.0%	94.0%	93.8%

Table 23: Remaining TACE activity in 20mM Tris pH7.4 and 50mM Tris pH7.4 on THP1 when TACE is inhibited by addition of 50µM TAPI-2 at different time points.

To make sure that the measured enzymatic activity was due to the action of TACE, we inhibited the enzyme with a specific inhibitor, TAPI-2 (Gutiérrez-López, et al., 2011; see Figure 26). 83% of TACE activity of THP1 cells incubated in 20mM Tris pH7.4 could be inhibited after 9.6 minutes of measurement, leaving 17% of the activity of uninhibited TACE (see Table 23). The maximum activity of TAPI-inhibited TACE reached about 49.7% of the activity of uninhibited TACE after an incubation period of about 52 minutes.

When incubated in 50mM Tris pH7.4 the activity of TACE could be reduced to about 16% after 14 minutes of incubation with the inhibitor and subsequently reached 94% of the activity of uninhibited TACE after 52 minutes.

Therefore we chose the 20mM Tris pH7.4 buffer as the final assay buffer because of the stronger difference in TACE activity that could be achieved by the addition of TAPI-2.

Neither the cells, nor the inhibitor TAPI-2, nor cells in combination with the TACE inhibitor TAPI-2 showed any fluorescence in the assay.
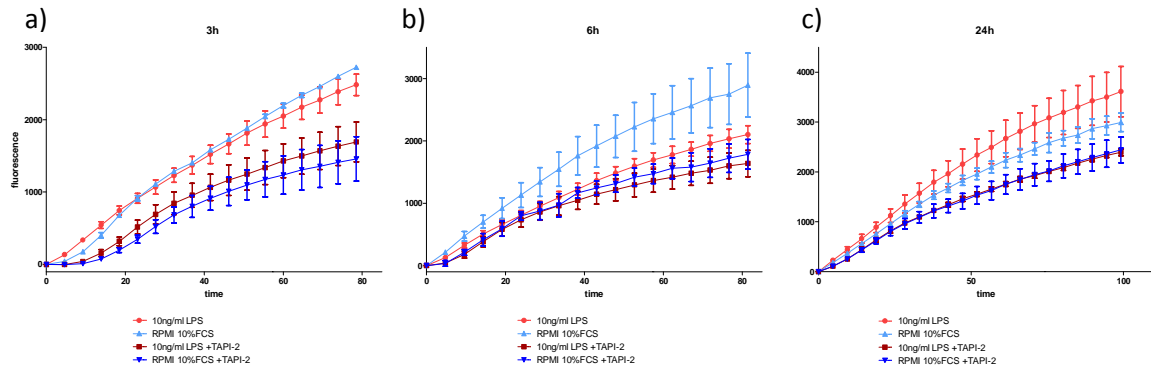
Results

Figure 27: TACE activity measured by hydrolysis of DABCYL-TNFα-Edans by THP1 incubated for a) 3 hours, b) 6 hours or c) 24 hours in RPMI-1640 10%FCS supplemented with 10ng/ml LPS or without LPS in the presents or absence of 50µM TAPI-2, respectively. Fluorescence was measured once per cycle at λ_{em}: 485nm when samples were excited at λ_{ex}: 360nm using 20mM Tris pH7.4 as buffer for measuring TACE activity. Starting values were arbitrarily set to 0 and values represent arbitrary units ±SD of duplicates.

We were further interested in the activity of TACE in LPS-induced THP1 cells in the presence or absence of the inhibitor TAPI-2. Therefore we incubated THP1 cells in RPMI supplemented with 10% FCS in the presence or absence of 10ng/ml LPS for 3 hours, 6 hours or 24 hours and measured the activity of TACE with or without 50µM TAPI-2 (see Figure 27).

TAPI-2 could inhibit the activity of TACE at each time point tested, but to different extents. After 78 minutes of measurement the activity of TACE was reduced to about 70% in THP1 which were incubated for 3 hours with LPS and to 54% in THP1 incubated in medium for 3 hours. Unfortunately, there was no difference in the activity of TACE of cells incubated with and without LPS, respectively.

TAPI-2 could reduce TACE activity in THP1 to about 78% after 80 minutes of measurement, when cells were incubated for 6 hours with LPS and to 62% when cells were incubated with medium. Surprisingly the activity of TACE on cells incubated with medium was 37% higher than the activity of cells incubated with LPS.

Incubating THP1 with LPS for 24 hours resulted in a 20% higher activity of TACE compared to cells incubated in medium. Addition of TAPI-2 led to a reduction of TACE activity to about 66% in LPS-induced cells and to about 82% in cells incubated in medium after 99 minutes of measurement.

Difference in TACE activity of THP1 cells depending on LPS concentration and incubation periods
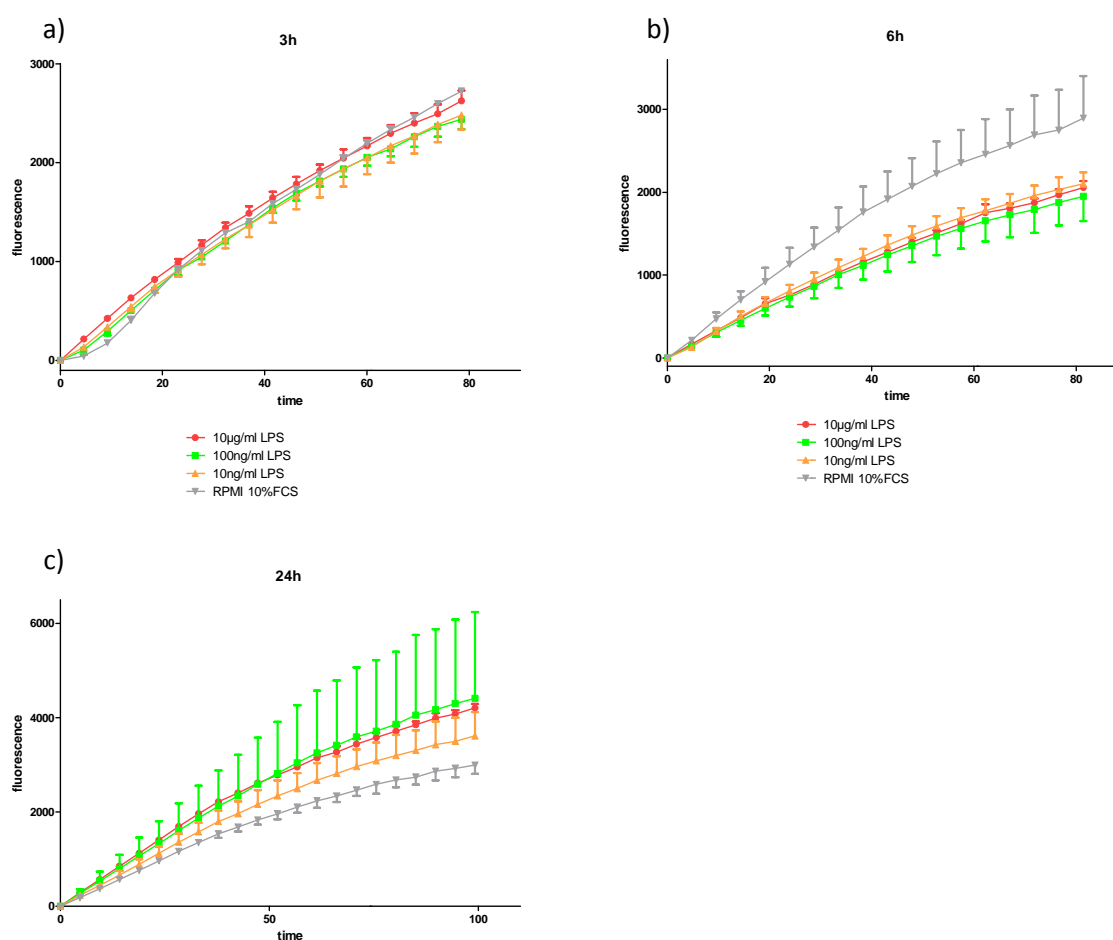

Figure 28: TACE activity measured by hydrolysis of DABCYL-TNFα-Edans by THP1 incubated for a) 3 hours, b) 6 hours or c) 24 hours in RPMI-1640 10%FCS supplemented with 10µg/ml LPS or 100ng/ml LPS or 10ng/ml LPS or without LPS, respectively. Fluorescence was measured at λ_{em}: 485nm when samples were excited at λ_{ex}: 360nm using 20mM Tris pH7.4 as buffer for measuring TACE activity. Starting values were arbitrarily set to 0 and values represent arbitrary units ±SD of duplicates.

Our next attempt was to find the appropriate conditions at which the difference in TACE activity between LPS-induced and uninduced cells was most prominent. Therefore THP1 cells were incubated for 3 hours, 6 hours or 24 hours, respectively, in RPMI supplemented with 10% FCS and either 10µg/ml LPS, 100ng/ml LPS or 10ng/ml LPS (see Figure 28). After 3 hours of incubation no difference in TACE activity could be detected.

The activity of LPS-induced cells after 6 hours was not significantly different, although the activity in medium treated cells was found to be higher.

LPS induction did also not result in different activities of TACE after 24 hours of treatment, although die average activity was higher than in medium treated cells.

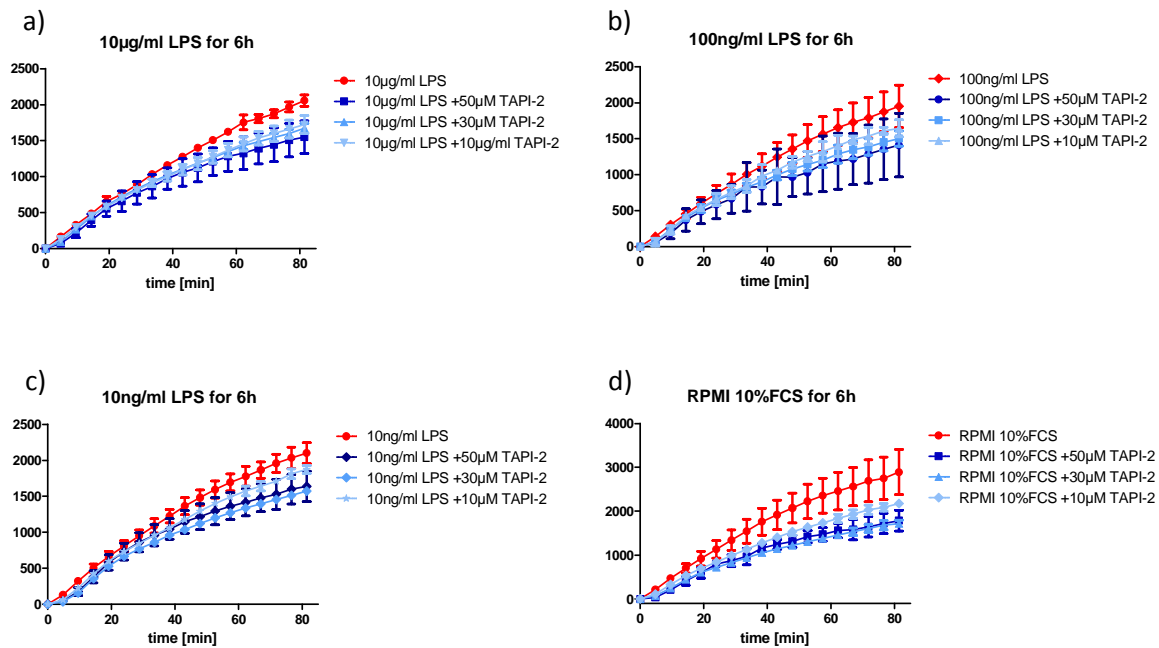*Extent of inhibition of TACE activity in THP1 depending on inhibitor concentration*

Figure 29: TACE activity measured by hydrolysis of DABCYL-TNFα-Edans by THP1 incubated for 6 hours in RPMI-1640 10%FCS supplemented with a) 10µg/ml LPS or b) 100ng/ml LPS or c) 10ng/ml LPS or d) without LPS in the presents or absence of 50µM or 30µM or 10µM TAPI-2, respectively. Fluorescence was measured once per cycle at λ_{em}: 485nm when samples were excited at λ_{ex}: 360nm using 20mM Tris pH7.4 as buffer for measuring TACE activity. Starting values were arbitrarily set to 0 and values represent arbitrary units ±SD of duplicates.

As we could not detect any difference in TACE activity of THP1 cells treated with different concentrations of LPS, TACE activity is either entirely unaffected by LPS or there is another regulation that affects inhibition of TACE. To test this second possibility, we used different concentrations of the TACE inhibitor TAPI-2 so see whether this would result in different TACE activities.

Therefore THP1 cells were incubated with increasing concentrations of LPS ranging from 10ng/ml to 10µg/ml for 6 hours. TACE activity of these induced cells was afterwards measured in the presence or absence of 10µM, 30µM or 50µM TAPI-2 for about 81 minutes (see Figure 29).

TACE activity could be inhibited in all cells regardless of the LPS concentration used, but the activities did not significantly decrease with increasing TAPI-2 concentration.
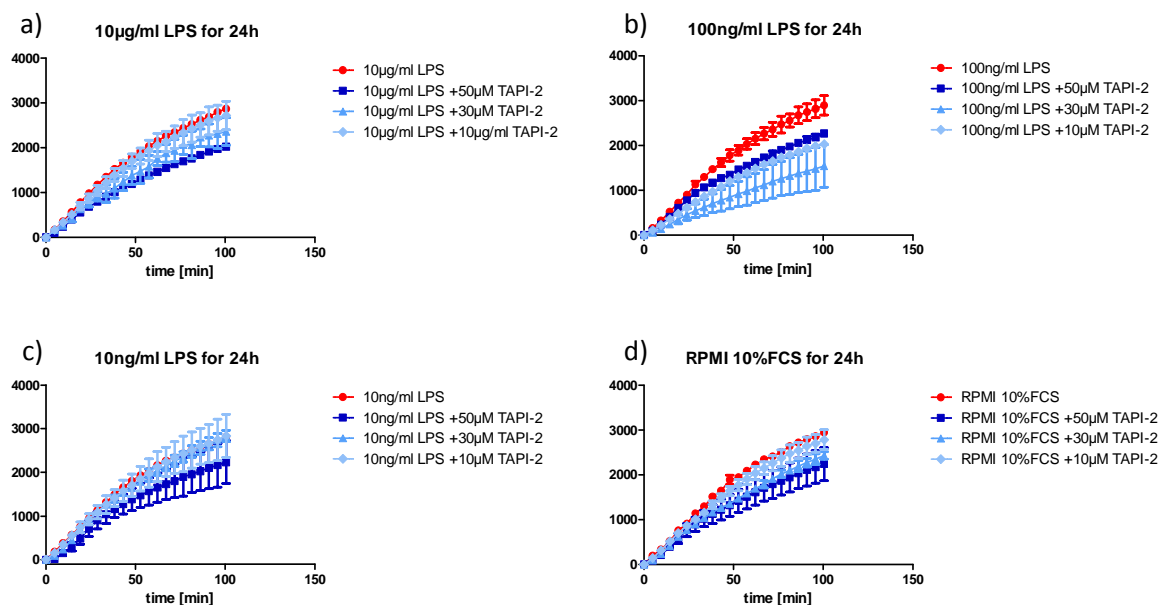
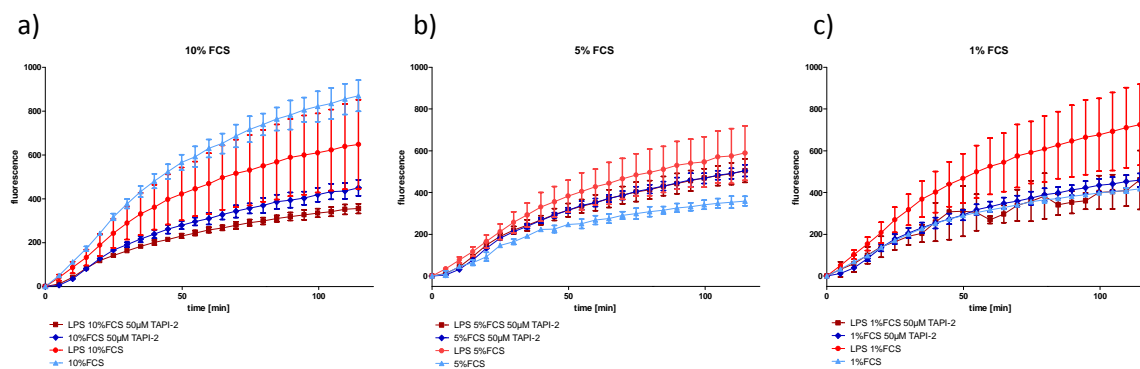**Figure 30: TACE activity measured by hydrolysis of DABCYL-TNFα-Edans by THP1 incubated for 6 hours in RPMI-1640 10%FCS supplemented with a) 10µg/ml LPS or b) 100ng/ml LPS or c) 10ng/ml LPS or d) without LPS in the presents or absence of 50µM or 30µM or 10µM TAPI-2, respectively. Fluorescence was measured once per cycle at λem: 485nm when samples were excited at λex: 360nm using 20mM Tris pH7.4 as buffer for measuring TACE activity. Starting values were arbitrarily set to 0 and values represent arbitrary units ±SD of duplicates**

TACE activities in the presence of different concentrations of TAPI-2did also not significantly differ in THP1 cells which were incubated for 24 hours with LPS (see Figure 30).

TACE activity in THP1 depending on serum concentration in treatment medium

Figure 31: TACE activity measured by hydrolysis of DABCYL-TNFα-Edans by THP1 incubated for 1 hour in RPMI-1640 supplemented with a) 10% FCS or b) 5% FCS or c) 1% FCS in the presents or absence of 50µM TAPI-2, respectively. Fluorescence was measured once per cycle at λ$_{em}$: 485nm when samples were excited at λ$_{ex}$: 360nm using 20mM Tris pH7.4 as buffer for measuring TACE activity. Starting values were arbitrarily set to 0 and values represent arbitrary units ±SD of duplicates.

As there might also be some proteinase inhibitors present in the serum of the medium, they could have an effect on TACE activity, although the assay itself is carried out in a simple Tris buffer without serum. Therefore THP1 cells were incubated for 1 hour with 10ng/ml LPS in RPMI-1640 medium supplemented with 1% FCS, 5% FCS or 10% FCS, respectively (see Figure 31). The TACE activity of LPS-induced THP1 in medium containing 10%FCS was found to be lower than the medium control itself. This effect could be detected in several, but not all experiments.

Results

TACE activities of THP1 cells which were induced with LPS in medium containing only 1% or 5% serum on the other hand, were found to be higher than TACE activities in control cells (see Figure 31 b and c). When inhibited with 50µM TAPI-2 TACE activities of cells kept in medium containing 5% serum with or without LPS, respectively, were higher than the activity of TACE of controls without inhibitor. TACE activity of LPS-induced cells incubated in medium containing 1% serum was higher than the activity of control cells. The activity of TACE of LPS-induced cells could be inhibited by the addition of TAPI-2, whereas TACE activity of control cells could not (Figure 31c).

TACE activity in THP1 depending on cell density
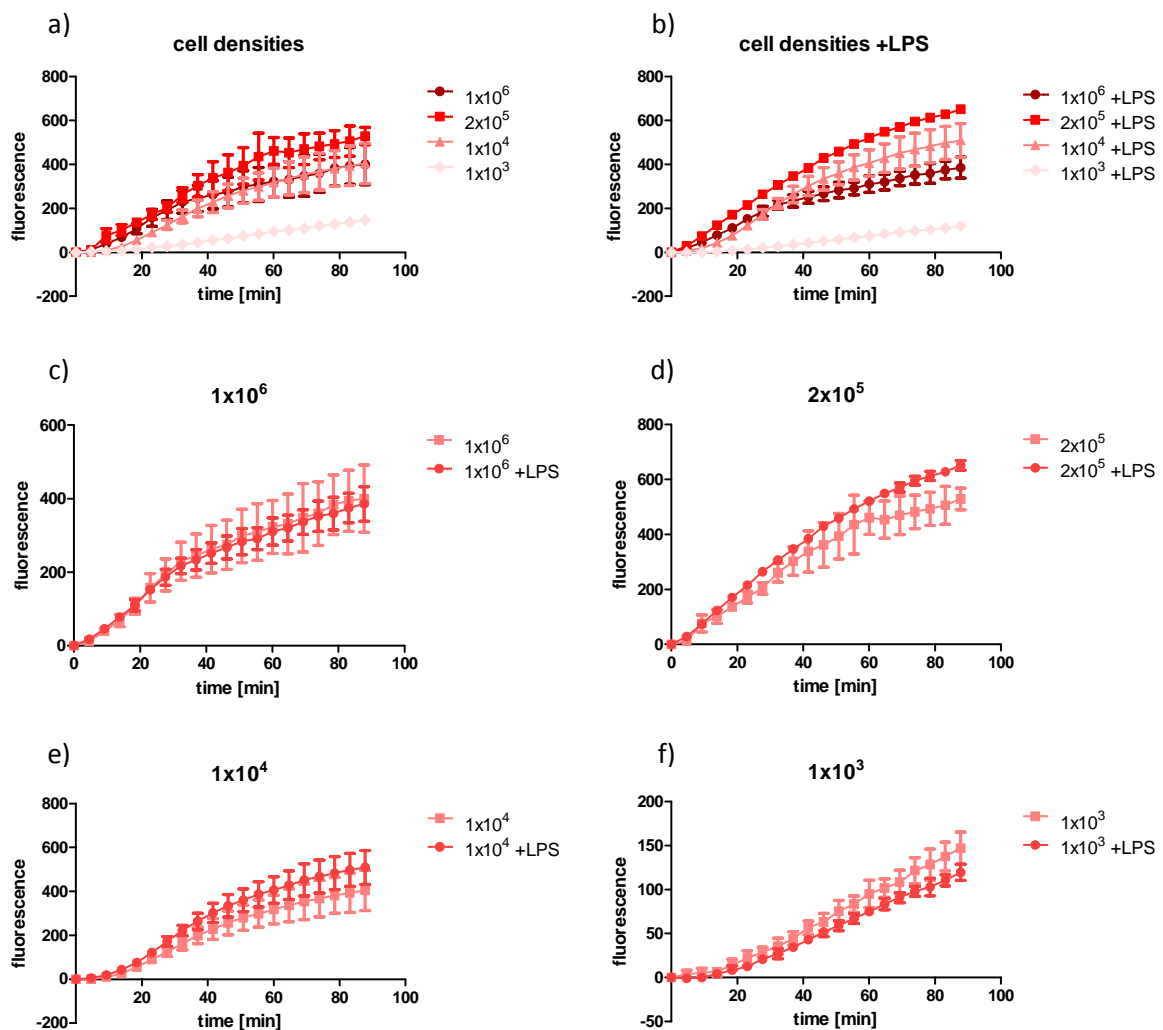
Figure 32: TACE activity measured by hydrolysis of DABCYL-TNFα-Edans by THP1 incubated for 1 hour in RPMI-1640 10% FCS in the presents or absence of 10ng/ml LPS, respectively. a) comparison of TACE activity at different cell densities incubated in medium or b) medium supplemented with LPS, c) TACE activity of $1x10^6$ THP1, d) TACE activity of $2x10^5$ THP1, e) TACE activity of $1x10^4$ THP1, f) TACE activity of $1x10^3$ THP1. Fluorescence was measured once per cycle at λ_{em}: 485nm when samples were excited at λ_{ex}: 360nm using 20mM Tris pH7.4 as buffer for measuring TACE activity. Starting values were arbitrarily set to 0 and values represent arbitrary units ±SD of duplicates.

To further evaluate the specificity and reproducibility of the assay we tested whether the measured activities of TACE correlate with cell densities as more available enzyme should result in faster cleavage of the substrate.

Therefore THP1 cells which were previously incubated for 1 hour with or without LPS, respectively, were plated at different densities ranging from $1x10^3$ to $1x10^6$ and TACE activity was measured. A correlation between cell density and activity could be detected at densities ranging from $1x10^3$ to $2x10^5$. In contrast, the activity of $1x10^6$ cells was almost as high as seen in $1x10^4$ cells (see Figure 32a). The same effects could be detected in cells which were treated with LPS previous to TACE activity measurement (see Figure 32b).

Induction of cells with LPS resulted in a slight increase in TACE activity compared to medium-treated control cells at densities of $1x10^4$ and $2x10^5$ (see Figure 32d and e). TACE activities of cells at densities of $1x10^3$ and $1x10^6$ cells were found to differ not significantly (see Figure 32c and f).

Results

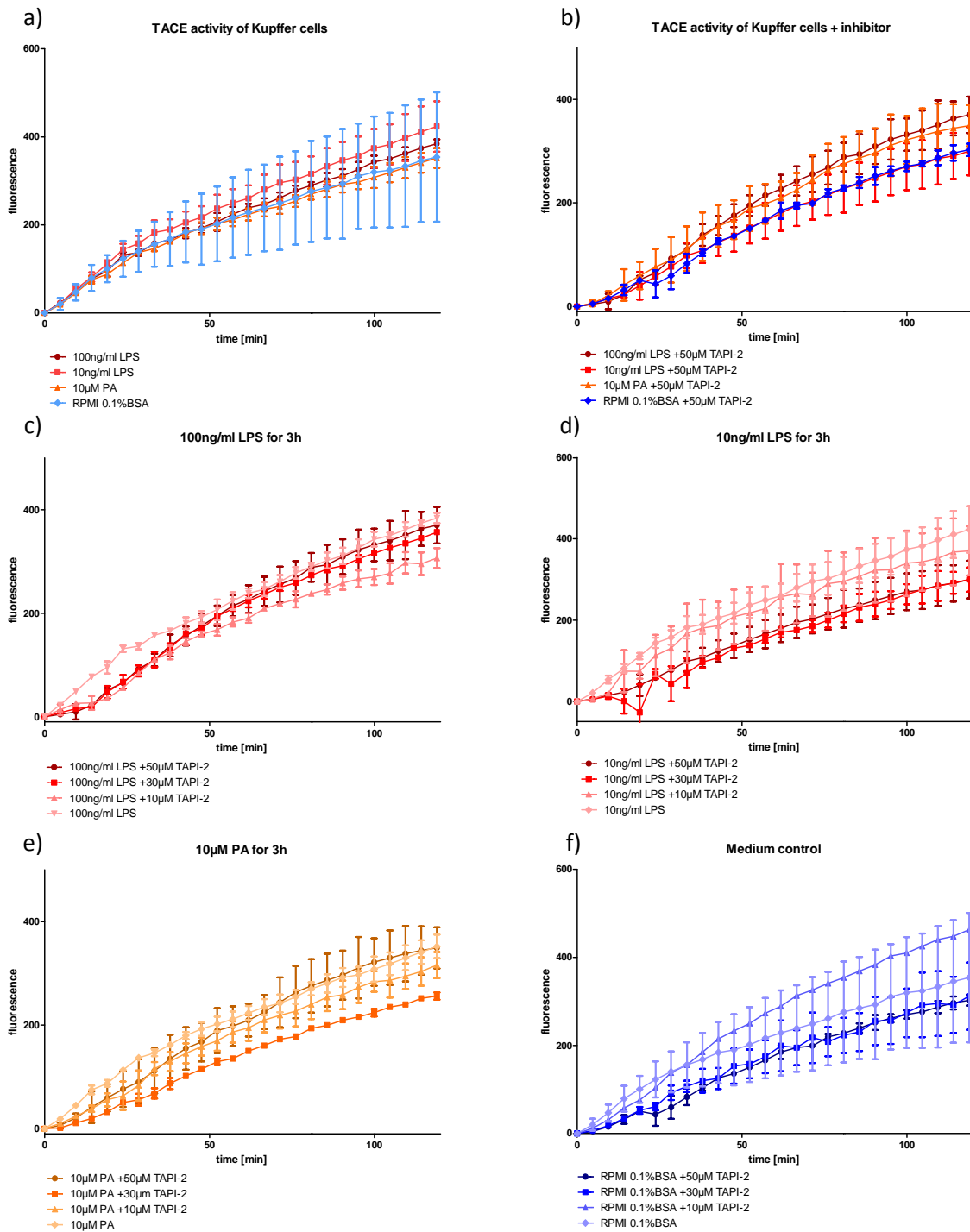*Activity and inhibition of TACE in native and induced primary rat Kupffer cells*

Figure 33: TACE activity measured by hydrolysis of DABCYL-TNFα-Edans by primary rat Kupffer cells incubated for 3 hours in RPMI-1640 0.1%BSA supplemented with 100ng/ml LPS, 10ng/ml LPS, 10μM palmitic acid (PA) or medium, respectively, in a) the absence or b) presence of 50μM TAPI-2. c) TACE activity of Kupffer cells incubated for 3 hours with 100ng/ml LPS, d) TACE activity of Kupffer cells incubated for 3 hours with 10ng/ml LPS, e) TACE activity of Kupffer cells incubated for 3 hours with 10μM PA, f) TACE activity of Kupffer cells incubated for 3 hours with RPMI 0.1%BSA. Fluorescence was measured in the absence or presence of 50μM, 30μM or 10μM TAPI-2, respectively, once per cycle at λ_{em}: 485nm when samples were excited at λ_{ex}: 360nm using 20mM Tris pH7.4 as buffer for measuring TACE activity. Starting values were arbitrarily set to 0 and values represent arbitrary units ±SD of duplicates.

We were further interested in the TACE activity of LPS-induced and native primary rat Kupffer cells. Therefore Kupffer cells were treated for 3 hours with 10ng/ml or 100ng/ml LPS and TACE activity was

measured in the presence or absence of the TACE inhibitor TAPI-2. Furthermore Kupffer cells were treated with 10µM palmitic acid followed by measurement of TACE activity (see Figure 33a-f).

TACE activity in primary rat Kupffer cells did not significantly differ in cells treated with LPS, palmitic acid or medium, respectively, although TACE activity was slightly higher in cells treated with 100ng/ml LPS than in cells treated with 10ng/ml LPS (see Figure 33a). TACE activities measured in the presence of TAPI-2 did also not differ significantly between treatments (see Figure 33b).

TACE activities of Kupffer cells treated with 100ng/ml LPS could be inhibited by the addition of TAPI-2, but activities did not decrease in a concentration dependent manner (see Figure 33c). TAPI-2 (30µM and 50µM) decreased TACE activity of Kupffer cells incubated with 10ng/ml LPS. A concentration of 10µM TAPI-2 just led to a slight decrease in TACE activity (see Figure 33d).

Treatment of Kupffer cells with palmitic acid could also just be slightly decreased by the addition of TAPI-2 and did therefore not significantly differ whether TACE was inhibited or not. Similarly, the TACE activity of medium treated cells showed no significant difference whether it was inhibited by different concentrations of TAPI-2 or not.
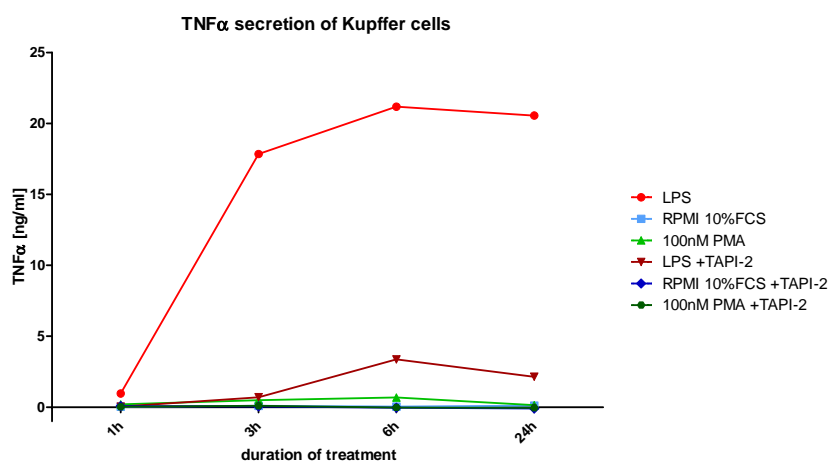

Figure 34: TNFα secretion into the supernatant of primary rat Kupffer cells in response to 10ng/ml LPS (LPS), medium (RPMI 10%FCS) and 100nM PMA in the absence or presents of 50µM TAPI-2.

TNFα [ng/ml]	LPS	RPMI 10%FCS	100nM PMA	LPS +TAPI-2	RPMI 10%FCS +TAPI-2	100nM PMA +TAPI-2
1h	0.959	0.030	0.198	0.037	0.073	0.033
3h	17.843	0.094	0.489	0.706	0.046	0.090
6h	21.178	0.040	0.678	3.367	-0.033	-0.025
24h	20.548	0.107	0.140	2.140	-0.087	-0.044

Table 24: TNFα concentrations [ng/ml] in the supernatant of Kupffer cells used in Figure 34.

Due to the inconclusive results of the measured TACE activities in primary rat Kupffer cells in response to treatment with LPS and palmitic acid, we measured the concentration of TNFα in the supernatant to verify the shedding of TNFα in our system (see Figure 34).

LPS treatment of primary rat Kupffer cells resulted in a strong release of TNFα, reaching the highest concentration after 6 hours of treatment. Neither treatment with PMA nor medium resulted in significant release of TNFα into the supernatant.

Addition of the TACE inhibitor TAPI-2 resulted in a significant decrease of TNFα release in LPS treated cells, resulting in a maximum concentration of TNFα of about 3.4ng/ml after 6 hours of treatment.

Effects of in-vivo oil treatment

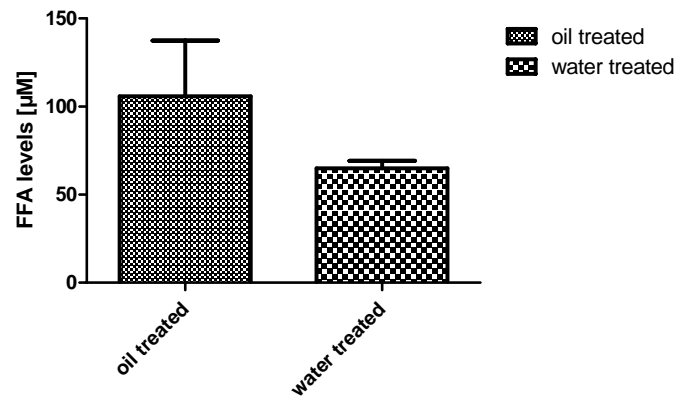### Effects of in-vivo oil treatment on FFA serum levels in rats after 20h

Figure 35: Levels of free fatty acids in the sera of oil treated and water treated rats, respectively. Values are mean ±SEM.

FFA [µM]	Mean	SEM	n
Oil treated	105,850	31,594	4
Water treated	64,875	4,286	4

Table 25: Mean, SEM and n of analyzed free fatty acid concentrations in sera of oil and water treated rats, respectively, used in Figure 35.

In order to evaluate changes in gene expression in oil-treated compared to water-treated rats, we were interested in the levels of free fatty acids in the sera of these rats. Therefore rats were given oil (1ml/100ml bodyweight) or water (1ml/100g bodyweight) by gavage and serum was extracted after 20 hours. FFA levels of oil-treated rats (105.85µM, see Figure 35 and Table 25) were found to be approx. 1.65-fold higher than in water-treated controls (64.88µM).

Micro-array analysis of mRNA of liver cells 20h and 6d after oil treatment

Since the levels of free fatty acids were about 2-fold higher in oil-treated rats compared to water-treated controls 20 hours after a single administration by gavage, we were interested in the resulting changes in gene expression in the liver. Therefore total RNA was isolated from mesenchymal and parenchymal cells of livers of oil-treated and water-treated rats and gene expression was analyzed using Affymetrix's GeneChip Rat Genome 230 array at the Core Facility Genomics of the Medical University of Vienna. Resulting gene expression data were delogarithmized and RMA-normalized and the values of each gene from oil-treated samples were divided by the mean of their respective controls. By calculating fold-controls of each oil-treated sample using control values from the same experiment instead of pooling oil-treated and water-treated samples from different experiments, we avoid to detect possible litter specific changes in gene expression. Gene expression in mesenchymal and parenchymal cells was than calculated as mean of these resulting fold-control values.

When we compared the gene expression in livers of oil-treated rats with water-treated controls 20 hours after oil or water administration, respectively, we found 18 genes more than 2-fold downregulated and 433 genes more than 2-fold upregulated (see Table 28) in mesenchymal cells and 3 genes more than 2-fold downregulated and 9 genes more than 2-fold upregulated in hepatocytes (see Table 29). Resulting gene lists were cleared of genes which appeared more than once and were

not regulated in the same way and of genes whose expression was changed in just one animal by comparison of standard deviations with means. This was followed by assigning genes to pathways as specific as possible. Resulting tables of regulated genes of interest assigned to pathways are listed below (Table 26 and Table 27) and tables of total regulated genes may be found in supplementary (Table 28and Table 29).

In lack of proper controls, the fold control of gene expression after 6 days of treatment was calculated by dividing the mean of gene expression values from oil-treated rats (6 days) by the mean of gene expression values of the water-treated controls from the one-time treatment experiment (20 hours).

Changes in gene expression in mesenchymal cells

Pathway	Gene title	Gene symbol	Public ID	Fold control 20h	Fold control 6d
Immune response	chemokine (C-C motif) ligand 4	Ccl4	U06434	0.489	0.490
	collagen, type I, alpha 2	Col1a2	BM388837	2.010	0.918
	laminin, beta 1	Lamb1	BI296460	2.162	1.487
	nuclear protein, transcriptional regulator, 1	Nupr1	NM_053611	2.247	1.925
	Vitronectin	Vtn	NM_019156	2.247	1.620
	arginase, liver	Arg1	NM_017134	2.390	2.573
	retinoic acid receptor responder (tazarotene induced) 2	Rarres2	BI282993	2.507	1.333
	orosomucoid 1	Orm1	NM_053288	2.758	1.348
	serine (or cysteine) peptidase inhibitor, clade A, member 3N	Serpina3n	NM_031531	3.168	2.035
Apoptosis	granzyme B	Gzmb	AI029386	0.497	0.435
	PERP, TP53 apoptosis effector	Perp	AI598971	2.127	1.596
Acute phase reaction	Haptoglobin	Hp	NM_012582	2.144	1.830
	inter alpha-trypsin inhibitor, heavy chain 4	Itih4	NM_019369	2.230	1.863
	fibrinogen gamma chain	Fgg	NM_012559	2.482	1.596
Oxidative stress	microsomal glutathione S-transferase 1	Mgst1	NM_134349	2.180	1.773
	glutathione S-transferase, theta 2	Gstt2	NM_012796	2.233	1.520
	glutathione S-transferase mu 2	Gstm2	AI169331	2.074	2.142
Complement system activation	mannose-binding lectin (protein A) 1	Mbl1	NM_012599	2.244	1.431
	complement component 9	C9	NM_057146	2.981	1.837
	complement component 8, alpha polypeptide	C8a	AA998638	3.147	1.874
	mannan-binding lectin serine peptidase 2	Masp2	AA996755	3.850	1.626
Complement system inhibition	complement factor I	Cfi	NM_024157	2.521	2.048
Amino acid metabolism	glutathione transferase zeta 1	Gstz1	AI169075	2.013	2.003
	cysteine dioxygenase, type I	Cdo1	NM_052809	2.026	1.726
	aminomethyltransferase	Amt	BF408907	2.114	1.735
	methionine adenosyltransferase I, alpha	Mat1a	AI454484	2.214	1.854
	nitrilase family, member 2	Nit2	AI411100	2.215	1.907
	guanidinoacetate N-methyltransferase	Gamt	NM_012793	2.318	2.003
	glycine C-acetyltransferase (2-amino-3-ketobutyrate-coenzyme A ligase)	Gcat	AW525471	2.329	1.695
	phenylalanine hydroxylase	Pah	NM_012619	2.444	1.914
	aldehyde oxidase 1	Aox1	NM_019363	2.606	2.607
	solute carrier family 38, member 4	Slc38a4	NM_130748	2.634	2.533
	N-acetylglutamate synthase	Nags	AI030790	2.662	2.120
	fumarylacetoacetate hydrolase	Fah	NM_017181	2.750	1.816
	choline dehydrogenase	Chdh	BI293004	2.856	1.853
	acireductone dioxygenase 1	Adi1	AA997430	2.896	2.670
	monoamine oxidase B	Maob	NM_013198	2.916	2.569

Results

Pathway	Gene title	Gene symbol	Public ID	Fold control 20h	Fold control 6d
	aldehyde dehydrogenase 1 family, member B1	Aldh1b1	AA997683	3.080	1.820
	glycine cleavage system protein H (aminomethyl carrier)	Gcsh	NM_133598	3.112	2.841
	tyrosine aminotransferase	Tat	M18340	3.313	2.113
	histidine ammonia lyase	Hal	NM_017159	3.562	1.424
	alanine-glyoxylate aminotransferase	Agxt	NM_030656	3.636	1.715
	homogentisate 1, 2-dioxygenase	Hgd	AI232328	3.647	2.055
	cystathionase (cystathionine gamma-lyase)	Cth	NM_017074	3.855	5.592
	cystathionine beta synthase	Cbs	NM_012522	4.247	2.057
Fatty acid degradation	acyl-CoA synthetase long-chain family member 1	Acsl1	D90109	2.020	2.063
	2-hydroxyacyl-CoA lyase 1	Hacl1	AJ245707	2.041	1.916
	acetyl-Coenzyme A acyltransferase 1 /// similar to 3-ketoacyl-CoA thiolase B, peroxisomal precursor (Beta-ketothiolase B)	Acaa1 /// RGD1562373	NM_012489	2.083	1.516
	peroxisomal D3,D2-enoyl-CoA isomerase	Peci	BI278268	2.083	1.791
	acyl-Coenzyme A dehydrogenase, C-2 to C-3 short chain	Acads	NM_022512	2.233	1.588
	acyl-CoA thioesterase 2	Acot2	AA899721	2.306	1.554
	cytochrome P450, family 4, subfamily a, polypeptide 3	Cyp4a3	M33936	2.308	1.535
	alcohol dehydrogenase 7 (class IV), mu or sigma polypeptide	Adh7	NM_134329	2.313	2.842
	cytochrome P450, family 2, subfamily c, polypeptide 12 (female specific)	Cyp2c12	NM_031572	2.339	2.188
	fatty acid binding protein 1, liver	Fabp1	NM_012556	2.358	2.239
	carnitine palmitoyltransferase 2	Cpt2	NM_012930	2.454	1.760
	acyl-Coenzyme A dehydrogenase, C-4 to C-12 straight chain	Acadm	NM_016986	2.485	1.796
	enoyl Coenzyme A hydratase domain containing 2	Echdc2	AI172274	2.499	2.190
	acyl-Coenzyme A oxidase 2, branched chain	Acox2	X95189	2.605	1.898
	hydroxyacyl-Coenzyme A dehydrogenase	Hadh	AA799574	2.654	2.169
	acyl-Coenzyme A dehydrogenase, long-chain	Acadl	NM_012819	2.748	2.187
	cytochrome P450, family 2, subfamily b, polypeptide 3	Cyp2b3	M20406	2.765	2.063
	phytanoyl-CoA 2-hydroxylase	Phyh	NM_053674	2.787	1.836
	acyl-CoA thioesterase 12	Acot12	NM_130747	2.853	2.070
	peroxisomal trans-2-enoyl-CoA reductase	Pecr	NM_133299	3.049	2.668
	cytochrome P450, family 4, subfamily a, polypeptide 2 /// cytochrome P450, family 4, subfamily a, polypeptide 3	Cyp4a2 /// Cyp4a3	AA893326	3.241	2.045
	dodecenoyl-Coenzyme A delta isomerase (3,2 trans-enoyl-Coenzyme A isomerase)	Dci	NM_017306	3.467	2.552
	2,4-dienoyl CoA reductase 2, peroxisomal	Decr2	AF044574	3.514	2.917
	acetyl-Coenzyme A acyltransferase 2	Acaa2	NM_130433	3.583	2.539
	fatty acid binding protein 2, intestinal	Fabp2	NM_013068	4.087	3.254
	glycerol kinase	Gk	AA945076	4.245	3.046
	enoyl-Coenzyme A, hydratase/3-hydroxyacyl Coenzyme A dehydrogenase	Ehhadh	NM_133606	4.901	3.881
	2,4-dienoyl CoA reductase 1, mitochondrial	Decr1	NM_057197	5.276	3.894
Regulation of lipid metabolism	Hepatocyte nuclear factor 4, alpha	Hnf4a	BI288517	2.518	1.540
Steroid biosynthesis	NAD(P) dependent steroid dehydrogenase-like	Nsdhl	BF407232	2.043	1.556
	phosphomevalonate kinase	Pmvk	BG378288	2.056	2.019
	transmembrane 7 superfamily member 2	Tm7sf2	BM390364	2.067	1.599
	hydroxysteroid (17-beta) dehydrogenase 7	Hsd17b7	NM_017235	2.073	1.982
	cytochrome P450, family 51	Cyp51	NM_012941	2.261	2.300
	hydroxysteroid (17-beta) dehydrogenase 4	Hsd17b4	NM_024392	2.362	1.957
	farnesyl diphosphate synthase (farnesyl pyrophosphate synthetase, dimethylallyltransferase, geranyltranstransferase)	Fdps	NM_031840	2.421	2.017

Pathway	Gene title	Gene symbol	Public ID	Fold control 20h	Fold control 6d
	protein kinase, AMP-activated, alpha 2 catalytic subunit	Prkaa2	NM_023991	3.051	2.272
	sulfotransferase family 2A, dehydroepiandrosterone (DHEA)-preferring, member 2	Sult2a2	D14989	3.328	3.489
	3-hydroxy-3-methylglutaryl-Coenzyme A synthase 1 (soluble)	Hmgcs1	NM_017268	3.799	3.134
	isopentenyl-diphosphate delta isomerase 1	Idi1	NM_053539	4.607	3.260
Lipoprotein assembly	cell death-inducing DFFA-like effector b	Cideb	AI137938	2.026	1.190
Triglyceride biosynthesis	1-acylglycerol-3-phosphate O-acyltransferase 2 (lysophosphatidic acid acyltransferase, beta)	Agpat2	AI012474	2.792	2.157
Bile acid	solute carrier organic anion transporter family, member 1a1	Slco1a1	NM_017111	2.053	3.209
	solute carrier family 27 (fatty acid transporter), member 5	Slc27a5	NM_024143	2.160	1.797
	solute carrier organic anion transporter family, member 1a4	Slco1a4	NM_131906	2.193	3.516
	nuclear receptor subfamily 1, group H, member 4	Nr1h4	NM_021745	2.458	1.880
	aldo-keto reductase family 1, member D1 (delta 4-3-ketosteroid-5-beta-reductase)	Akr1d1	D17309	2.541	2.838
	cytochrome P450, family 7, subfamily a, polypeptide 1	Cyp7a1	NM_012942	3.009	1.698
	solute carrier family 10 (sodium/bile acid cotransporter family), member 1	Slc10a1	NM_017047	3.097	2.480
	bile acid Coenzyme A: amino acid N-acyltransferase (glycine N-choloyltransferase)	Baat	NM_017300	3.746	2.272
Lipid transport	apolipoprotein C-IV	Apoc4	AA998783	2.867	1.929
	lecithin cholesterol acyltransferase	Lcat	NM_017024	3.070	1.924
	apolipoprotein A-IV	Apoa4	NM_012737	3.150	1.584
	apolipoprotein A-I	Apoa1	NM_012738	4.021	3.806
	butyrobetaine (gamma), 2-oxoglutarate dioxygenase (gamma-butyrobetaine hydroxylase) 1	Bbox1	NM_022629	3.477	2.291
Ketone bodies	3-hydroxybutyrate dehydrogenase, type 1	Bdh1	NM_053995	3.580	2.358
	3-hydroxy-3-methylglutaryl-Coenzyme A synthase 2 (mitochondrial)	Hmgcs2	M33648	4.954	2.408
Retinoic acid metabolism	retinol binding protein 1, cellular	Rbp1	NM_012733	2.876	2.067
	dehydrogenase/reductase (SDR family) member 4	Dhrs4	AB062758	3.559	3.142
	retinol dehydrogenase 7	Rdh7	NM_133543	3.924	2.254
	cytochrome P450, family 2, subfamily c, polypeptide 22	Cyp2c22	M58041	4.169	5.477
Vitamin E transport	tocopherol (alpha) transfer protein	Ttpa	NM_013048	3.245	3.596
Liver regeneration	hepatocyte growth factor activator	Hgfac	BE119649	2.042	1.866
	heat-responsive protein 12	Hrsp12	NM_031714	2.167	2.219
	apolipoprotein A-V	Apoa5	AF202888	2.597	1.591
	transmembrane 4 L six family member 4	Tm4sf4	NM_053785	4.238	2.647
Detoxification	aldehyde dehydrogenase 3 family, member A2	Aldh3a2	NM_031731	2.114	1.528
	aldo-keto reductase family 7, member A2 (aflatoxin aldehyde reductase)	Akr7a2	NM_134407	2.228	1.544
	cytochrome P450, family 3, subfamily a, polypeptide 9	Cyp3a9	U46118	2.558	2.522
	flavin containing monooxygenase 5	Fmo5	AI454611	2.663	1.603
	cytochrome P450, family 1, subfamily a, polypeptide 2	Cyp1a2	K02422	2.728	1.483
Eicosanoid biosynthesis	fatty acid desaturase 2	Fads2	NM_031344	2.642	2.991
	arginine vasopressin receptor 1A	Avpr1a	NM_053019	2.922	1.483
	elongation of very long chain fatty acids (FEN1/Elo2, SUR4/Elo3, yeast)-like 2	Elovl2	BG666735	4.083	2.272
	acyl-CoA thioesterase 4	Acot4	AI411493	7.244	4.348
Purine metabolism	urate oxidase	Uox	M24396	2.514	2.776
	similar to transthyretin (4L369)	RGD1309350	BM387540	3.512	2.771
DNA repair	uracil-DNA glycosylase	Ung	AA848420	2.048	1.632
Metabolism of sugars	aldolase B, fructose-bisphosphate	Aldob	M10149	2.188	1.711

Results

Pathway	Gene title	Gene symbol	Public ID	Fold control 20h	Fold control 6d
	sorbitol dehydrogenase	Sord	NM_017052	2.391	1.480
	pyruvate carboxylase	Pc	NM_012744	2.855	1.342
	fructose-1,6-bisphosphatase 1	Fbp1	NM_012558	2.938	1.846
	amylase, alpha 1A (salivary)	Amy1a	AB057450	3.852	4.055
	glycogen synthase 2	Gys2	NM_013089	4.023	2.695
G-Protein coupled receptors	adrenergic, alpha-1B-, receptor	Adra1b	NM_016991	2.029	1.996
	purinergic receptor P2Y, G-protein coupled, 2	P2ry2	NM_017255	2.956	1.893
Kinin-Kallikrein-system	kininogen 2	Kng2	NM_012741	2.186	1.636
	serine (or cysteine) proteinase inhibitor, clade A (alpha-1 antiproteinase, antitrypsin), member 4	Serpina4	U51017	2.443	1.797
	kininogen 1 /// kininogen 1-like 1 /// kininogen 2	Kng1 /// Kng1l1 /// Kng2	NM_012696	2.911	1.986
Blood coagulation	coagulation factor X	F10	NM_017143	2.775	1.862
	coagulation factor IX	F9	AA963815	2.899	2.100
Inhibition of Coagulation	serine (or cysteine) peptidase inhibitor, clade D, member 1	Serpind1	NM_024382	2.186	1.785
	serine (or cysteine) peptidase inhibitor, clade C (antithrombin), member 1	Serpinc1	BG377322	2.222	1.812
	protein C	Proc	NM_012803	2.602	2.184
	apolipoprotein H (beta-2-glycoprotein I)	Apoh	AI180413	2.635	1.786
Regulation of blood pressure	angiotensin II receptor, type 1a	Agtr1a	NM_030985	2.505	1.324
Cell cycle	interferon regulatory factor 6	Irf6	BF557891	2.240	1.818
	activating transcription factor 5	Atf5	BM391471	4.366	3.126
Hyperlipidemia associated	angiopoietin-like 3	Angptl3	AI058911	2.138	1.673
	apolipoprotein C-I	Apoc1	NM_012824	2.181	1.612
Obesity development	solute carrier family 27 (fatty acid transporter), member 2	Slc27a2	NM_031736	2.377	2.224
Miscellaneous	dimethylarginine dimethylaminohydrolase 1	Ddah1	NM_022297	2.512	1.955
	regucalcin (senescence marker protein-30)	Rgn	NM_031546	2.579	1.735
	SEC16 homolog B (S. cerevisiae)	Sec16b	NM_053571	2.676	2.038
	G0/G1switch 2	G0s2	AI406939	2.718	1.565
	phosphatidylethanolamine N-methyltransferase	Pemt	NM_013003	2.989	1.627
	retinol binding protein 4, plasma	Rbp4	AA858962	3.201	2.239
	cytochrome P450, family 3, subfamily a, polypeptide 23/polypeptide 1	Cyp3a23/3a1	NM_013105	3.332	21.992[1]
	cytochrome P450, family 2, subfamily f, polypeptide 4	Cyp2f4	NM_019303	3.338	2.505
	growth factor receptor bound protein 14	Grb14	NM_031623	3.390	2.350
	choline phosphotransferase 1	Chpt1	BF282951	3.457	2.683
	keratin 18	Krt18	BI286012	3.653	2.198
	glutathione S-transferase A2 /// LOC494499 protein	Gsta2 /// LOC494499	NM_017013	3.711	6.790[2]
	interferon-induced protein with tetratricopeptide repeats 1	Ifit1	NM_020096	3.740	2.875
	keratin 8	Krt8	BF281337	4.207	2.080
	asialoglycoprotein receptor 1	Asgr1	NM_012503	4.216	2.836
	pantothenate kinase 1	Pank1	AA850195	4.465	3.245
	kidney expressed gene 1	Keg1	AB019693	4.890	6.959

Table 26: list of selected genes whose expression was more than 2-fold changed in primary mesenchymal cells of the livers of oil-treated vs. water-treated rats 20 hours after a single treatment and after 6 days of daily treatment.

---

[1] Cyp3a23/3a1 was found to be 16.6-fold upregulated in just one rat.
[2] Gsta2 was found to be 62.8-fold upregulated in just one rat.

Changes in gene expression in hepatocytes

Pathway	Gene title	Gene symbol	Public ID	Fold control 20h	Fold control 6d
Immune response	activating transcription factor 3	Atf3	NM_012912	0.484	0.694
Amino acid transport	solute carrier family 7 (cationic amino acid transporter, y+ system), member 7	Slc7a7	AF200684	2.100	1.384
Retinoic acid metabolism	cytochrome P450, family 2, subfamily a, polypeptide 2	Cyp2a2	NM_012693	2.336	3.245
Fatty acid degradation	acyl-CoA thioesterase 2	Acot2	AA899721	2.384	1.914
	fatty acid binding protein 2, intestinal	Fabp2	NM_013068	2.577	2.274
Miscellaneous	Sialophorin	Spn	BF550890	2.459	1.320
	vanin 1	Vnn1	BI289085	5.508	6.147

Table 27: list of selected genes whose expression was more than 2-fold changed in primary hepatocytes of oil-treated vs. water-treated rats 20 hours after a single treatment and after 6 days of daily treatment.

Discussion

Effects of in-vitro FFA treatment on primary rat liver cells

We isolated and purified primary rat hepatocytes and mesenchymal cells and treated these different cell types with α-linolenic acid, an n3-PUFA. Effects of treatment of primary rat liver cells with n6-PUFAs and peroxidized fatty acids have already been studied by our group (Sagmeister, 2009).

As the solvent had no significant effect on the viability of hepatocytes (Figure 9), the slight decrease in viability observed when the cells were treated with α-linolenic acid (Figure 10) is due to the fatty acid itself. Interestingly, primary rat mesenchymal cells are more susceptible to α-linolenic acid treatment using a concentration of 500μM. This observed difference between hepatocytes and mesenchymal cells is most probably due to a higher uptake and metabolic conversion or even storage of fatty acids in hepatocytes, as uptake of FFAs doesn't seem to be tightly regulated in the liver leading to steatosis in some individuals (Greenfield, Cheung, & Sanyal, 2008) (Savage & Semple, 2010).

Treatment with α-linolenic acid (ALA) did not change secretion of TNFα from rat mesenchymal cells (Figure 11) compared to the solvent control. α-linoleic acid (LH) and palmitic acid (PA) did not change TNFα shedding either, although at least saturated fatty acids were reported to increase expression of TNFα in a TLR-mediated way in a monocyte cell line (Lee, Zhao, & Hwang, 2009) and increase in TNFα secretion into the medium of primary rat mesenchymal cells in response to palmitic acid could be detected by ELISA by our group (unpublished data). However, an elevation in TNFα concentration of up to 15.5ng/ml (~6.9-fold, Table 15) could be observed after 6 hours of treatment with bacterial lipopolysaccharide (LPS), thereby confirming that primary rat mesenchymal cells after liver perfusion are capable of TNFα shedding and are therefore an applicable system which resembles the in-vivo situation as close as possible. The usefulness of the system is further supported by the observation that neither the solvents (EtOH and DMSO) nor an inhibitor for CD36 (SSO) had any influence on TNFα shedding.

Treatment of primary rat mesenchymal cells with ALA did not increase the phosphorylation status (Figure 12a) and thereby the activation of p38MAPK, a kinase activated during cellular stress, which induces COX2 and regulates the production of TNFα and IL-6 (Wagner & Nebreda, 2009), compared to the solvent control for up to a treatment period of 1 hour. After 24 hours phosphorylation was up to 2.6-fold increased (Table 16). This might rather be an effect of culturing of primary cells or even nutrient deprivation (although this is rather unlikely) than a real effect of the FFA treatment, as cellular stress resulting in activation of p38MAPK is a quite immediate event that would occur within 1 hour (own, unpublished data). The second, already stated cause might just be the generally low phosphorylation of p38MAPK in ALA-treated and control cells. Thereby every minor change in blot intensity results in a quite significant alteration of the fold-change ratio.

Activation of ERK1/2, as measured by phosphorylation, was also not affected by ALA treatment compared to solvent control (Figure 12b). ERK1/2 activation is involved in FFA mediated GPR signaling and is downregulated by n3-PUFA (Gleissman, Johnsen, & Kogner, 2010). This could not be reproduced in our system of primary rat cells.

Our next step in assessing the effects of ALA treatment on primary rat liver cells was assaying gene expression of the inflammation associated genes COX2, iNOS, TNFα and IL-6. COX-2 mRNA levels could not be detected in hepatocytes when they were treated with ALA or LH. The expression of iNOS and TNFα in LH-treated hepatocytes (see Figure 13) could just be detected after 6 hours of treatment, whereas expression of both mRNAs was detectable in ALA-treated hepatocytes. As cells were still viable after 24 hours of treatment, this phenomenon could not be explained. Treatment with ALA resulted in an approximately 2-fold decrease of TNFα mRNA levels after 6 hours and an almost 2-fold increase after 24 hours. As n3-PUFA are reported to reduce or even inhibit the production of TNF (Boutros, Somasundar, Razzak, Helton, & Espat, 2010), substantiated by our finding of a 2-fold decrease in TNFα expression after 6 hours, the increase in TNFα mRNA production after 24 hours seem contradictory. As LH did not lead to measurable TNFα mRNA levels that could be compared to the mRNA levels caused by ALA-treatment, other effects than FFA-treatment contributing to this increase cannot be completely excluded.

COX2 expression in primary rat mesenchymal cells was unchanged by treatment with ALA or LH (see Figure 14a), but was decreased by treatment with palmitic acid after 6 hours. Conversely, an increase in COX2 expression upon PA-treatment was reported in a murine macrophage cell line and myoblasts (Lee, Zhao, & Hwang, 2009). The discrepancy might be explained by the lower concentration of PA (10μM) used in our experimental setting, as higher concentrations showed toxic effects in our system of primary cells. LPS, which was used as a positive control for inducing inflammation, resulted in a 4.5-fold increase in COX2 expression after 24 hours, confirming the ability of primary mesenchymal cells to induce COX2 mRNA. iNOS mRNA levels were solely elevated by LPS-treatment (see Figure 14b), although saturated fatty acids were reported to increase its expression in a macrophage cell line (Lee, Zhao, & Hwang, 2009). Again, as in the case of COX2, we used primary cells and therefore lower concentrations of fatty acids to avoid cytotoxic effects. In contrast, the expression of TNFα was increased in PA-treated mesenchymal cells, leading to a 2-fold elevation, which was as high as observed in LPS-treated cells (see Figure 14c). Treatment with LH led to a slight decrease in TNFα expression after 6 hours which was at the level of solvent treated cells after 24 hours. This indicates that there is a difference in how primary cells react to FFA-treatment compared to cell lines, namely by elevation of TNFα mRNA levels (rather than COX2 or iNOS mRNA levels) at a low concentration where no cytotoxic effects could be observed. Nevertheless, the increase in TNFα expression in cells treated with palmitic acid was as high as observed in LPS-treated cells confirming the TNFα-inducing effects of PA.

Effects of inhibition of CD36 on primary rat liver cells

As CD36 might be the translocase/transporter for free fatty acids into the liver (Silverstein & Febbraio, 2009) (He, Lee, Febbraio, & Xie, 2011), we were interested whether its inhibition would result in changes in gene expression of COX2, iNOS and TNFα and phosphorylation p38MAPK and Erk1/2, indicating a role of CD36 in binding and FFA-mediated signaling in our system. To make sure that CD36 was expressed in primary rat liver cells, as reported, we assayed its expression in hepatocytes, Kupffer cells and endothelial cells (see Figure 15). CD36 RNA was detectable in all three types of cells after 39 cycles of PCR using cDNA as template.

Since palmitic acid induced expression of TNFα in mesenchymal cells we decided to use this fatty acid for our inhibition experiments. mRNA levels of COX2, iNOS and TNFα did not differ significantly

Discussion

between PA-treated and PA+SSO-treated cells (see Figure 17). Cells treated with SSO (in the presence of EtOH) or with the solvent control (EtOH+DMSO) did not show any changes in gene expression levels compared to controls.

As the mesenchymal cell fraction comprises many different celltypes including endothelial cells, Kupffer cells and stellate cells and the ratio between these cell types may vary, we decided to further separate Kupffer cells from endothelial cells and assay gene expression levels of PA-treated and PA+SSO treated cells separately.

Endothelial cells did not significantly change gene expression of COX2 or iNOS when treated with palmitic acid, although the combination of PA with SSO resulted in a decrease of iNOS expression after 6 hours and an increase after 24 hours, as did the treatment with PA alone (see Figure 18). TNFα expression was decreased after 6 hours by both, PA and PA+SSO treatment which was also cause by the solvent. Over all, the expression of inflammation associated genes varied a lot which could also be demonstrated by the treatment with LPS and the solvent. These findings might also in part explain the variations in gene expression observed with total mesenchymal cells and which might further be aggravated by different ratios of cell type number in rat livers thereby demonstrating the need for cell type separation when studying inflammatory responses in primary cells.

COX2 expression was increased 3-fold and 2-fold in PA-treated Kupffer cells after 6 hours and 24 hours of treatment, respectively, and this could be attenuated by the addition of the CD36 inhibitor SSO (see Figure 19a). iNOS mRNA levels were elevated after 6 hours of treatment with PA which could be decreased by inhibition of CD36. Expression levels were still slightly elevated after 24 hours of treatment which was independent of CD36 inhibition. Both, iNOS and COX2, expression were not as highly induced as they were by LPS, whereas in contrast TNFα expression was. Inhibition of CD36 by SSO led to a decrease in TNFα expression after 6 hours of treatment and mRNA levels of PA and PA+SSO-treated cells were almost at the level of the solvent control after 24 hours. Palmitic acid was unable to induce expression of IL-6 and addition of SSO did not change expression either. Nevertheless, IL-6 expression by primary rat Kupffer cells could be demonstrated by treatment with LPS, thereby showing the ability of these cells for inducing IL-6 production. Taken together, these results indicate the ability of palmitic acid to induce an - at least partially - CD36-mediated expression of the inflammation associated genes COX2, iNOS and TNFα in primary rat Kupffer cells, which seem to be the cell population which shows the highest response to FFA-treatment. Each of these genes showed stronger induction at the earlier time point investigated with COX2 levels being still 2-fold elevated after 24 hours of treatment, indicating an immediate response in iNOS and TNFα expression and an a prolonged expression for COX2. In every analyzed expression of inflammation associated genes, LPS-treatment led to an increase in transcription, whereas the solvent showed no influence thereby demonstrating the reliability of our primary cell system.

The phosphorylation status of p38MAPK and Erk1/2 was investigated when CD36 was inhibited by SSO and cells were treated with palmitic acid (see Figure 16). After 10min phosphorylation of p38MAPK was slightly reduced in PA-treated cells and was further reduced in PA+SSO-treated cells. At time point 30min only PA+SSO-treated cells showed a slight reduction in p38 phosphorylation. At later time points there was no significant difference between treatments and compared to solvent control be detected, although CD36 inhibition tended to reduce p38 phosphorylation compared to PA-treatment. Phosphorylation of Erk1/2 was not affected by treatment with palmitic acid and

inhibition of CD36 had no significant influence either. As CD36 inhibition did not change Erk1/2 phosphorylation, there might be no CD36-mediated downstream signaling affecting Erk1/2 activation in primary rat mesenchymal cells in response to palmitic acid. p38MAPK activation might in part be influenced by CD36, as shown by the difference of phosphorylation between PA and PA+SSO-treated cells after 10 minutes. But phopsphorylation of PA-treated cells was slightly decreased compared to the solvent control, although saturated fatty acids where reported to activate p38 (Silverstein, Li, Park, & Rahaman, 2010) in a CD36 dependent manner.

Development of a real-time measurement assay of ADAM17/TACE

ADAM17/TACE is supposed to be the main enzyme responsible for the shedding of TNFα. As it is reported to be upregulated in chronic liver injury and in HCC (Berasain, Castillo, Perugorria, Latasa, Prieto, & Avila, 2009) and is also responsible for the shedding of other factors involved in modulation of inflammation or cancer growth like TGFα, amphiregulin, HB-EGF, p55 TNFαR, p75 TNFαRII, IL-6R, ICAMs, VCAM and VEGFRs, we were interested whether its activity is influenced by free fatty acids. We were able to demonstrate TNFα gene expression to be elevated in response to palmitic acid in primary rat Kupffer cells (see Figure 19c) but could not show secretion of TNFα (Figure 11). We therefore attempted to develop an enzyme measurement assay using live cells and a fluorogenic substrate.

First of all, a suitable buffer for the reaction had to be chosen, which would not interfere with the measurement of fluorescence at the used wavelengths and would not promote any unspecific hydrolysis of the substrate. Buffers with minimal changes in fluorescence during the measurement were PBS, aqua bidest., 20mM Tris pH7.4, 50mM Tris pH 7.4 and TBS (Figure 20). The stability of the substrate DABCYL-TNFα-EDANS was the second important aspect for the selection of an appropriate buffer, so the fluorescence of the substrate in each buffer was measured (see Figure 21a). The fluorescence of buffer alone was subtracted from the fluorescences of substrate in the respective buffer to evaluate the stability of the substrate (see Figure 21b). The third aspect to be considered in chosing a buffer was its property to allow the cleavage of the substrate. To evaluate the most appropriate buffer, the substrate was incubated with typsin and the cleavage was followed by measuring the fluorescene of formed cleavage product. The highest increase in fluorescence was found in the Tris-buffers (20mM Tris pH7.4, 50mM Tris pH7.4, 250mM Tris pH7.4 and TBS), which is necessary to yield maximal sensitivity.

After calculating the signal:background ratio (see Figure 23) the Tris-buffers (20mM Tris pH7.4, 50mM Tris pH7.4, 250mM Tris pH7.4 and TBS) together with PBS showed the highest specificity in substrate cleavage. Therefore these Tris-buffers and HAM's medium were chosen as assay buffers for the cell based TACE assay.

For the cell-based assay, human THP1 cells were incubated for 24 hours with or without PMA, as this phorbol ester was reported to increase TACE activity on DRM cells (murine monocytes) (Doedens, Mahimkar, & Black, 2003) and on MonoMac-6 cells (Alvarez-Iglesias, Wayne, O'Dea, Amour, & Takata, 2005) followed by addition of LPS for another 3 hours. LPS is reported to increase TACE activity on THP1 cells (Alvarez-Iglesias, Wayne, O'Dea, Amour, & Takata, 2005) and on primary human monocytes (Scott, et al., 2011). Both activating agents are reported to increase TACE activity on the cell surface without changing TACE abundance. As fluorescence resulting from cleaved

Discussion

DABCYL-TNFα-EDANS was hightest using 20mM and 50mM Tris pH7.4 (see Figure 25c and d) we used these two buffers for further experiments, although the most significant difference in induced THP1 cells compared to uninduced cells was found in 250mM Tris pH7.4 and TBS. This might seem counterproductive, but fluorescence in 20mM and 50mM Tris was almost twice as high as in 250mM Tris and TBS, resulting in higher sensitivity when using these buffers.

Next, we had to evaluate whether the observed enzyme activity was due to TACE. Therefore we inhibited the enzyme with the specific inhibitor TAPI-2 (Gutiérrez-López, et al., 2011) and found 83% of TACE activity on THP1 cells inhibited by TAPI-2 after 9.6 minutes of incubation using 20mM Tris pH7.4 as an assay buffer (see Figure 26a). At the end of the measurement after about 52 minutes less than 50% of TACE activity could be observed. Inhibition using 50mM Tris pH7.4 was found to be less effective, resulting in 93.8% remaining TACE activity after 52 minutes of incubation (see Figure 26b). This was due to two facts, first, the activity of uninhibited THP1 cells was lower than observed in 20mM Tris pH7.4 and second, the activity of inhibited THP1 cells was higher compared to TAPI-2-treated cells in 20mM Tris pH7.4. Furthermore, no increase in fluorescence of sole THP1 cells, the inhibitor TAPI-2, nor the combination of cells with TAPI-2 could be observed, thereby proving that the measured fluorescence resulted solely from substrate cleavage.

TACE activity of LPS-induced and TAPI-2-inhibited THP1 cells was also tested to see whether activities could be decreased to the level of uninduced THP1 cells. This was done after different incubation periods in the presence or absence of LPS (see Figure 27). TACE activities of LPS-induced and uninduced THP1 cells after 3 hours of incubation were found to be quite similar, except in the first 15 minutes, indicating a slight increase in TACE activity in LPS-induced cells. TAPI-2 inhibited TACE activities to similar levels as already observed (~50-60% of remaining activity) and was found to be slightly higher in LPS-induced than in uninduced cells, especially within the first 30 minutes of measurement. After 6 and 24 hours of incubation, respectively, inhibition of LPS-induced and uninduced THP1 cells resulted in similar remaining activities which were also higher than after 3 hours of incubation when compared to the respective uninhibited activities. This may point to a probable reduction of TACE abundancy after longer incubation periods with LPS given that the used substrate concentration is high enough to ensure enzyme saturation or to a reduction in the responsiveness to LPS as it is reported in PMA-treated THP1 cells (Daigneault, Preston, Marriott, Whyte, & Dockrell, 2010). Nevertheless, TACE activity of LPS-treated cells was about 20% higher than in untreated cells.

Therefore we used higher concentrations of LPS than 10ng/ml. THP1 cells were incubated for 3, 6 or 24 hours with 10ng/ml, 100ng/ml or even 10µg/ml LPS (see Figure 28). No significant difference in TACE activity could be detected when cells were treated with different LPS concentrations; we therefore considered using higher concentrations than 10ng/ml of LPS unnecessary. This was further supported by the finding that TACE activities of induced and uninduced cells could also be inhibited using lower concentrations than of TAPI-2, but inhibition did not decrease with decreasing concentration of TAPI-2 (see Figure 29 and Figure 30).

A further explanation for the absence of a significant difference between TACE activities in LPS-induced and uninduced THP1 cells is the possible presence of TACE inhibitors in the serum (Doedens, Mahimkar, & Black, 2003). Although the assay is performed in a buffer without serum, there might still be inhibitors bound to TACE from the incubation with LPS. To test this hypothesis, THP1 cells were incubated with and without LPS in medium containing 1% or 5% FCS (see Figure 31). The TACE

72

activity of uninduced cells (without LPS) incubated in 5% FCS prior to the assay was lower than the activities of TAPI-2-inhibited cells. After LPS treatment of cells in medium containing 1% FCS, measured TACE activities were significantly higher in LPS-induced than in noninduced cells. This supports the possible presence of inhibitor of TACE in the serum which may interfere with the assay even though the medium is changed for the assay buffer. Apparently, some inhibitors are still present after medium removal. Inhibition of TACE by TAPI-2 reduced substrate cleavage of LPS-induced cells significantly. Surprisingly, the activity of TACE on noninduced cells could not further be inhibited, assuming, that in low serum TACE is either inactivated or not expressed unless cells are preincubated with LPS.

Substrate cleavage was further found to correlate with cell density (see Figure 32) and increased with increasing cell number independent of LPS treatment with the exception of the highest used density of 1×10^6 cells. This points to a limitation in cell density above which substrate cleavage is impaired.

TACE activities in primary rat Kupffer cells were not significantly different when cells were preincubated with medium, palmitic acid or two different concentrations of LPS for 3 hours (see Figure 33). Substrate cleavage could be inhibited by addition of TAPI-2 but not in a clear, dose-dependet manner, except when cells were preincubated with 100ng/ml LPS (see Figure 33c). Therefore, primary rat Kupffer cells may not respond to LPS with a significantly increased TACE activity. The expression of TACE in primary rat Kupffer cells was previously demonstrated by members of our group (Bintner, 2011). Further experiments are therefore required to test whether a shorter period of incubation with LPS using medium with just 1% FCS would result in more significant differences of TACE activities.

To make sure that there is a response of Kupffer cells to the LPS treatment, the secretion of TNFα into the supernatant was measured by ELISA (see Figure 34). TNFα could be detected in the supernatant of LPS treated cells at all time points investigated. Secretion of TNFα was also significantly decreased by the addition of TAPI-2, indicating that TACE is the primary sheddase for TNFα in primary rat Kupffer cells. Cells kept in medium or incubated with PMA, which is reported to increase TACE activity on DRM-cells (Doedens, Mahimkar, & Black, 2003) and MonoMac-6 cells (Scott, et al., 2011), did not secrete significant amounts of TNFα into the supernatant, although some shedding occurred after 6 hours in PMA-treated cells (about 680pg/ml; see Table 24). Nevertheless, TNFα concentrations after 6 hours in the supernatant of LPS-induced and TACE-inhibited (TAPI-2) cells was higher than in the supernatant of PMA-treated cells indicating that LPS is a far stronger inducer of TACE activity than PMA in primary rat Kupffer cells.

The fact that cleavage of the substrate could never be completely abrogated by the TACE specific inhibitor TAPI-2 indicates that further proteinases are involved in substrate cleavage on the membrane of primary rat Kupffer cells. Furthermore, it has to be taken into account that there might as well be inhibitors present in the incubation medium (FCS) that still inhibit TACE activity after changing the medium for the assay buffer, as it seems to be the case with THP1 cells. Another fact that has to be considered in establishing a fluorescence based assay is the stability of the used substrate DABCYL-TNFα-EDANS. In every assay that was performed, a positive control for the cleavage of the substrate was included. In this postitive control, trypsin was used for the cleavage of the substrate. The measured maximal fluorescent values (of trypsin-cleaved substrate after 68 min of assay time) decreased from 8500 arbitrary units to 2400 arbitrary units within 12 weeks during which aliquots of the substrate in assay buffer remained stored at -20°C. To achieve maximum sensitivity in

the sense of highest measureable fluorescence, experiments should be carried out within the first few weeks after solubilisation of the substrate to avoid loss of sensitivity.

Effects of in-vivo oil treatment on FFA serum levels and gene expression

Apart from in-vitro experiments we were interested in the in-vivo effects of oil ingestion, particularly in the transcriptional changes in the liver. Therefore rats were administered oil (1ml/100g body weight) or the same volume of water by gavage. The rats were sacrified 20 hours after administration and the concentration of free fatty acids in the sera and the gene expression in the liver was analyzed. Furthermore, another group of rats was administered oil daily on 6 consecutive days by gavage and gene expression in mesenchymal and parenchymal cells of the liver was compared with water-treated controls from the one-time administration experiment (20 hours).

The concentration of free fatty acids in the sera of oil-treated rats was found to be almost twice as high as in water-treated controls (see Figure 35 and Table 25) 20 hours after a one-time administration. After this period of time the administered oil is therefore already taken up and transported throughout the body and reaches the liver.

As inflammatory responses in the liver are mainly mediated by cells of the mesenchyme, we focused on the transcriptional changes in these cells, but also investigated changes in hepatocytes. Surprisingly, more genes were differentially expressed in mesenchymal cells (18 genes downregulated and 433 genes upregulated) than in parenchymal cells (3 genes downregulated and 9 upregulated) between oil-treatment and water-control. This leads to the assumption that oil-treatment has a greater effect on mesenchymal cells than on hepatocytes. The latter might not have to adapt their gene expression to a higher content of lipids in total metabolites as they basically represent the center of lipid metabolism and distribution in the body.

Genes with differential expression in mesenchymal cells of the livers of oil-treated animals compared to water-treated controls are involved in several pathways including immune response/inflammation, apoptosis, acute phase reactions, oxidative stress, regulation of the complement system, sugar, amino acid, purine and lipid metabolism, bile acid metabolism, lipid transport and lipoprotein assembly, ketone bodies and retinoic acid metabolism, liver regeneration, detoxification, eicosanoid production, the kinin-kallikrein-system, regulation of blood coagulation and blood pressure, cell cycle and genes associated with hyperlipidemia and obesity among others that will be discussed separately. The pathways involving most of the upregulated genes were metabolic ones including amino acid metabolism, fatty acid degradation (mitochondrial and peroxisomal), steroid and triglyceride biosynthesis and regulation and transport of lipids in lipoprotein particles as well as genes involved in bile acid metabolism and production of ketone bodies indicating the need of mesenchymal cells to adapt to a higher lipid content in metabolites.

Nine genes could be assigned to having a role in immune response with Ccl4 being 2-fold downregulated 20 hours after treatment as well as after 6 days of treatment; the other eight genes were found to be upregulated. Nupr1, for example, was reported to be a transcription factor upregulated in inflammatory processes regulating cell proliferation and tissue stress and is also induced by LPS via TNFα and NF-κB signaling in rat hepatoma cells (Kallwellis, Grempler, Günther, Päth, & Walther, 2006). Arginase, an enzyme of the urea cycle which enables mammals to dispose

otherwise toxic ammonia, was also found to play a role in regulating immune responses in the liver (Thomson & Knolle, 2010) and in cell proliferation of endothelial cells by the production of essential polyamines (Li, Meininger, Kelly, Hawker, Morris, & Wu, 2002). Rarres2 is a chemoattractant for cells of the innate and adaptive immune system (via binding to the receptors CCRL2 and GPR1 on immune cells), its plasma level correlates with BMI and its expression was also found to be induced by TNFα and IL-1β, whereas its loss was shown to affect the expression of GLUT4, DGAT2, leptin and adiponectin, all of which are involved in metabolism (Ernst & Sinal, 2010). Orm1 (also termed α_1-acid glycoprotein, AAG) is a typical acute phase reactant and inflammation associated protein in rats comparable to C-reactive protein in humans (Kuribayashi, Tomizawa, Seita, Tagata, & Yamamoto, 2011). A further acute phase reactant is haptoglobin, a hemoglobin-binding protein and antioxidant. Its expression is induced by IL-6 via STAT3 signaling and it is hypothesized to regulate the level and duration of inflammatory processes (Wang, Kinzie, Berger, Lim, & Baumann, 2001). Expression of inter alpha-trypsin inhibitor, heavy chain 4 (Itih4), together with haptoglobin, was found to be induced in hepatoma cells treated with IL-6 (Piñeiro, et al., 1999). Fgg, together with others, was found to be increased during CCl_4 induced liver fibrosis in rats (Cai, Shen, Zhou, & Wang, 2006). Most of these genes were not more than 2-fold upregulated anymore after 6 days of daily treatment, except for arginase (2.573-fold) and Serpina3n (2.035-fold), indicating that oil-treatment might induce an acute inflammatory response in the liver mesenchyme of rats which is attenuated after some days of treatment, pointing to an adaption to high fat content.

Genes of the complement system were also found to be upregulated including Mbl1, C9, C8a, Masp2 and Cfi. Upregulation of all genes 20 hours after the one-time oil treatment was attenuated after 6 days of treatment, with the exception of Cfi, which is an inhibitor of the C3 convertase, thus, indicating an induction and a concomitant, prolonging inhibition of the complement system. Linked to this system is the Kinin-kallikrein system, of which Kng1 and Kng2 were found to be induced 20 hours after the one-time oil administration. As it was the case in activation of the complement system, an inhibitor, Serpina4, was also found to be induced by the oil administration. The human homolog of Serpina4, kallistatin, was reported to inhibit kallikrein, the proteinase that cleaves and activates kininogens into mature kinins (Chao, Miao, Chen, Chen, & Chao, 2001). The third system besides the complement system and the kinin-kallikrein system that is regulated by factor F12 is blood coagulation of which the factors F9, F10, Serpinc1, Serpind1, Proc and Apoh were found to be upregulated. Serpinc1 is an inhibitor for F9, which in turn activates F10. Protein C (Proc) inhibits activation of F5 which would further activate thrombin which is also inhibited by Serpind1. Apoh was found to be an inhibitor of the intrinsic pathway of blood coagulation (Schousboe, 1985). With angiotensin II receptor 1a being also upregulated, this indicates to an overall increase of mRNA of components of systems regulating inflammation, blood pressure and coagulation including immature precursors and inhibitors. Although the upregulation of these genes was mostly just detectable after a one-time administration of oil (with the exception of Proc, F9 and Cfi) this might be the pathways responsible for the development of hypertension and chronic inflammation upon long-time challenge of the body with high contents of lipids.

Factors contributing to liver regeneration (Hgfac, Hrsp12, Apoa5 and Tm4sf4) were found to be upregulated. Hepatocyte growth factor activator (Hgfac) converts immature hepatocyte growth factor (HGF) into its mature, active form, which is involved in the recovery of the injured liver (Kaibori, et al., 2002). Heat-responsive protein 12 (Hrsp12) was also found to be upregulated during liver regeneration and probably acts as a fatty acid inducible protein in enterocytes (Kanouchi, et al.,

2006) (Kanouchi, et al., 2006). Apoa5 is also reported to be upregulated during liver regeneration, more specifically during the early phase (van der Vliet, et al., 2001). Transmembrane 4 L six family member 4 (Tm4sf4) was found to be overexpressed during CCl_4-induced liver injury and also seems to accelerate it by affecting TNFα and TNFR1 expression (Qiu, et al., 2007). Altogether, upregulation of these genes, two of which (Hrsp12 and Tm4sf4) were still more than 2-fold upregulated after 6 days of treatment, leads to the assumption that some stress or even damage occurs in the liver upon oil administration leading to the expression of genes involved in regeneration of this organ. This is further supported by the finding of the upregulation of genes involved in oxidative stress responses (Mgst1, Gstt2 and Gstm2) and the high increase in a vitamin E transporter (Ttpa), of which Gstm2 and Ttpa were still 2.14-fold and 3.59-fold, respectively, upregulated after 6 days of oil-treatment compared to controls. Furthermore, genes involved in detoxification reactions were upregulated, such as Aldh3a2, which is responsible for the detoxification of lipid peroxidation products (Demozay, et al., 2004) which arise and accumulate in livers after ingestion of peroxidized oil (Sagmeister, 2009). Among these were also genes responsible for the detoxification of xenobiotics like aflatoxin or nicotine (Akr7a2, Cyp3a9, Fmo5 and Cyp1a2).

In addition, factors reported to be overexpressed or involved in the development of obesity or of its symptom, hypertriglyceridemia, were found to be upregulated after oil administration. Solute carrier family 27 (fatty acid transporter), member 2 (Slc27a2) is implicated in lipid biosynthesis and fatty acid degradation and was found to be overexpressed in a diet-induced obesity model of rats and might be a possible marker for overweight development as its overexpression correlates with body weight increase (Caimari, Oliver, Rodenburg, Keijer, & Palou, 2010). Angiopoietin-like 3 (Angptl3) is a LXR induced, liver specific gene whose expression accounts for hypertriglyceridemia and its absence leads to triglyceride accumulation in the liver (Inaba, et al., 2003). Similarly apolipoprotein C-I (Apoc1) inhibits the binding of lipoprotein particles to the LDL-receptor, thereby aggravating hypertriglyceridemia (Jong, Hofker, & Havekes, 1999). Of these only Slc27a2 was found to be still upregulated after 6 days of daily oil administration supporting the hypothesis of a possible marker for overweight development.

Further genes found to be upregulated included dimethylarginine dimethylaminohydrolase 1 (Ddah1) which metabolizes asymmetric dimethylarginine, an inhibitor of nitric oxide synthesis. Overexpression of Ddah1 was shown to increase NO production and expression of VEGF resulting in increased angiogenesis and seems to play an important role in tumor associated angiogenesis (Kostourou, Robinson, Cartwright, & Whitley, 2002). Induction of similar intensity was found for regucalcin (Rgn) which is a calcium-induced gene reported to suppress NO production in the cytosol of rat livers (Yamaguchi, Takahashi, & Tsurusaki, 2003). In addition the transcription factor or regucalcin, Sec16b, was also found to be upregulated. Overexpression of Sec16b was shown to inhibit the gene expression of Casp3 and Casp8, thereby suppressing cell death (Yamaguchi, 2009). This shows additionally the increased expression of genes involved in the regulation of critical pathways implicated in inflammation (NO production) and cancer related angiogenesis. G0/G1switch2 was reported to be a direct PPARγ and probable PPARα target gene which is expressed in the liver and is upregulated during adipogenesis (Zandbergen, et al., 2005). Rbp4 is an adipokine produced by adipose tissue and liver and was found to contribute to insulin resistance development and positively correlates with blood pressure (Ou, Wu, Yang, Wu, Cheng, & Chang, 2011). Further, Grb14, a negative regulator of insulin signaling in the liver (Desbuquois, Béréziat, Authier, Girard, & Burnol, 2008), was 3.39-fold upregulated upon oil administration and was still upregulated 2.35-fold

after 6 days of oil administration. Asialoglycoprotein receptor 1 (Asgr1) mRNA and protein are downregulated in ethanol-induced fatty livers of rats as shown by Casey and colleagues (Casey, McVicker, Donohue, McFarland, Wiegert, & Nanji, 2004). Conversely, we found Asgr1 4.2-fold and 2.8-fold upregulated in livers of rats treated once or for 6 days with oil, respectively, compared to water-treated controls. Casey et al. compared fish-oil and ethanol treated rats with medium-chain triglyceride and ethanol treated rats and found a more pronounced downregulation of Asgr1 in the fish-oil treated group. As also ethanol was present in both groups of rats and Asgr1 is already downregulated in ethanol-treated rats, Asgr1 might be a possible 'marker' for distinguishing between alcohol caused and non-alcohol-caused steatosis. Kidney expressed gene 1 (Keg1, HP33) expression is stimulated in the regenerating liver and in hepatocellular carcinoma and also seems to play a role in the interphase of the cell cycle.

The gene showing the highest upregulation in hepatocytes was vanin-1 (vnn1) which was 5.5-fold increased in rats administered oil once compared to water-treated controls and was even 6.15-fold increased in livers of rats treated with oil for 6 days. Vanin-1 is a pantetheine hydrolase and catalyzes the conversion of pantetheine into cysteamine (an anti-oxidant) and pantothenate (or pantothenic acid, vitamin B5), therefore indicating a role for vanin-1 in fatty acid metabolism, inflammation, oxidative stress response (detoxification of lipid peroxidation products) and numerous diseases. Vanin-1 knockout mice showed enhanced resistance to oxidative stress and reduced oxidative stress-induced tissue inflammation. As the gene might also show anti-inflammatory and protective properties, its expression has to be tightly controlled to avoid deregulation resulting in a disease state (Kaskow, Proffit, Blangero, Moses, & Abraham, 2012).

Taking all the expressed genes and pathways together, this forms the picture of an increased metabolism (lipid, steroid, sugar, and bile acid), increased immune response (inflammation, complement), upregulation of components involved in the regulation of blood pressure and clotting, liver regeneration, oxidative stress response, regulation of NO-production and angiogenesis and factors involved in the development of insulin resistance, hypertriglyceridemia and obesity development. Although these genes were mostly found to be upregulated after a one-time administration of oil and just some of them were still upregulated after a 6 day oil-treatment, these genes might be the first ones of many whose deregulation contributes to the development of the various symptoms of the metabolic syndrome, one of which is the fatty liver that clearly predisposes towards NASH and HCC.

Abstract

Hepatocellular carcinoma (HCC) is the most common form of liver cancer and the third most common cause of cancer death. It develops in the background of chronic liver inflammation which might arise in a fatty liver. Predisposing conditions for the development of non-alcoholic steatohepatitis (NASH) are obesity and non-alcoholic fatty liver disease (NAFLD), both of which were shown to dramatically increase the risk of developing cancer, especially HCC. As inflammation plays a major role in the development and progression of HCC, we tried to elucidate the role of free fatty acids in the onset of inflammation, since their concentration is increased in obesity and NAFLD.

Therefore we performed in-vitro experiments treating primary rat mesenchymal and parenchymal cells with free fatty acids and taking a closer look at protein phosphorylation, gene expression and secretion of the pro-inflammatory cytokine TNFα. As ADAM17/TACE, a 'sheddase', seems to be involved in the conversion of inflammation-associated precursors into their mature forms and this sheddase is also found to be overexpressed in chronic liver injury and HCC, we were interested whether its activity could be increases by free fatty acids and therefore aimed to develop a real-time enzyme assay using live cells. In order to estimate in-vivo changes caused by a high lipid content in food, rats were administered oil by gavage and we analysed the content of free fatty acids in the plasma and the changes of gene expression in the liver.

We found that treatment of primary rat mesenchymal cells which palmitic acid, a saturated fatty acid, led to a 2-fold increase in the mRNA level of TNFα which seemed mainly be mediated by Kupffer cells. Endothelial cells did not respond to FFA-treatment by increasing the expression of COX-2, iNOS or TNFα, thereby masking the upregulation of these genes in total mesenchymal cells, as also COX-2 and iNOS expression were only found to be elevated in Kupffer cells. Inhibition of CD36, a fatty acid receptor and translocase, which is expressed in hepatocytes, endothelial cells and Kupffer cells, resulted in a reduction of COX-2, iNOS and TNFα expression levels in palmitic acid treated Kupffer cells. CD36-mediated downstream signaling seemed to be independent of p38MAPK or Erk1/2 since we found no activating phosphorylation of these kinases in palmitic acid treated cells.

In-vivo oil administration to rats resulted in a 2-fold increase in the concentration of free fatty acids in the serum and in the upregulation of genes involved in metabolism (fatty acids, steroids and sugars), immune responses (inflammation and complement system), regulation of blood pressure and coagulation, oxidative stress, angiogenesis and liver regeneration in cells of the liver mesenchyme indicating the increased challenge of the liver by the ingestion of food which contains a high lipid content. Among the upregulated genes were also some which were reported to correlate with the development of insulin resistance, hypertriglyceridemia and obesity, all of which contribute to the metabolic syndrome and predispose towards non-alcoholic steatohepatitis and HCC. Most changes in gene expression were found to occur in mesenchymal cells rather than in parenchymal cells indicating a substantial contribution of the liver mesenchyme and most probably of Kupffer cells in the early onset of immune reactions. Additionally, the highest upregulated gene found in hepatocytes was vanin-1 which seems to connect fatty acids metabolism with inflammation and oxidative stress responses urging the need for a tight regulation and control of this gene in the cell.

Zusammenfassung

Das Hepatozellulare Karzinom ist die häufigste Form des Leberkrebses und die dritthäufigste Krebstodesursache. Es entsteht in Folge einer chronischen Leberentzündung, deren Ursache häufig eine Fettleber ist. Fettleibigkeit und die entstehende Fettleber (nichtalkoholische Fettleber; NAFLD) sind prädestinierende Vorrausetzungen für die Entwicklung einer Fettleberentzündung (nichtalkoholische Fettleberentzündung, NASH). In beiden Erkrankungen zeigt sich ein erhöhtes Risiko für die Entstehung von Krebs, speziell für das hepatozellulare Karzinom. Da Entzündungen eine große Rolle bei der Entstehung und weiteren Entwicklung von Leberkrebs spielen, haben wir versucht, die Rolle der freien Fettsäuren, deren Konzentration bei Fettleibigkeit und Fettlebererkrankungen erhöht ist, aufzuklären.

Dafür haben wir in-vitro Experimente mit mesenchymalen und parenchymalen Primärzellen der Ratte durchgeführt, in denen die Zellen mit freien Fettsäuren behandelt und anschließend die Proteinphosphorylierung, die Genexpression und die Sekretion des pro-inflammatorischen Zytokins TNFα analysiert wurde. Da die „Sheddase" ADAM17/TACE in der Konvertierung von Vorstufen von entzündungsbeteiligten Faktoren in ihre lösliche, aktive Form beteiligt zu sein scheint, und des Weiteren auch in chronischen Lebererkrankungen und Leberkrebs überexprimiert sein dürfte, waren wir daran interessiert zu sehen, ob ihre Enzymaktivität sich durch freie Fettsäuren erhöhen würde. Daher haben wir versucht, eine Möglichkeit zu entwickeln, die Enyzmaktivität auf lebenden Zellen zu messen. Um die in-vivo Veränderungen, die durch eine fettreiche Nahrung entstehen, abschätzen zu können, wurde Ratten Öl mittels Schlundsonde verabreicht und die freien Fettsäuren im Plasma bestimmt und die Änderungen der Genexpression in der Leber analysiert.

Die Behandlung von primären Rattenzellen mit Palmitinsäure, einer gesättigten Fettsäure, führte zu einem zweifachen Anstieg der TNFα mRNA, was hauptsächlich durch Kupfferzellen versucht wurde. Endothelzellen reagierten auf die Fettsäurebehandlungen nicht mit einer Veränderung in der Genexpression von COX-2, iNOS oder TNFα, was auch die Expressionsänderung in der mesenchymalen Zellenfraktion maskiert haben dürfte, da diese Gene nur in Kupfferzellen erhöht exprimiert wurden. Die Inhibierung von CD36, einem Fettsäurerezeptor und -transporter, der von Hepatozyten, Endothelzellen und Kupfferzellen exprimiert wird, resultierte in einer verminderten Expression von COX-2, iNOS und TNFα in palmitinsäurebehandelten Kupfferzellen. Die durch CD36 verursachte Signalweiterleitung scheint unabhängig von den Kinasen p38 und Erk zu sein, da keine aktivierenden Phosphorylierungen in palmitinsäurebehandelten Zellen gefunden wurde.

Die Ölschlundierung von Ratten führte zu einer zweifachen Erhöhung der freien Fettsäuren im Serum der Tiere und zu der Expression von Genen, die im Metabolismus (von Fetten, Steroiden und Zuckern), in der Immunantwort (Entzündungen und Komplementsystem), in der Regulierung des Blutdrucks und der –koagulation, bei oxidativem Stress, Angiogenese sowie in der Leberregenerierung involviert sind. Das deutet auf eine erhöhte Forderung der Leber durch fettreiche Nahrung hin. Unter den erhöht exprimierten Genen waren solche, die mit der Entstehung von Insulinresistenz, Hypertriglyceridämien und Fettleibigkeit korrelieren. All diese Erkrankungen tragen zum Metabolischen Syndrom bei und erhöhen das Risiko für Leberentzündung und Krebs. Die meisten Veränderungen in der Genexpression wurden in mesenchymalen Zellen beobachtet, was auf deren wesentliche Rolle (und im Speziellen von Kupfferzellen) in der frühen Entstehung von Immunreaktionen hindeuten könnte. Zusätzlich scheint das am Höchsten raufregulierte Gen in

79

Zusammenfassung

Hepatozyten (Vanin-1) den Fettsäuremetabolismus mit Entzündungsreaktionen und oxidativem Stress zu verknüpfen, was es besonders notwendig erscheinen lässt, dass dieses Gen ganz genau in den Zellen reguliert und kontrolliert wird.

Appendix

List of tables

Appendix

List of figures

Appendix

List of abbreviations

ACOX – acyl coenzyme A oxidase 1
ADAM17 – a disintegrin and metalloproteinase 17 (synonym for TACE)
AhR – aryl hydrocarbon receptor
ALA – α-linolenic acid
ALT – alanine aminotransferase
AST – aspartate aminotransferase
ATGL – Adipose triglyceride lipase
BMI – Body-mass-index
BSA – bovine serum albumin
cAMP – cyclic adenosine monophosphate
COX2 – cyclooxygenase 2, prostaglandin synthase 2
CPT-I – carnitine palmitoyltransferase-I
CRP – C-reactive-protein
DAMP – damage-associated molecular pattern
DEN – diethylnitrosamine
DGAT – diacylglycerol acyl transferase
DHA – docosahexaenoic acid
DMSO – dimethyl sulfoxide
DNL – de-novo lipogenesis
EC – endothelial cell
EGFR – epidermal growth factor receptor
EMT – epithelial-mesenchymal transition
EPA – eicosapentaenoic acid
EtOH – ethanol
FFA – free fatty acid (synonym for NEFA)
GPR – G-protein-coupled receptor
HB-EGF – heparin-binding epidermal growth factor
HBV – hepatitis B virus
HC – hepatocytes
HCC – hepatocellular carcinoma
HCV – hepatitis C virus
HFD – high fat diet
HGF – hepatocyte growth factor
IL6 – interleukin 6
iNOS – inducible nitric oxide synthase
JAK – Janus Kinase
KC – Kupffer cell
LH – linolic acid
LOX – lipoxygenase
LXR – liver X receptor
MAPK – mitogen-activated protein kinase
MCP-I – monocyte chemoattractant protein 1, (synonym for CCL2)
MIF – macrophage migration inhibitory factor
MMP – Matrix metalloproteinase
NAFLD – non-alcoholic fatty liver disease
NASH – non-alcoholic steatohepatitis
NEFA – non-esterified fatty acid (synonym for FFA)
NOD – Nucleotide-binding oligomerization domain protein
NPC – non-parenchymal cell, mesenchymal cell
PA – palmitic acid
PAMP – pathogen-associated molecular pattern

Appendix

PGE2 – prostaglandin E_2
PKA – protein kinase A
PMA – phorbol 12-myristate 13-acetate
PRR – pattern recognition receptor
PUFA – polyunsaturated fatty acid
PXR – pregnane X receptor
ROS – reactive oxygen species
SFA – saturated fatty acid
SOCS – suppressor of cytokine signaling
SREBP – sterol regulatory element-binding protein
SSO - Sulfosuccinimidyl oleate sodium
STAT – signal transducer and activator of transcription
T2D – type 2 diabetes
TACE – TNFα converting enzyme (synonym for ADAM17)
TAK – TGFβ activated kinase
TG – triglyceride
TNFα – tumor necrosis factor alpha
UPR – unfolded protein response
VEGFR – vascular endothelial growth factor
VLDL – very low-density lipoprotein
WHO – World Health Organization

Supplementary data

Changes in gene expression in mesenchymal cells after 20h

Affymetrix ID	Public ID	Gene Symbol	Gene Title	fold control	SD
1378690_at	BI291986	Ly6al	lymphocyte antigen 6 complex, locus A-like	0,195	0,244
1387839_at	NM_012646	RT1-N1 /// RT1-N2	RT1 class Ib, locus N1 /// RT1 class Ib, locus N2	0,395	0,160
1391279_at	AI112564	Scin	Scinderin	0,417	0,128
1388275_at	AW919577	Tcrb	T-cell receptor beta chain	0,422	0,085
1388968_at	BF402642	Mpped1	metallophosphoesterase domain containing 1	0,431	0,151
1376908_at	AW531805	Ifit3	interferon-induced protein with tetratricopeptide repeats 3	0,433	0,196
1370499_at	M62891	Klrb1a	killer cell lectin-like receptor subfamily B, member 1A	0,439	0,085
1377626_at	AA924350	LOC690768	Hypothetical protein LOC690768	0,445	0,162
1382999_at	AI411747	Art2b	ADP-ribosyltransferase 2b	0,450	0,102
1379653_a_at	AI176327	Sh2d1a	SH2 domain protein 1A	0,474	0,152
1380967_at	BE101670	Nts	neurotensin	0,478	0,098
1373994_at	BM388789	Aplf	aprataxin and PNKP like factor	0,483	0,201
1392309_at	BI300426	Jam2	junctional adhesion molecule 2	0,484	0,211
1377163_at	BM385741	Inhbb	inhibin beta-B	0,485	0,205
1370394_at	L22654	IgG-2a	gamma-2a immunoglobulin heavy chain	0,486	0,373
1370832_at	U06434	Ccl4	chemokine (C-C motif) ligand 4	0,489	0,133
1371015_at	X52711	Mx1	myxovirus (influenza virus) resistance 1	0,493	0,088
1379794_at	AI029386	Gzmb	granzyme B	0,497	0,111
1380066_at	BF401956	Tfr2	transferrin receptor 2	2,005	0,736
1370019_at	AF394783	Sult1a1	sulfotransferase family, cytosolic, 1A, phenol-preferring, member 1	2,008	1,677
1373134_at	BE329450	Fahd2a	fumarylacetoacetate hydrolase domain containing 2A	2,010	1,204
1370155_at	BM388837	Col1a2	collagen, type I, alpha 2	2,010	1,300
1388526_at	AI169075	Gstz1	glutathione transferase zeta 1	2,013	1,808
1387372_at	NM_133623	Slc6a13	solute carrier family 6 (neurotransmitter transporter, GABA), member 13	2,016	1,082
1370939_at	D90109	Acsl1	acyl-CoA synthetase long-chain family member 1	2,020	0,984
1367598_at	NM_012681	Ttr	transthyretin	2,022	1,381
1391538_at	AI137938	Cideb	cell death-inducing DFFA-like effector b	2,026	1,474
1367755_at	NM_052809	Cdo1	cysteine dioxygenase, type I	2,026	1,414
1370821_at	AF120100	Tpmt	thiopurine S-methyltransferase	2,026	1,228
1372158_at	BI295768	Macrod1	MACRO domain containing 1	2,028	1,397
1382235_at	BF549700	RGD1306809	similar to hypothetical protein FLJ30596	2,028	1,499
1371379_at	AI011738	RGD1563422	similar to Brain protein 44	2,029	0,896
1370547_at	M84000	Pzp	pregnancy-zone protein	2,029	1,386
1368574_at	NM_016991	Adra1b	adrenergic, alpha-1B-, receptor	2,029	0,635
1377192_a_at	BM384629	Clpx	ClpX caseinolytic peptidase X homolog (E. coli)	2,031	1,423
1370676_at	AF436847	RGD1564614	similar to complement factor H-related protein	2,033	1,043
1371012_at	AJ245707	Hacl1	2-hydroxyacyl-CoA lyase 1	2,041	0,857
1381006_at	BE119649	Hgfac	hepatocyte growth factor activator	2,042	1,049
1368702_at	U05989	Pawr	PRKC, apoptosis, WT1, regulator	2,042	0,837
1392988_at	BF407232	Nsdhl	NAD(P) dependent steroid dehydrogenase-like	2,043	1,377
1369531_at	NM_133547	Sult1c2	sulfotransferase family, cytosolic, 1C, member 2	2,048	1,182
1389738_at	AA848420	Ung	uracil-DNA glycosylase	2,048	0,845
1387567_at	NM_017111	LOC100360270 /// Slco1a1	solute carrier organic anion transporter family member 1A1-like /// solute carrier organic anion transporter family, member 1a1	2,053	1,205
1368964_at	NM_030856	Lrrn3	leucine rich repeat neuronal 3	2,054	1,361
1368536_at	NM_057104	Enpp2	ectonucleotide pyrophosphatase/phosphodiesterase 2	2,055	0,766
1373243_at	BG378288	Pmvk	phosphomevalonate kinase	2,056	1,462
1368931_at	NM_031238	Sh3gl3	SH3-domain GRB2-like 3	2,064	1,319
1393239_at	BI296413	Mtfr1	Mitochondrial fission regulator 1	2,066	1,376
1389725_at	BM390364	Tm7sf2	transmembrane 7 superfamily member 2	2,067	0,786
1367818_at	NM_019187	Coq3	coenzyme Q3 homolog, methyltransferase (S. cerevisiae)	2,068	1,017
1371094_at	L06804	Lhx2	LIM homeobox 2	2,072	1,308
1387233_at	NM_017235	Hsd17b7	hydroxysteroid (17-beta) dehydrogenase 7	2,073	1,237
1370952_at	AI169331	Gstm2	glutathione S-transferase mu 2	2,074	1,532
1387783_a_at	NM_012489	Acaa1 /// RGD1562373	acetyl-Coenzyme A acyltransferase 1 /// similar to 3-ketoacyl-CoA thiolase B, peroxisomal precursor (Beta-ketothiolase B)	2,083	1,178
1388908_at	BI278268	Peci	peroxisomal D3,D2-enoyl-CoA isomerase	2,083	1,181
1369720_at	NM_053986	Myo1b	myosin Ib	2,088	1,057
1369657_at	NM_016998	Cpa1	carboxypeptidase A1	2,091	1,527

Appendix

Affymetrix ID	Public ID	Gene Symbol	Gene Title	fold control	SD
1393241_at	BI295197	Prss32	protease, serine, 32	2,091	1,169
1389551_at	AI008160	Lactb2	lactamase, beta 2	2,097	1,165
1376847_at	BI302283	Mosc1	MOCO sulphurase C-terminal domain containing 1	2,100	0,759
1368244_at	NM_080890	As3mt	arsenic (+3 oxidation state) methyltransferase	2,100	1,278
1368943_at	NM_020082	Rnase4	ribonuclease, RNase A family 4	2,101	1,407
1378536_at	AI638960	Hook1	hook homolog 1 (Drosophila)	2,102	1,310
1370377_at	M25143	Cyp2d1 /// Cyp2d5	cytochrome P450, family 2, subfamily d, polypeptide 1 /// cytochrome P450, family 2, subfamily d, polypeptide 5	2,108	1,086
1368316_at	NM_019158	Aqp8	aquaporin 8	2,109	1,422
1392825_at	AA923852	RGD1559600	RGD1559600	2,111	1,416
1386904_a_at	AF007107	Cyb5a	cytochrome b5 type A (microsomal)	2,111	1,106
1374947_at	BI286041	Bcar3	breast cancer anti-estrogen resistance 3	2,112	0,858
1368365_at	NM_031731	Aldh3a2	aldehyde dehydrogenase 3 family, member A2	2,114	0,934
1383920_at	BF408907	Amt	aminomethyltransferase	2,114	1,182
1387821_at	NM_017313	Rab3ip	RAB3A interacting protein (rabin3)	2,118	0,973
1389177_at	AI598971	Perp	PERP, TP53 apoptosis effector	2,127	1,373
1368418_a_at	AF202115	Cp	ceruloplasmin	2,133	0,952
1385668_at	AI044864	LOC683460	hypothetical protein LOC683460	2,135	1,446
1393403_at	AI058911	Angptl3	angiopoietin-like 3	2,138	1,863
1376733_at	AI407898	Igsf11	immunoglobulin superfamily, member 11	2,141	1,588
1391806_at	AA957557	LOC498793	similar to inter-alpha-inhibitor H2 chain	2,142	1,476
1368087_a_at	NM_133545	Ptpn21	protein tyrosine phosphatase, non-receptor type 21	2,143	1,103
1370148_at	NM_012582	Hp	haptoglobin	2,144	1,390
1390172_at	AI409946	Dhtkd1	dehydrogenase E1 and transketolase domain containing 1	2,145	1,180
1398252_at	NM_017209	Mecr	mitochondrial trans-2-enoyl-CoA reductase	2,153	1,113
1387082_at	NM_053348	Fetub	fetuin B	2,154	1,642
1394483_at	AW535310	Adamts5	ADAM metallopeptidase with thrombospondin type 1 motif, 5	2,155	0,747
1387325_at	NM_024143	Slc27a5	solute carrier family 27 (fatty acid transporter), member 5	2,160	1,438
1373210_at	BI296460	Lamb1	laminin, beta 1	2,162	1,743
1372260_at	BI296304	Rogdi	rogdi homolog (Drosophila)	2,163	1,659
1390131_at	BE112936	Srr	serine racemase	2,166	1,492
1379606_at	BM392291	Rab30	RAB30, member RAS oncogene family	2,167	1,276
1368060_at	NM_031714	Hrsp12	heat-responsive protein 12	2,167	1,517
1387825_at	NM_031533	Ugt2b	UDP glycosyltransferase 2 family, polypeptide B	2,170	1,823
1383826_at	AA924620	Rab40b	Rab40b, member RAS oncogene family	2,179	1,984
1367612_at	NM_134349	Mgst1	microsomal glutathione S-transferase 1	2,180	1,481
1383469_at	BG377269	Aldh1a3	aldehyde dehydrogenase 1 family, member A3	2,180	1,410
1368587_at	NM_012824	Apoc1	apolipoprotein C-I	2,181	1,458
1370396_x_at	AF198441	Rup2	urinary protein 2	2,182	1,666
1387531_at	NM_053307	Msra	methionine sulfoxide reductase A	2,185	1,373
1369225_at	NM_012741	Kng2	kininogen 2	2,186	1,744
1398260_a_at	NM_024382	Serpind1	serine (or cysteine) peptidase inhibitor, clade D, member 1	2,186	1,376
1370299_at	M10149	Aldob	aldolase B, fructose-bisphosphate	2,188	1,459
1376546_at	BE120498	RGD1565432	similar to hypothetical protein	2,190	1,299
1387093_at	NM_131906	Slco1a4	solute carrier organic anion transporter family, member 1a4	2,193	1,618
1374959_at	AA945624	Nqo2	NAD(P)H dehydrogenase, quinone 2	2,196	1,340
1388884_at	BM390774	RGD1310224	similar to RIKEN cDNA 1810022C23	2,199	1,083
1368662_at	NM_134374	Rnf39	ring finger protein 39	2,203	1,397
1391491_a_at	BG377084	Rad23b	RAD23 homolog B (S. cerevisiae)	2,204	1,203
1368824_at	BM392106	Cald1	caldesmon 1	2,214	1,643
1371031_at	AI454484	Mat1a	methionine adenosyltransferase I, alpha	2,214	1,450
1388441_at	BG379987	LOC689574	hypothetical protein LOC689574	2,214	1,359
1372438_at	AI411100	Nit2	nitrilase family, member 2	2,215	1,325
1392090_at	BG377322	Serpinc1	serine (or cysteine) peptidase inhibitor, clade C (antithrombin), member 1	2,222	1,433
1367843_at	NM_134407	Akr7a2	aldo-keto reductase family 7, member A2 (aflatoxin aldehyde reductase)	2,228	1,387
1368707_at	NM_019369	Itih4	inter alpha-trypsin inhibitor, heavy chain 4	2,230	1,314
1368409_at	NM_012796	Gstt2	glutathione S-transferase, theta 2	2,233	1,325
1367828_at	NM_022512	Acads	acyl-Coenzyme A dehydrogenase, C-2 to C-3 short chain	2,233	1,325
1388422_at	BI275904	Lims2	LIM and senescent cell antigen like domains 2	2,234	1,468
1375530_at	BG374612	Gnpnat1	glucosamine-phosphate N-acetyltransferase 1	2,236	1,471
1386568_at	BF557891	Irf6	interferon regulatory factor 6	2,240	1,661
1393242_at	BE104107	Snrnp25	small nuclear ribonucleoprotein 25 (U11/U12)	2,242	1,373
1387765_at	NM_012599	Mbl1	mannose-binding lectin (protein A) 1	2,244	1,440
1367847_at	NM_053611	Nupr1	nuclear protein, transcriptional regulator, 1	2,247	1,653
1368380_at	NM_019156	Vtn	vitronectin	2,247	1,501

Affymetrix ID	Public ID	Gene Symbol	Gene Title	fold control	SD
1386954_at	NM_030986	Ak2	adenylate kinase 2	2,249	1,213
1375056_at	AA943310	LOC100365923	rCG57079-like	2,254	2,009
1369840_at	NM_134379	UST4r	integral membrane transport protein UST4r	2,259	1,595
1367979_s_at	NM_012941	Cyp51	cytochrome P450, family 51	2,261	1,236
1387145_at	NM_017251	Gjb1	gap junction protein, beta 1	2,261	1,431
1374478_at	AA819329	RGD1305347	similar to RIKEN cDNA 2610528J11	2,265	2,046
1371083_at	D00752	LOC299282	Serine protease inhibitor	2,269	1,652
1367917_at	NM_012730	Cyp2d2	cytochrome P450, family 2, subfamily d, polypeptide 2	2,273	1,603
1369960_at	NM_031648	Fxyd1	FXYD domain-containing ion transport regulator 1	2,278	2,217
1367720_at	NM_012899	Alad	aminolevulinate, delta-, dehydratase	2,288	1,242
1368431_at	NM_017112	Hpn	hepsin	2,300	1,042
1391433_at	AA899721	Acot2	acyl-CoA thioesterase 2	2,306	1,083
1383654_a_at	BE112523	Fn3k	fructosamine 3 kinase	2,308	1,456
1370397_at	M33936	Cyp4a3	cytochrome P450, family 4, subfamily a, polypeptide 3	2,308	1,399
1372000_at	AI180187	Net1	neuroepithelial cell transforming 1	2,312	1,445
1369072_at	NM_134329	Adh7	alcohol dehydrogenase 7 (class IV), mu or sigma polypeptide	2,313	1,845
1393061_at	AI030103	Ttc36	tetratricopeptide repeat domain 36	2,316	1,738
1368253_at	NM_012793	Gamt	guanidinoacetate N-methyltransferase	2,318	1,809
1372440_at	BI275818	Serpine2	serine (or cysteine) peptidase inhibitor, clade E, member 2	2,318	1,656
1392189_at	BE105136	Rfx4	Regulatory factor X, 4 (influences HLA class II expression)	2,328	1,172
1382325_at	AW525471	Gcat	glycine C-acetyltransferase (2-amino-3-ketobutyrate-coenzyme A ligase)	2,329	1,804
1387228_at	NM_012879	Slc2a2	solute carrier family 2 (facilitated glucose transporter), member 2	2,335	2,119
1368155_at	NM_031572	Cyp2c12	cytochrome P450, family 2, subfamily c, polypeptide 12	2,339	1,791
1381574_at	BF403907	Tmem195	transmembrane protein 195	2,340	1,738
1368397_at	NM_031980	Ugt2b36	UDP glucuronosyltransferase 2 family, polypeptide B36	2,344	2,178
1376537_at	AW435010	Ptpn3	Protein tyrosine phosphatase, non-receptor type 3	2,346	1,583
1368304_at	NM_053433	Fmo3	flavin containing monooxygenase 3	2,347	2,288
1368583_a_at	NM_133428	Hrg	histidine-rich glycoprotein	2,348	2,472
1388569_at	AI179984	Serpinf1	serine (or cysteine) peptidase inhibitor, clade F, member 1	2,354	1,606
1388617_at	AW914746	Bphl	biphenyl hydrolase-like (serine hydrolase)	2,357	1,634
1373748_at	AW532566	Pdzrn3	PDZ domain containing RING finger 3	2,357	0,371
1369111_at	NM_012556	Fabp1	fatty acid binding protein 1, liver	2,358	1,452
1367672_at	NM_024392	Hsd17b4	hydroxysteroid (17-beta) dehydrogenase 4	2,362	1,160
1370496_at	AB008424	Cyp2d3	cytochrome P450, family 2, subfamily d, polypeptide 3	2,366	1,519
1379744_at	AI137930	Saa4	serum amyloid A4, constitutive	2,366	2,045
1388537_at	BF554891	Nipsnap1	4-nitrophenylphosphatase domain and non-neuronal SNAP25-like protein homolog 1 (C. elegans)	2,371	1,875
1368150_at	NM_031736	Slc27a2	solute carrier family 27 (fatty acid transporter), member 2	2,377	1,613
1396103_at	BF556107	Cmbl	carboxymethylenebutenolidase homolog (Pseudomonas)	2,382	1,760
1368266_at	NM_017134	Arg1	arginase, liver	2,390	1,643
1369635_at	NM_017052	Sord	sorbitol dehydrogenase	2,391	1,813
1373924_at	AI712686	Cpped1	calcineurin-like phosphoesterase domain containing 1	2,398	1,268
1370235_at	AI175009	Dbi	diazepam binding inhibitor (GABA receptor modulator, acyl-Coenzyme A binding protein)	2,402	1,704
1376765_at	BF283408	Mro	maestro	2,412	1,895
1377018_at	BF284124	Pamr1	peptidase domain containing associated with muscle regeneration 1	2,414	1,751
1374625_at	AI176616	Hes6	hairy and enhancer of split 6 (Drosophila)	2,416	1,251
1393751_at	AA859029	Fabp12	Fatty acid binding protein 12	2,421	2,195
1367667_at	NM_031840	Fdps	farnesyl diphosphate synthase (farnesyl pyrophosphate synthetase, dimethylallyltranstransferase, geranyltranstransferase)	2,421	1,699
1371615_at	BI279069	Dgat2	diacylglycerol O-acyltransferase homolog 2 (mouse)	2,422	1,486
1373625_at	AI412012	Shmt1	serine hydroxymethyltransferase 1 (soluble)	2,422	1,426
1368400_at	NM_053370	Timm8a1	translocase of inner mitochondrial membrane 8 homolog a1 (yeast)	2,424	1,563
1382864_at	AI231808	Palmd	palmdelphin	2,426	1,676
1375504_at	BM390747	Polg2	polymerase (DNA directed), gamma 2, accessory subunit	2,430	1,881
1371519_at	AA851258	Etfdh	electron-transferring-flavoprotein dehydrogenase	2,430	1,571
1369764_at	NM_012516	C4bpa	complement component 4 binding protein, alpha	2,441	1,774
1389648_at	AI170382	Ripk4	receptor-interacting serine-threonine kinase 4	2,442	1,681
1370836_at	U51017	Serpina4	serine (or cysteine) proteinase inhibitor, clade A (alpha-1 antiproteinase, antitrypsin), member 4	2,443	1,671
1377048_at	H31813	Dak	dihydroxyacetone kinase 2 homolog (S. cerevisiae)	2,443	1,483
1387034_at	NM_012619	Pah	phenylalanine hydroxylase	2,444	1,684
1368336_at	NM_017126	Fdx1	ferredoxin 1	2,444	2,178
1386274_at	AI169925	Slc17a2	solute carrier family 17 (sodium phosphate), member 2	2,444	1,537
1384512_at	AI072137	LOC100363441	hypothetical protein LOC100363441	2,444	1,827

Appendix

Affymetrix ID	Public ID	Gene Symbol	Gene Title	fold control	SD
1377758_at	BF415386	Hsd17b13	hydroxysteroid (17-beta) dehydrogenase 13	2,448	1,838
1386927_at	NM_012930	Cpt2	carnitine palmitoyltransferase 2	2,454	1,213
1369073_at	NM_021745	Nr1h4	nuclear receptor subfamily 1, group H, member 4	2,458	1,720
1370414_at	M94043	Rab38	RAB38, member RAS oncogene family	2,463	2,139
1391417_at	AA925145	Bhmt2	betaine-homocysteine methyltransferase 2	2,476	1,792
1384628_at	AI549292	Iyd	iodotyrosine deiodinase	2,478	1,628
1398516_at	BF283013	Golt1a	golgi transport 1 homolog A (S. cerevisiae)	2,481	1,885
1370086_at	NM_012559	Fgg	fibrinogen gamma chain	2,482	1,973
1367702_at	NM_016986	Acadm	acyl-Coenzyme A dehydrogenase, C-4 to C-12 straight chain	2,485	1,712
1379592_at	AI045151	Slc25a13	solute carrier family 25, member 13 (citrin)	2,495	1,590
1374527_at	AI172274	Echdc2	enoyl Coenzyme A hydratase domain containing 2	2,499	1,756
1368814_at	NM_031057	Aldh6a1	aldehyde dehydrogenase 6 family, member A1	2,500	1,651
1376174_at	AI137506	Serpina11	serine (or cysteine) peptidase inhibitor, clade A (alpha-1 antiproteinase, antitrypsin), member 11	2,505	1,843
1369291_at	NM_030985	Agtr1a	angiotensin II receptor, type 1a	2,505	0,714
1387905_at	AB062135	Dnajc12	DnaJ (Hsp40) homolog, subfamily C, member 12	2,506	1,756
1371691_at	BI282993	Rarres2	retinoic acid receptor responder (tazarotene induced) 2	2,507	1,370
1390789_at	BI296347	Acad11	acyl-Coenzyme A dehydrogenase family, member 11	2,508	1,467
1387111_at	NM_022297	Ddah1	dimethylarginine dimethylaminohydrolase 1	2,512	2,311
1387963_a_at	M24396	Uox	urate oxidase	2,514	1,595
1367871_at	NM_031543	Cyp2e1	cytochrome P450, family 2, subfamily e, polypeptide 1	2,516	2,054
1393947_at	BG377383	Slc25a15	Solute carrier family 25 (mitochondrial carrier; ornithine transporter) member 15	2,517	1,394
1391679_at	AA944639	LOC691083	hypothetical protein LOC691083	2,517	1,892
1382496_at	BI288517	Hnf4a	Hepatocyte nuclear factor 4, alpha	2,518	1,448
1391483_at	BF282264	Creb3l3	cAMP responsive element binding protein 3-like 3	2,519	1,613
1368205_at	NM_024157	Cfi	complement factor I	2,521	1,821
1377051_at	AA849966	LOC100366119	Mpv17 transgene, kidney disease mutant-like (predicted)-like	2,526	2,221
1372860_at	BE112971	Lhpp	phospholysine phosphohistidine inorganic pyrophosphate phosphatase	2,531	2,079
1370511_at	U05675	Fgb	fibrinogen beta chain	2,537	1,961
1367885_at	NM_031587	Pxmp2	peroxisomal membrane protein 2	2,537	1,736
1377921_at	AA875050	Etnk2	ethanolamine kinase 2	2,540	1,634
1387955_at	M31109	Ugt2b5	UDP glucuronosyltransferase 2 family, polypeptide B5	2,540	2,335
1398310_at	D17309	Akr1d1	aldo-keto reductase family 1, member D1 (delta 4-3-ketosteroid-5-beta-reductase)	2,541	1,570
1372765_a_at	BM390774	Peci /// RGD1310224	peroxisomal D3,D2-enoyl-CoA isomerase /// similar to RIKEN cDNA 1810022C23	2,557	1,442
1385767_at	BF411017	LOC304000	cell adhesion molecule JCAM	2,557	1,878
1370387_at	U46118	Cyp3a9	cytochrome P450, family 3, subfamily a, polypeptide 9	2,558	2,086
1384103_at	BE106350	RGD1561416	similar to novel protein (HT036)	2,559	1,688
1370420_at	J05035	Srd5a1	steroid-5-alpha-reductase, alpha polypeptide 1 (3-oxo-5 alpha-steroid delta 4-dehydrogenase alpha 1)	2,561	1,914
1371542_at	BI284599	Tuba4a	tubulin, alpha 4A	2,567	2,278
1390421_at	AI232524	Npl2	N-acetylneuraminate pyruvate lyase 2 (putative)	2,576	2,050
1368627_at	NM_031546	Rgn	regucalcin (senescence marker protein-30)	2,579	1,865
1386571_at	BF567145	RGD1562626	Similar to adaptor molecule SRCASM	2,580	1,890
1395041_at	BM385230	Mttp	microsomal triglyceride transfer protein	2,581	1,771
1376792_at	AW251313	Fam176a	family with sequence similarity 176, member A	2,582	1,271
1368686_at	NM_012901	Ambp	alpha-1-microglobulin/bikunin precursor	2,585	1,838
1383165_at	BM390462	RGD1310209	similar to KIAA1324 protein	2,586	2,230
1388988_at	AI175070	Abhd14b	abhydrolase domain containing 14b	2,587	1,969
1398267_at	NM_053537	Slc22a7	solute carrier family 22 (organic anion transporter), member 7	2,588	1,555
1379833_at	BE110171	Lingo4 /// Rorc	leucine rich repeat and Ig domain containing 4 /// RAR-related orphan receptor C	2,589	1,843
1370936_at	AA892345	Dmgdh	dimethylglycine dehydrogenase	2,589	1,981
1387121_a_at	NM_133583	Ndrg2	N-myc downstream regulated gene 2	2,593	1,679
1369011_at	AF202888	Apoa5	apolipoprotein A-V	2,597	1,695
1368467_at	NM_019623	Cyp4f1	cytochrome P450, family 4, subfamily f, polypeptide 1	2,599	2,401
1369286_at	NM_012803	Proc	protein C	2,602	1,652
1371137_at	X95189	Acox2	acyl-Coenzyme A oxidase 2, branched chain	2,605	1,612
1387376_at	NM_019363	Aox1	aldehyde oxidase 1	2,606	1,712
1369206_at	NM_053617	Cpb2	carboxypeptidase B2 (plasma)	2,607	1,942
1377407_at	BI290154	Acsm5	acyl-CoA synthetase medium-chain family member 5	2,616	1,983
1382678_at	AA859019	Cfhl1	complement component factor h-like 1	2,631	2,234
1369074_at	NM_130748	Slc38a4	solute carrier family 38, member 4	2,634	1,923
1389350_at	AI180413	Apoh	apolipoprotein H (beta-2-glycoprotein I)	2,635	2,018

Affymetrix ID	Public ID	Gene Symbol	Gene Title	fold control	SD
1368453_at	NM_031344	Fads2	fatty acid desaturase 2	2,642	1,647
1377672_at	BI300997	RGD1559960 /// Sult1c2	similar to Sulfotransferase K1 (rSULT1C2) /// sulfotransferase family, cytosolic, 1C, member 2	2,648	2,188
1370237_at	AA799574	Hadh	hydroxyacyl-Coenzyme A dehydrogenase	2,654	1,766
1373386_at	AI179953	Gjb2	gap junction protein, beta 2	2,660	1,511
1391907_at	AI030790	Nags	N-acetylglutamate synthase	2,662	1,786
1383248_at	AI454611	Fmo5	flavin containing monooxygenase 5	2,663	1,904
1387511_at	NM_012692	Cyp2a1	cytochrome P450, family 2, subfamily a, polypeptide 1	2,671	2,348
1387209_at	NM_053571	Sec16b	SEC16 homolog B (S. cerevisiae)	2,676	1,430
1387926_at	AB052846	Sc5dl	sterol-C5-desaturase (ERG3 delta-5-desaturase homolog, S. cerevisiae)-like	2,680	1,766
1368178_at	NM_031712	Pdzk1	PDZ domain containing 1	2,683	1,864
1372462_at	AI412322	Acat2	acetyl-Coenzyme A acetyltransferase 2	2,685	1,779
1393826_at	AI043761	Apon	apolipoprotein N	2,691	1,832
1388605_at	BM384938	Wfdc3	WAP four-disulfide core domain 3	2,707	2,527
1369492_at	NM_020538	Aadac	arylacetamide deacetylase (esterase)	2,717	2,161
1388395_at	AI406939	G0s2	G0/G1switch 2	2,718	1,245
1387243_at	K02422	Cyp1a2	cytochrome P450, family 1, subfamily a, polypeptide 2	2,728	1,506
1368794_at	NM_020076	Haao	3-hydroxyanthranilate 3,4-dioxygenase	2,729	2,058
1367994_at	NM_031027	Dpyd	dihydropyrimidine dehydrogenase	2,735	1,609
1393397_at	AI576488	Cpa2	carboxypeptidase A2 (pancreatic)	2,741	2,534
1387223_at	NM_017193	Aadat	aminoadipate aminotransferase	2,745	2,206
1367735_at	NM_012819	Acadl	acyl-Coenzyme A dehydrogenase, long-chain	2,748	1,577
1368092_at	NM_017181	Fah	fumarylacetoacetate hydrolase	2,750	2,203
1382384_at	BM383783	Rassf6	Ras association (RalGDS/AF-6) domain family member 6	2,752	2,211
1373452_at	AI232273	Rcl1	RNA terminal phosphate cyclase-like 1	2,753	2,239
1386754_at	BF521617	Trim14	tripartite motif-containing 14	2,756	1,751
1368731_at	NM_053288	Orm1	orosomucoid 1	2,758	1,710
1370475_at	M20406	Cyp2b3	cytochrome P450, family 2, subfamily b, polypeptide 3	2,765	1,945
1369863_at	NM_017270	Adh4 /// LOC100364917	alcohol dehydrogenase 4 (class II), pi polypeptide /// alcohol dehydrogenase 4-like	2,768	1,858
1368121_at	NM_013215	Akr7a3	aldo-keto reductase family 7, member A3 (aflatoxin aldehyde reductase)	2,770	2,042
1387503_at	NM_053526	Cpn1	carboxypeptidase N, polypeptide 1	2,770	1,701
1368401_at	M85035	Gria2	glutamate receptor, ionotropic, AMPA 2	2,772	2,068
1369746_a_at	AF147740	Slco1b3	solute carrier organic anion transporter family, member 1b3	2,775	1,890
1369852_at	NM_017143	F10	coagulation factor X	2,775	1,960
1373337_at	AI412065	Grhpr	glyoxylate reductase/hydroxypyruvate reductase	2,782	1,945
1393221_at	AA866264	RGD1564865	similar to 20-alpha-hydroxysteroid dehydrogenase	2,786	2,329
1387271_at	NM_053674	Phyh	phytanoyl-CoA 2-hydroxylase	2,787	2,033
1374570_at	AI012474	Agpat2	1-acylglycerol-3-phosphate O-acyltransferase 2 (lysophosphatidic acid acyltransferase, beta)	2,792	2,146
1388358_at	AW252650	Etfb	electron-transfer-flavoprotein, beta polypeptide	2,818	2,007
1370943_at	AI168953	Sult1c2 /// Sult1c2a	sulfotransferase family, cytosolic, 1C, member 2 /// sulfotransferase family, cytosolic, 1C, member 2a	2,826	2,276
1369493_at	NM_012630	Prlr	prolactin receptor	2,837	1,863
1368289_at	AA944965	Gc	group specific component	2,840	2,371
1369485_at	NM_130747	Acot12	acyl-CoA thioesterase 12	2,853	1,794
1386917_at	NM_012744	Pc	pyruvate carboxylase	2,855	1,456
1377666_at	BI293004	Chdh	choline dehydrogenase	2,856	2,028
1384417_at	AA998783	Apoc4	apolipoprotein C-IV	2,867	2,471
1367939_at	NM_012733	Rbp1	retinol binding protein 1, cellular	2,876	1,370
1393464_at	BM383378	RGD1311251	similar to RIKEN cDNA 4930550C14	2,895	2,331
1389363_at	AA997430	Adi1	acireductone dioxygenase 1	2,896	1,825
1370698_at	M13506	Ugt2b1	UDP glucuronosyltransferase 2 family, polypeptide B1	2,898	2,341
1369275_s_at	NM_012692	Cyp2a1 /// Cyp2a2	cytochrome P450, family 2, subfamily a, polypeptide 1 /// cytochrome P450, family 2, subfamily a, polypeptide 2	2,898	2,347
1380104_at	AA963815	F9	coagulation factor IX	2,899	2,488
1369799_at	U29701	Abat	4-aminobutyrate aminotransferase	2,903	2,655
1387050_s_at	NM_012696	Kng1 /// Kng1l1 /// Kng2	kininogen 1 /// kininogen 1-like 1 /// kininogen 2	2,911	2,117
1389654_at	BM392070	Pls1	Plastin 1 (I isoform)	2,914	1,755
1368514_at	NM_013198	Maob	monoamine oxidase B	2,916	2,087
1374828_at	AI045590	Pdia5	protein disulfide isomerase family A, member 5	2,917	2,416
1369727_at	NM_013112	Apoa2	apolipoprotein A-II	2,918	2,853
1369664_at	NM_053019	Avpr1a	arginine vasopressin receptor 1A	2,922	2,472

Appendix

Affymetrix ID	Public ID	Gene Symbol	Gene Title	fold control	SD
1370108_a_at	AF090134	Lin7a	lin-7 homolog a (C. elegans)	2,928	2,549
1370241_at	AA800502	Cyp2c7 /// LOC100361347	cytochrome P450, family 2, subfamily c, polypeptide 7 /// cytochrome P450 2C7-like	2,928	1,837
1368695_at	NM_016995	C4bpb	complement component 4 binding protein, beta	2,931	2,755
1393260_at	BG661061	LOC360228	WDNM1 homolog	2,936	2,282
1378739_at	AA818135	Cidec	cell death-inducing DFFA-like effector c	2,936	2,309
1368077_at	NM_012558	Fbp1	fructose-1,6-bisphosphatase 1	2,938	2,188
1384934_at	AA893454	Slc41a2	Solute carrier family 41, member 2	2,942	2,100
1387994_at	U89280	Hsd17b6	hydroxysteroid (17-beta) dehydrogenase 6	2,948	3,135
1368940_at	NM_017255	P2ry2	purinergic receptor P2Y, G-protein coupled, 2	2,956	2,137
1379246_at	AI169938	RGD1308742	similar to Complement C5 precursor	2,958	2,668
1369296_at	NM_031732	Sult1c3	sulfotransferase family, cytosolic, 1C, member 3	2,968	2,934
1373803_a_at	AI170771	Ghr	growth hormone receptor	2,969	2,612
1388948_at	AI104759	Stard10	StAR-related lipid transfer (START) domain containing 10	2,974	2,510
1368741_at	NM_057146	C9	complement component 9	2,981	2,338
1391194_at	BG377337	Sall1	Sal-like 1 (Drosophila)	2,982	2,561
1369581_at	NM_013003	Pemt	phosphatidylethanolamine N-methyltransferase	2,989	2,442
1397419_at	AI101314	Mpp6	Membrane protein, palmitoylated 6 (MAGUK p55 subfamily member 6)	3,000	2,694
1373686_at	AA893495	Serpina6	serine (or cysteine) peptidase inhibitor, clade A, member 6	3,006	2,479
1378819_at	AW435096	Aspdh	aspartate dehydrogenase domain containing	3,006	2,194
1370580_a_at	M18336	Cyp2c6 /// LOC293989	cytochrome P450, family 2, subfamily c, polypeptide 6 /// cytochrome P450-like	3,008	2,302
1368458_at	NM_012942	Cyp7a1	cytochrome P450, family 7, subfamily a, polypeptide 1	3,009	2,656
1387234_at	NM_012826	Azgp1	alpha-2-glycoprotein 1, zinc-binding	3,019	2,358
1374006_at	BI295878	Kat3 /// LOC100361841	kynurenine aminotransferase III /// kynurenine aminotransferase III-like	3,022	2,279
1374512_at	AI232341	LOC684314	similar to CG9886-like	3,039	2,423
1368016_at	NM_133299	Pecr	peroxisomal trans-2-enoyl-CoA reductase	3,049	2,367
1369654_at	NM_023991	Prkaa2	protein kinase, AMP-activated, alpha 2 catalytic subunit	3,051	2,704
1371824_at	AA891949	Ak3l1	adenylate kinase 3-like 1	3,052	2,058
1390326_at	BF564217	Ang1	angiogenin, ribonuclease A family, member 1	3,058	2,417
1398634_at	AI030835	LOC678836	hypothetical protein LOC678836	3,059	2,767
1367887_at	NM_017024	Lcat	lecithin cholesterol acyltransferase	3,070	1,843
1387282_at	NM_053612	Hspb8	heat shock protein B8	3,072	2,244
1383472_at	AA997683	Aldh1b1	aldehyde dehydrogenase 1 family, member B1	3,080	1,966
1372485_at	BF281220	Pcbd1	pterin-4 alpha-carbinolamine dehydratase/dimerization cofactor of hepatocyte nuclear factor 1 alpha	3,084	2,509
1398282_at	NM_053902	Kynu	kynureninase (L-kynurenine hydrolase)	3,089	2,893
1368609_at	NM_017047	Slc10a1	solute carrier family 10 (sodium/bile acid cotransporter family), member 1	3,097	2,544
1384499_at	BG373566	Bucs1	butyryl Coenzyme A synthetase 1	3,100	2,335
1387314_at	NM_022513	Sult1b1	sulfotransferase family, cytosolic, 1B, member 1	3,107	2,609
1367908_at	NM_133598	Gcsh	glycine cleavage system protein H (aminomethyl carrier)	3,112	2,449
1384834_at	AI028942	Cobl	cordon-bleu homolog (mouse)	3,116	2,057
1397740_at	AA964229	Sfxn1	sideroflexin 1	3,117	1,933
1382554_at	AA998638	C8a	complement component 8, alpha polypeptide	3,147	2,462
1398326_at	BI282332	Chchd10	coiled-coil-helix-coiled-coil-helix domain containing 10	3,149	2,762
1368520_at	NM_012737	Apoa4	apolipoprotein A-IV	3,150	2,256
1374176_at	AI408727	RGD1308059	similar to DNA segment, Chr 4, Brigham & Womens Genetics 0951 expressed	3,154	2,254
1373947_at	BI278545	Dpt	dermatopontin	3,154	2,169
1387284_at	NM_031705	Dpys	dihydropyrimidinase	3,163	2,965
1368224_at	NM_031531	Serpina3n	serine (or cysteine) peptidase inhibitor, clade A, member 3N	3,168	2,485
1394022_at	BE116009	Id4	inhibitor of DNA binding 4	3,170	2,650
1383606_at	BI302544	Tc2n	tandem C2 domains, nuclear	3,186	2,261
1372841_at	BG376982	Reep6	receptor accessory protein 6	3,194	2,434
1371762_at	AA858962	Rbp4	retinol binding protein 4, plasma	3,201	2,482
1370352_at	AB023630	Cesl1 /// Es22 /// LOC100125372	carboxylesterase-like 1 /// esterase 22 /// carboxylesterase ES-4	3,202	2,130
1383904_at	BM386541	Fgl1	fibrinogen-like 1	3,203	2,658
1373108_at	BM390827	Ppp1r3c	protein phosphatase 1, regulatory (inhibitor) subunit 3C	3,220	3,075
1369491_at	NM_053626	Dao	D-amino-acid oxidase	3,222	3,348
1383732_at	AA819810	RGD1307603	similar to hypothetical protein MGC37914	3,238	2,780
1391652_at	AI411140	Glyat	glycine-N-acyltransferase	3,239	2,655

Affymetrix ID	Public ID	Gene Symbol	Gene Title	fold control	SD
1394844_s_at	AA893326	Cyp4a2 /// Cyp4a3	cytochrome P450, family 4, subfamily a, polypeptide 2 /// cytochrome P450, family 4, subfamily a, polypeptide 3	3,241	2,298
1369435_at	NM_013048	Ttpa	tocopherol (alpha) transfer protein	3,245	2,749
1368569_at	NM_053781	Akr1b7	aldo-keto reductase family 1, member B7	3,251	3,013
1383692_at	BG377830	Prelid2	PRELI domain containing 2	3,257	2,978
1369663_at	NM_022936	Ephx2	epoxide hydrolase 2, cytoplasmic	3,281	2,763
1368362_a_at	M16347	Asgr2	asialoglycoprotein receptor 2	3,282	2,590
1374816_at	AI103939	Gcom1	GRINL1A complex locus	3,283	3,099
1386980_at	NM_019373	Apom	apolipoprotein M	3,284	2,974
1369790_at	M18340	Tat	tyrosine aminotransferase	3,313	2,120
1387936_at	D14989	Sult2a2	sulfotransferase family 2A, dehydroepiandrosterone (DHEA)-preferring, member 2	3,328	2,906
1372297_at	AI234527	Gsta4	glutathione S-transferase alpha 4	3,329	3,000
1387118_at	NM_013105	Cyp3a23/3a1	cytochrome P450, family 3, subfamily a, polypeptide 23/polypeptide 1	3,332	3,131
1368608_at	NM_019303	Cyp2f4	cytochrome P450, family 2, subfamily f, polypeptide 4	3,338	3,127
1370563_at	D17310	Akr1c14	aldo-keto reductase family 1, member C14	3,354	2,824
1387877_at	BE096729	Ftcd	formiminotransferase cyclodeaminase	3,371	2,477
1368618_at	NM_031623	Grb14	growth factor receptor bound protein 14	3,390	2,438
1367937_at	AF230096	Miox	myo-inositol oxygenase	3,391	2,397
1383395_at	AI028979	Agmat	agmatine ureohydrolase (agmatinase)	3,431	2,705
1379770_at	BF282951	Chpt1	choline phosphotransferase 1	3,457	3,447
1367659_s_at	NM_017306	Dci	dodecenoyl-Coenzyme A delta isomerase (3,2 trans-enoyl-Coenzyme A isomerase)	3,467	2,396
1388432_at	BI294994	Optn	optineurin	3,470	2,754
1369546_at	NM_022629	Bbox1	butyrobetaine (gamma), 2-oxoglutarate dioxygenase (gamma-butyrobetaine hydroxylase) 1	3,477	2,546
1383437_at	AI547691	Rab17	RAB17, member RAS oncogene family	3,481	2,821
1368790_at	NM_133617	Serpina10	serine (or cysteine) peptidase inhibitor, clade A (alpha-1 antiproteinase, antitrypsin), member 10	3,490	2,749
1387396_at	NM_053469	Hamp	hepcidin antimicrobial peptide	3,510	2,058
1367758_at	NM_012493	Afp	alpha-fetoprotein	3,511	3,618
1377660_at	BM387540	RGD1309350	similar to transthyretin (4L369)	3,512	2,758
1370818_at	AF044574	Decr2	2,4-dienoyl CoA reductase 2, peroxisomal	3,514	2,881
1387018_at	NM_053770	Sorbs2	sorbin and SH3 domain containing 2	3,520	3,069
1390944_at	BM384937	Chmp4c	chromatin modifying protein 4C	3,548	2,364
1370814_at	AB062758	Dhrs4	dehydrogenase/reductase (SDR family) member 4	3,559	2,890
1387307_at	NM_017159	Hal	histidine ammonia lyase	3,562	2,662
1390591_at	AI169163	Slc17a3	solute carrier family 17 (sodium phosphate), member 3	3,563	2,964
1368387_at	NM_053995	Bdh1	3-hydroxybutyrate dehydrogenase, type 1	3,580	2,984
1386880_at	NM_130433	Acaa2	acetyl-Coenzyme A acyltransferase 2	3,583	2,627
1393612_a_at	AI059270	Depdc7	DEP domain containing 7	3,594	2,715
1371363_at	BI277042	Gpd1	glycerol-3-phosphate dehydrogenase 1 (soluble)	3,599	2,658
1367804_at	NM_017170	Apcs	amyloid P component, serum	3,619	2,767
1394112_at	AA945123	Hao1	hydroxyacid oxidase (glycolate oxidase) 1	3,633	2,939
1387215_at	NM_030656	Agxt	alanine-glyoxylate aminotransferase	3,636	2,725
1398514_at	AI232328	Hgd	homogentisate 1, 2-dioxygenase	3,647	3,442
1388155_at	BI286012	Krt18	keratin 18	3,653	2,861
1368180_s_at	NM_017013	Gsta2 /// LOC494499	glutathione S-transferase A2 /// LOC494499 protein	3,711	3,081
1369836_at	NM_020096	Ifit1	interferon-induced protein with tetratricopeptide repeats 1	3,740	2,446
1387508_at	NM_017300	Baat	bile acid Coenzyme A: amino acid N-acyltransferase (glycine N-choloyltransferase)	3,746	2,864
1367932_at	NM_017268	Hmgcs1	3-hydroxy-3-methylglutaryl-Coenzyme A synthase 1 (soluble)	3,799	2,971
1382569_at	BF386242	Paqr9	Progestin and adipoQ receptor family member IX	3,842	3,398
1387006_at	NM_012695	Sult2al1	sulfotransferase family 2A, dehydroepiandrosterone (DHEA)-preferring-like 1	3,844	3,478
1371098_a_at	AA996755	Masp2	mannan-binding lectin serine peptidase 2	3,850	2,653
1370359_at	AB057450	Amy1a	amylase, alpha 1A (salivary)	3,852	3,201
1367838_at	NM_017074	Cth	cystathionase (cystathionine gamma-lyase)	3,855	4,180
1392172_at	AI169984	Ccl9	chemokine (C-C motif) ligand 9	3,858	3,599
1379400_at	AI044556	Aldh1l2	aldehyde dehydrogenase 1 family, member L2	3,875	2,925
1393123_at	BM392153	C8g	complement component 8, gamma polypeptide	3,920	3,591
1387240_at	NM_133543	Rdh7	retinol dehydrogenase 7	3,924	3,064
1385707_at	BF550221	Lect2	leukocyte cell-derived chemotaxin 2	3,954	3,167
1368335_at	NM_012738	Apoa1	apolipoprotein A-I	4,021	2,810
1368328_at	NM_013089	Gys2	glycogen synthase 2	4,023	2,684

Affymetrix ID	Public ID	Gene Symbol	Gene Title	fold control	SD
1371030_at	BI291181	Spp2	secreted phosphoprotein 2	4,064	3,307
1374657_at	AA848437	Anks4b	ankyrin repeat and sterile alpha motif domain containing 4B	4,067	3,289
1391534_at	BG666735	Elovl2	elongation of very long chain fatty acids (FEN1/Elo2, SUR4/Elo3, yeast)-like 2	4,083	3,861
1369195_at	NM_013068	Fabp2	fatty acid binding protein 2, intestinal	4,087	3,319
1381976_at	BE103004	Kif21a	kinesin family member 21A	4,155	2,601
1387949_at	M58041	Cyp2c22	cytochrome P450, family 2, subfamily c, polypeptide 22	4,169	3,139
1371530_at	BF281337	Krt8	keratin 8	4,207	3,343
1370149_at	NM_012503	Asgr1	asialoglycoprotein receptor 1	4,216	3,431
1391397_at	BF418393	LOC684055	hypothetical protein LOC684055	4,232	3,214
1368706_at	NM_053785	Tm4sf4	transmembrane 4 L six family member 4	4,238	3,639
1391661_at	AA945076	Gk	glycerol kinase	4,245	3,801
1387178_a_at	NM_012522	Cbs	cystathionine beta synthase	4,247	3,751
1370024_at	NM_030832	Fabp7	fatty acid binding protein 7, brain	4,286	4,368
1372601_at	BM391471	Atf5	activating transcription factor 5	4,366	3,706
1373963_at	BF284337	Hdhd3	haloacid dehalogenase-like hydrolase domain containing 3	4,410	2,903
1382924_at	AA850195	Pank1	pantothenate kinase 1	4,465	4,081
1379326_at	AI169837	RGD1305679	similar to 9530008L14Rik protein	4,542	4,079
1370167_at	BG668421	Sdc2	syndecan 2	4,552	3,670
1368878_at	NM_053539	Idi1	isopentenyl-diphosphate delta isomerase 1	4,607	5,003
1372755_at	AI102073	Mal2	mal, T-cell differentiation protein 2	4,623	4,813
1368720_at	NM_022403	Tdo2	tryptophan 2,3-dioxygenase	4,701	4,205
1379452_at	AI411492	Gas2	growth arrest-specific 2	4,707	4,533
1370334_at	AF081582	Plekhb1	pleckstrin homology domain containing, family B (evectins) member 1	4,786	4,635
1369509_a_at	AJ302031	A1bg	alpha-1-B glycoprotein	4,795	3,588
1387022_at	NM_022407	Aldh1a1	aldehyde dehydrogenase 1 family, member A1	4,874	4,798
1370592_at	AB019693	Keg1	kidney expressed gene 1	4,890	3,638
1368283_at	NM_133606	Ehhadh	enoyl-Coenzyme A, hydratase/3-hydroxyacyl Coenzyme A dehydrogenase	4,901	4,931
1370310_at	M33648	Hmgcs2	3-hydroxy-3-methylglutaryl-Coenzyme A synthase 2 (mitochondrial)	4,954	4,214
1382084_at	AA850264	RGD1562988	Similar to EHM2	4,964	4,152
1393139_at	BM385272	Apoc2	apolipoprotein C-II	4,995	4,292
1369502_a_at	NM_031502	Amy1a /// Amy2 /// Amy2-2	amylase, alpha 1A (salivary) /// amylase 2, pancreatic /// amylase 2-2, pancreatic	5,243	6,756
1367777_at	NM_057197	Decr1	2,4-dienoyl CoA reductase 1, mitochondrial	5,276	4,030
1391429_at	AW434961	Hfe2	hemochromatosis type 2 (juvenile) homolog (human)	5,286	5,286
1368934_at	NM_016999	Cyp4a1 /// Cyp4a10	cytochrome P450, family 4, subfamily a, polypeptide 1 /// cytochrome P450, family 4, subfamily a, polypeptide 10	5,507	3,953
1377037_at	AI411493	Acot4	acyl-CoA thioesterase 4	7,244	6,750
1369765_at	NM_022384	Ascl1	achaete-scute complex homolog 1 (Drosophila)	10,821	12,681

Table 28: Affymetrix IDs, public IDs, gene symbols, full gene titles, mean fold control of gene expression compared to controls (NPC 24h oil-treated, n=4, fold NPC 20h water treated, n=3) and SD of genes which were at least 2-fold up- or downregulated in primary rat mesenchymal cells.

Changes in gene expression in hepatocytes after 20h

Affymetrix ID	Public ID	Gene Symbol	Gene Title	fold control	SD
1395403_at	BM385735	Stac3	SH3 and cysteine rich domain 3	0,450	0,319
1384525_at	AI549335	Dock11	dedicator of cytokinesis 11	0,479	0,406
1369268_at	NM_012912	Atf3	activating transcription factor 3	0,484	0,392
1387808_at	AF200684	Slc7a7	solute carrier family 7 (cationic amino acid transporter, y+ system), member 7	2,100	1,327
1367553_x_at	NM_033234	Hbb	hemoglobin, beta	2,268	1,956
1369424_at	NM_012693	Cyp2a2	cytochrome P450, family 2, subfamily a, polypeptide 2	2,336	0,995
1391433_at	AA899721	Acot2	acyl-CoA thioesterase 2	2,384	1,372
1370987_at	BF550890	Spn	sialophorin	2,459	0,884
1369195_at	NM_013068	Fabp2	fatty acid binding protein 2, intestinal	2,577	1,566
1384064_at	AI502703	Krt23	keratin 23 (histone deacetylase inducible)	2,673	2,104
1369765_at	NM_022384	Ascl1	achaete-scute complex homolog 1 (Drosophila)	3,025	1,864
1389253_at	BI289085	Vnn1	vanin 1	5,508	4,764

Table 29: Affymetrix IDs, public IDs, gene symbols, full gene titles, mean fold control of gene expression compared to controls (HC 24h oil-treated, n=4, fold HC 20h water treated, n=3) and SD of genes which were at least 2-fold up- or downregulated in primary rat hepatocytes.

Appendix

References

Alvarez-Iglesias, M., Wayne, G., O'Dea, K., Amour, A., & Takata, M. (August 2005). Continuous real-time measurement of tumor necrosis factor-α converting enzyme activity on live cells. *Laboratory Investigation 85* , S. 1440-1448.

Arribas, J., & Borroto, A. (February 2002). Protein Ecotdomain Shedding. *Chemical Reviews* , S. 4627-4637.

Becker, B. F., Gilles, S., Sommerhoff, C. P., & Zahler, S. (November 2002). Application of Peptides Containing the Cleavage Sequence of Pro-TNFα in Assessing TACE Activity of Whole Cells. *Biological Chemistry* , S. 1821-1826.

Berasain, C., Castillo, J., Perugorria, M., Latasa, M., Prieto, J., & Avila, M. (2009). Inflammation and Liver Cancer. *Annals of the New York Academy of Sciences* , S. 206-221.

Berk, P., & Stump, D. (1999). Mechanisms of cellular uptake of long chain free fatty acids. *Molecular and Cellular Biochemistry 192* , S. 17-31.

Bintner, N. (2011). *The role of non-genotoxic carcinogens and their impact on the expression of growth factors and cytokines in liver cells.* Wien: Universität Wien.

Blonski, W., Kotlyar, D. S., & Forde, K. A. (2010). Non-viral causes of hepatocellular carcinoma. *World J Gastroenterol* , S. 3603-3615.

Boutros, C., Somasundar, P., Razzak, A., Helton, S., & Espat, J. (June 2010). Omega-3 fatty acids - Investigations from cytokine regulation to pancreatic cancer gene suppression. *Archives of surgery* , S. 515-519.

Cai, Y., Shen, X. Z., Zhou, C. H., & Wang, J. Y. (November 2006). Abnormal expression of Smurf2 during the process of rat liver fibrosis. *Chinese Journal of Digestive Diseases* , S. 237-245.

Caimari, A., Oliver, P., Rodenburg, W., Keijer, J., & Palou, A. (May 2010). Slc27a2 expression in peripheral blood mononuclear cells as a molecular marker for overweight development. *International Journal of Obesity. Vol 34(5)* , S. 831-839.

Calle, E. E., Rodriguez, C., Walker-Thurmond, K., & Thun, M. J. (April 2003). Overweight, Obesity, and Mortality from Cancer in a Prospectively Studied Cohort of U.S. Adults. *The New England Journal of Medicine Vol.348* , S. 1625-1638.

Casey, C. A., McVicker, B. L., Donohue, T. M., McFarland, M. A., Wiegert, R. L., & Nanji, A. A. (January 2004). Liver asialoglycoprotein receptor levels correlate with severity of alcoholic liver damage in rats. *Journal of Applied Physiology. Vol 96(1)* , S. 76-80.

Chao, J., Miao, R., Chen, V., Chen, L., & Chao, L. (January 2001). Novel roles of kallistatin, a specific tissue kallikrein inhibitor, in vascular remodeling. *Biological Chemistry* , S. 15-21.

Cohen, J. C., Horton, J. D., & Hobbs, H. H. (June 2011). Human Fatty Liver Disease: Old Questions and New Insights. *Science Vol. 332* , S. 1519-1523.

Daigneault, M., Preston, J. A., Marriott, H. M., Whyte, M. K., & Dockrell, D. H. (January 2010). The Identification of Markers of Macrophage Differentiation in PMA-Stimulated THP-1 Cells and Monocyte-Derived Macrophages. *PLoS ONE* .

de Lima, T. M., de Sa Lima, L., Scavone, C., & Curi, R. (2006). Fatty acid control of nitric oxide production by macrophages. *FEBS Letters 580* , S. 3287-3295.

Demozay, D., Rocchi, S., Mas, J.-C., Grillo, S., Pirola, L., Chavey, C., et al. (February 2004). Fatty aldehyde dehydrogenase: potential role in oxidative stress protection and regulation of its gene expression by insulin. *Journal of Biological Chemistry Vol.279(8)* , S. 6261-6270.

Desbuquois, B., Béréziat, V., Authier, F., Girard, J., & Burnol, A.-F. (September 2008). Compartmentalization and in vivo insulin-induced translocation of the insulin-signaling inhibitor Grb14 in rat liver. *The FEBS Journal. Vol 275(17)* , S. 4363-4377.

Doedens, J. R., Mahimkar, R. M., & Black, R. A. (2003). TACE/ADAM17 enzymatic activity is increased in response to cellular stimulation. *Biochemical and Biophysical Research Communications 308* , S. 331-338.

El-Serag, H. B., & Rudolph, K. L. (2007). Hepatocellular Carcinoma: Epidemiology and Molecular Carcinogenesis. *GASTROENTEROLOGY* , S. 2557–2576.

Ernst, M. C., & Sinal, C. J. (November 2010). Chemerin: at the crossroads of inflammation and obesity. *Trends in Endocrinology and Metabolism* , S. 660-667.

Gao, B., Jeong, W.-I., & Tian, Z. (2008). Liver: An Organ with Predominant Innate Immunity. *Hepatology* , S. 729-736.

Gleissman, H., Johnsen, J. I., & Kogner, P. (2010). Omega-3 fatty acids in cancer, the protectors of good and the killers of evil? *Experimental Cell Research* , S. 1365-1373.

Greenfield, V., Cheung, O., & Sanyal, A. J. (2008). Recent advances in nonalcoholic fatty liver disease. *Current Opinion in Gastroenterology* , S. 320-327.

Grivennikov, S. I., & Karin, M. (2011). Inflammatory cytokines in cancer: tumour necrosis factor and interleukin 6 take the stage. *Annals of the rheumatic diseases* , S. 104-108.

Gutiérrez-López, M. D., Gilsanz, A., Yanez-Mo, M., Ovalle, S., Lafuente, E. M., Domínguez, C., et al. (January 2011). The sheddase activity of ADAM17/TACE is regulated by the tetraspanin CD9. *Cellular and Molecular Life Sciences* .

Hanahan, D., & Weinberg, R. A. (2011). Hallmarks of Cancer: The next Generation. *Cell, Vol.144* , S. 646-674.

Hanahan, D., & Weinberg, R. A. (January 2000). The Hallmarks of Cancer. *Cell, Vol.100* , S. 57–70.

He, J., Lee, J. H., Febbraio, M., & Xie, W. (2011). The emerging roles of fatty acid translocase/CD36 and the aryl hydrocarbon receptor in fatty liver disease. *Experimental Biology and Medicine 236* , S. 1116-1121.

Appendix

Inaba, T., Matsuda, M., Shimamura, M., Takei, N., Terasaka, N., Ando, Y., et al. (June 2003). Angiopoietin-like protein 3 mediates hypertriglyceridemia induced by the liver X receptor. *Journal of Biological Chemistry. Vol 278(24)* , S. 21344-21351.

Jong, M. C., Hofker, M. H., & Havekes, L. M. (March 1999). Role of ApoCs in Lipoprotein Metabolism: Functional Differences Between ApoC1, ApoC2, and ApoC3 . *Arteriosclerosis, Thrombosis, and Vascular Biology. Vol 19(3)* , S. 472-484.

Kaibori, M., Inoue, T., Oda, M., Naka, D., Kawaguchi, T., Kitamura, N., et al. (January 2002). Exogenously administered HGF activator augments liver regeneration through the production of biologically active HGF. *Biochemical and Biophysical Research Communications Vol290(1)* , S. 475-481.

Kakehashi, A., Inoue, M., Wei, M., Fukushima, S., & Wanibuchi, H. (July 2009). Cytokeratin 8/18 overexpression and complex formation as an indicator of GST-P positive foci transformation into hepatocellular carcinomas. *Toxicology and Applied Pharmacology. Vol 238(1)* , S. 71-79.

Kallwellis, K., Grempler, R., Günther, S., Päth, G., & Walther, R. (September 2006). Tumor necrosis factor alpha induces the expression of the nuclear protein p8 via a novel NF kappaB binding site within the promoter. *Hormone and Metabolic Research* , S. 570-574.

Kang, H. S., Okamoto, K., Kim, Y.-S., Takeda, Y., Bortner, C. D., Dang, H., et al. (2011, January). Nuclear orphan receptor TAK1/TR4-deficient mice are protected against obesity-linked inflammation, hepatic steatosis and insulin resistance. *Diabetes* , pp. 177-188.

Kanouchi, H., Miyamoto, M., Oka, T., Matsumoto, M., Okamoto, T., Tone, S., et al. (September 2006). Perchloric acid-soluble protein is expressed in enterocytes and goblet cells in the intestine and upregulated by dietary lipid. *Biochimica et Biophysica Acta (BBA) - General Subjects. Vol1760(9)* , S. 1380–1385.

Kanouchi, H., Taga, M., Okamoto, T., Yamasaki, M., Oka, T., Yamada, K., et al. (January 2006). Reduced Expression of Perchloric Acid-Soluble Protein after Partial Hepatectomy in Rats. *Bioscience, Biotechnology, and Biochemistry Vol70(1)* , S. 290-292.

Kaskow, B. J., Proffit, J. M., Blangero, J., Moses, E. K., & Abraham, L. J. (2012). Diverse biological activities of the vascular non-inflammatory molecules – The Vanin pantetheinases. *Biochemical and Biophysical Research Communications. Vol 417* , S. 653–658.

Kostourou, V., Robinson, S. P., Cartwright, J. E., & Whitley, G. S. (September 2002). Dimethylarginine dimethylaminohydrolase I enhances tumour growth and angiogenesis. *British Journal of Cancer. Vol 87(6)* , S. 673-680.

Kuribayashi, T., Tomizawa, M., Seita, T., Tagata, K., & Yamamoto, S. (July 2011). Relationship between production of acute-phase proteins and strength of inflammatory stimulation in rats. *Laboratory Animals* , S. 215-218.

Lee, J. Y., Zhao, L., & Hwang, D. H. (2009). Modulation of pattern recognition receptor-mediated inflammation and riks of chronic diseases by dietary fatty acids. *Nutrition Reviews* , S. 38-61.

Li, C.-C., Lii, C.-K., Liu, K.-L., Yang, J.-J., & Chen, H.-W. (2006). n-6 and n-3 polyunsaturated fatty acids down-regulate cytochrome P-450 2B1 gene expression induced by phenobarbital in primary rat hepatocytes. *Journal of Nutritional Biochemistry* , S. 707-715.

Li, H., Meininger, C., Kelly, K., Hawker, J. J., Morris, S. J., & Wu, G. (January 2002). Activities of arginase I and II are limiting for endothelial cell proliferation. *American Journal of Physiology. Regulatory, integrative and comparative physiology.* , S. R64-R69.

Li, N., Grivennikov, S. I., & Karin, M. (April 2011). The Unholy Trinity: Inflammation, Cytokines, and STAT3 Shape the Cancer Microenvironment. *Cancer Cell Vol 19* , S. 429-431.

Masterton, G., Plevris, J., & Hayes, P. (2010). Omega-3 fatty acids - a promising novel therapy for non-alcoholic fatty liver disease. *Alimentary Pharmacology and Therapeutics* , S. 679-692.

Oh, D. Y., Talukdar, S., Bae, E. J., Imamura, T., Mornaga, H., Fan, W., et al. (September 2010). GPR120 is an Omega-3 Fatty Acid Receptor Mediating Potent Anti-inflammatory and Insulin-Sensitizing Effects. *Cell 142* , S. 687-698.

Ou, H.-Y., Wu, H.-T., Yang, Y.-C., Wu, J.-S., Cheng, J.-T., & Chang, C.-J. (May 2011). Elevated Retinol Binding Protein 4 Contributes to Insulin Resistance in Spontaneously Hypertensive Rats. *Hormone and metabolic research. Vol 43(5)* , S. 312-318.

Oyagbemi, A., Azeez, O., & Saba, A. (March 2010). Hepatocellular carcinoma and the underlying mechanisms. *African Health Sciences Vol 10* , S. 93-98.

Park, E. J., Lee, J. H., Yu, G.-Y., He, G., Raza Ali, S., Holzer, R. G., et al. (January 2010). Dietary and Genetic Obesity Promote Liver Inflammation and Tumorigenesis by Enhancing IL-6 and TNF Expression. *Cell Vol. 140* , S. 197-208.

Parzefall, W., Monschau, P., & Schulte-Hermann, R. (1989). Induction by cyproterone acetate of DNA synthesis and mitosis in primary cultures of adult rat hepatocytes in serum free medium. *Archives of Toxicology* , S. 456-461.

Pertoft, H., & Smedsrod, B. (1987). Separation and characterization of liver cells. *Cell separation: methods and selected applications Vol 4* , S. 1-24.

Piñeiro, M., Alava, M. A., González-Ramón, N., Osada, J., Lasierra, P., Larrad, L., et al. (September 1999). ITIH4 serum concentration increases during acute-phase processes in human patients and is up-regulated by interleukin-6 in hepatocarcinoma HepG2 cells. *Biochemical and Biophysical Research Communications* , S. 224-229.

Qiu, J., Liu, Z., Da, L., Li, Y., Xuan, H., Lin, Q., et al. (February 2007). Overexpression of the gene for transmembrane 4 superfamily member 4 accelerates liver damage in rats treated with CCl4. *Journal of Hepatology. Vol 46(2)* , S. 266-275.

Richieri, G. V., Anel, A., & Kleinfeld, A. M. (1993). Interactions of Long-chain Fatty Acids and Albumin: Determination of Free Fatty Acid Levels Using the Fluorescent Probe ADIFAB. *Biochemistry 32* , S. 7574-7580.

Sagmeister, S. (2009). *Epithelial-mesenchymal interactions in early and late hepatocarcinogenesis with focus on the role of linoleic acid and its hydroperoxides.* Wien: Universität Wien.

Savage, D. B., & Semple, R. K. (2010). Recent insights into fatty liver, metabolic dyslipidaemia and their links to insulin resistance. *Current Opinion in Lipidology* , S. 329-336.

Scheller, J., Chalaris, A., Garbers, C., & Rose-John, S. (August 2011). ADAM17: a molecular switch to control inflammation and tissue regeneration. *Trends in Immunology Vol 32* , S. 380-387.

Schenk, S., Saberi, M., & Olefsky, J. M. (September 2008). Insulin sensitivity: modulation by nutrients and inflammation. *The Journal of Clinical Investigation* , S. 2992-3002.

Schousboe, I. (November 1985). beta 2-Glycoprotein I: a plasma inhibitor of the contact activation of the intrinsic blood coagulation pathway. *Blood Vol 66(5)* , S. 1086-1091.

Scott, A. J., O'Dea, K., O'Callaghan, D., Williams, L., Dokpesi, J. O., Tatton, L., et al. (October 2011). Reactive Oxygen Species and p38MAPK mediate TNF-alpha converting enzyme (TACE/ADAM17) activation in primary human monocytes. *Journal of Biological Chemistry* , S. 35466-35476.

Seglen, P. (1976). Preparation of isolated rat liver cells. *Methods in cell biology 13* , S. 29-83.

Silverstein, R. L., & Febbraio, M. (2009). CD36, a Scavenger Receptor involved in Immunity, Metabolism, Angiogenesis, and Behavior. *Science Signaling Vol 2 Issue 72* .

Silverstein, R. L., Li, W., Park, Y. M., & Rahaman, S. O. (2010). Mechanisms of cell signaling by the scavenger receptor CD36; implications in atherosclerosis and thrombosis. *Transactions of the American Clinical and Climatological Association Vol 121* , S. 207-220.

Stewart, C. R., Stuart, L. M., Wilkinson, K., van Gils, J. M., Deng, J., Halle, A., et al. (February 2010). CD36 ligands promote sterile inflammation through assembly of a Toll-like receptor 4 and 6 heterodimer. *Nature immunology Vol 11* , S. 155-162.

Thomson, A. W., & Knolle, P. A. (November 2010). Antigen-presenting cell function in the tolerogenic liver environment. *Nature Reviews Immunology* , S. 753-766.

Toffanin, S., Friedman, S. L., & Llovet, J. M. (February 2010). Obesity, Inflammatory Signaling, and Hepatocellular Carcinoma - An Enlarging Link. *Cancer Cell Vol 17* , S. 115-117.

van der Vliet, H. N., Sammels, M. G., Leegwater, A. C., Levels, J. H., Reitsma, P. H., Boers, W., et al. (September 2001). Apolipoprotein A-V: a novel apolipoprotein associated with an early phase of liver regeneration. *Journal of Biological Chemistry. Vol 276(48)* , S. 44512-44520.

Wagner, E. F., & Nebreda, Á. R. (August 2009). Signal integration by JNK and p38 MAPK pathways in cancer development. *Nature Reviews. Cancer.* , S. 537-549.

Wall, R., Ross, P., Fitzgerald, G. F., & Stanton, C. (2010). Fatty acids from fish: the anti-inflammatory potential of long-chain omega-3 fatty acids. *Nutrition Reviews* , S. 280-289.

Wang, Y., Kinzie, E., Berger, F., Lim, S., & Baumann, H. (2001). Haptoglobin, an inflammation-inducible plasma protein. *Redox Report* , S. 379-385.

Yamaguchi, M. (July 2009). Novel protein RGPR-p117: its role as the regucalcin gene transcription factor. *Molecular and Cellular Biochemistry. Vol 327* , S. 53-63.

Yamaguchi, M., Takahashi, H., & Tsurusaki, Y. (April 2003). Suppressive role of endogenous regucalcin in the enhancement of nitric oxide synthase activity in liver cytosol of normal and regucalcin transgenic rats. *Journal of Cellular Biochemistry.Vol 88(6)* , S. 1226-1234.

Yang, J. D., & Roberts, L. R. (2010). Hepatocellular carcinoma: a global view. *Nat. Rev. Gastroenterol. Hepatol. 7* , S. 448–458.

Zandbergen, F., Mandard, S., Escher, P., Tan, N. S., Patsouris, D., Jatkoe, T., et al. (December 2005). The G0/G1 switch gene 2 is a novel PPAR target gene. *The Biochemical Journal. Vol 392(Pt2)* , S. 313–324.

Appendix

Curriculum vitae

Persönliche Informationen

- Name: Mario Kuttke
- Geburtsdatum: 23. Dezember 1985
- Geburtsort: Wien
- Adresse: Kaiser-Ebersdorferstraße 79/7/1, 1110 Wien
- E-Mail: mario.kuttke@gmx.at
- Staatsbürgerschaft: Österreich

Ausbildung

Sept. 2010 – Sept. 2011	Durchführung der Diplomarbeit am Institut für Krebsforschung der Medizinischen Universität Wien bei a.o.Univ.Prof. Dr. Bettina Grasl-Kraupp
2010	Bachelorstudium Biologie/Molekulare Biologie an der Universität Wien
Okt. 2005 - heute	Studium der Molekularen Biologie an der Universität Wien
1996 – 2004	BRG Geringergasse, Wien 11
1992 - 1996	VS Wilhelm Kress Platz, Wien 11

Kongresse

ASTOX-Symposium (Austrian Society for Toxicology), Wien, 25. Nov 2011

Kurzvortrag: "Do free fatty acids in native or peroxidized form trigger the outbreak of liver inflammation?"

M. Kuttke, T. Böhm, S. Sagmeister, N. Rohr-Udilova, H. Berger, W. Huber, B. Grasl-Kraupp